In the Name of God

Journal of
Information Systems & Telecommunication
Vol. 8, No.3, July-September 2020, Serial Number 31

Research Institute for Information and Communication Technology
Iranian Association of Information and Communication Technology
Affiliated to: Academic Center for Education, Culture and Research (ACECR)

Print ISSN: 2322-1437
Online ISSN: 2345-2773
Publication License: 91/13216
Editorial Office Address: No.5, Saeedi Alley, Kalej Intersection., Enghelab Ave., Tehran, Iran,
P.O.Box: 13145-799 Tel: (+9821) 88930150 Fax: (+9821) 88930157
E-mail: info@jist.ir , infojist@gmail.com
URL: www.jist.ir

Indexed by:
- SCOPUS www. Scopus.com
- Index Copernicus International www.indexcopernicus.com
- Islamic World Science Citation Center (ISC) www.isc.gov.ir
- Directory of open Access Journals www.Doaj.org
- Scientific Information Database (SID) www.sid.ir
- Regional Information Center for Science and Technology (RICeST) www.ricest.ac.ir
- Iranian Magazines Databases www.magiran.com

Publisher:
Iranian Academic Center for Education, Culture and Research **(ACECR)**

This Journal is published under scientific support of
Advanced Information Systems (AIS) Research Group and
Digital & Signal Processing Research Group, ICTRC

Acknowledgement

JIST Editorial-Board would like to gratefully appreciate the following distinguished referees for spending their valuable time and expertise in reviewing the manuscripts and their constructive suggestions, which had a great impact on the enhancement of this issue of the JIST Journal.

(A-Z)

- Ahmadizad, Arman, University of Kurdistan, Kurdistan, Iran
- Asgari Tabatabaee, Mohammad Javad, University Of Torbat Heydarieh, Razavi Khorasan, Iran
- Agahi, Hamed, Islamic Azad University ,Shiraz, Iran
- Badie, Kambiz, Tehran University, Iran
- Borna, Keyvan, Kharazmi University,Tehran, Iran
- Chauhan, Ritu, Amity University, Noida, India
- Ebadati, Omid Mahdi, Kharazmi University,Tehran, Iran
- Ebrahimi, Seyed Babak, K. N. Toosi University of Technology, Tehran, Iran
- Fasanghari, Mehdi, Iran Telecommunication Research Center (ITRC), Tehran, Iran
- Farrokhbakht Foumani, Mehdi, Islamic Azad University Fouman , Rasht, Iran
- Ghayoomi, Masood, Institute for Humanities and Cultural Studies, Tehran, Iran
- Ghafari, Ali, Islamic Azad University, Tabriz, Iran
- Haghbin, Afrooz, Science and Research university, Tehran , Iran
- Kasaei, Shohreh, Sharif University, Tehran, Iran
- Kashef, Seyed Sadra, Urmia University, Iran
- Mavadati, Samira, Mazandaran University, Mazandaran, Iran
- Masoomi, Mohsen, Islamic Azad University, Tehran, Iran
- Mahdieh, omid, Zanjan University, Iran
- Mahmoudzadeh, Mahmood, Islamic Azad University, Tehran, Iran
- Maleki Sadr, Mohammad Amin, K. N. Toosi University of Technology, Tehran, Iran
- Mavaddati, Samira, Mazandaran University, Iran
- Mohebbi, Keyvan, Islamic Azad University, Mobarakeh, Najafabad, Iran
- Nezafati, Navid, Shahid Beheshti University, Tehran, Iran
- Rasi, Habib , University of Technology, Shiraz, Iran
- Reshadat, Vahideh, Malek-Ashtar University of Technology, Tehran, Iran
- Shiri, Mohammad Ebrahim, Amirkabir, Tehran, Iran
- Siadat, Hossein, Kharazmi University,Tehran, Iran
- Tanhaei, Mohammad, Ilam University, Ilam , Iran
- Vahidi, Javad, University of Science and Technology, Tehran, Iran
- Yaghoobi, Kaebeh, Ale Taha Institute of Higher Education, Tehran, Iran

Table of Contents

Optical Power Distributions for 4×4 MIMO Visible Light Communications in Indoor Environment

Lwaa Faisal Abdulameer*
Faculty of Information and Communication Engineering, University of Baghdad, Baghdad, Iraq
lwaa@kecbu.uobaghdad.edu.iq
Ahmed K. Hassan
Faculty of Information and Communication Engineering, University of Baghdad, Baghdad, Iraq
akadhim@kecbu.uobaghdad.edu.iq
Aliaa T. Obeed
Information and Communication Engineering, University of Baghdad, Baghdad, Iraq
aliaarariq2222@gmail.com
Aye N. Dahir
Information and Communication Engineering, University of Baghdad, Baghdad, Iraq
oshynaeem300@gmail.com

Received: 18/Dec/2019 Revised: 24/Sep/2020 Accepted: 24/Oct/2020

Abstract

Visible Light Communication (VLC) has emerged as a powerful technique for wireless communication systems. Providing high data rate and increasing capacity are the major problems in VLC. Recent evidence suggests that Multiple Input Multiple Output (MIMO) technique can offers improved data rates and increased link range. This paper describes the design and implementation of visible light communication system in indoor environment exploring the benefits of MIMO. The specific objective of this research was to implement a 4×4 Multiple Input (LEDs) Multiple Output (photodetectors)-VLC communication system, where a 16 white power LEDs in four arrays are setting up at transmitter and four RX modules are setting up at receiver side without the need for additional power or bandwidth as well as analyze a mathematical model for a VLC- 4 ×4 MIMO with different modes such as the suitable angles to cover the entire room.

The research designs practically an electronic circuit for the transmitter and receiver with inexpensive components. The power distribution of different propagation modes is calculated for Single Input Single Output (SISO) and MIMO channels in typical room dimensions. The results in this paper indicate that the power is distributed uniformly for entire room when implemented VLC-MIMO as compared to VLC-SISO. Furthermore, a 4×4 MIMO implementing VLC is compared in term of BER vs. SINR with SISO communication system for both Line of Sight (LOS) and Non Line of Sight (NLOS) propagation modes. Comparing the two results of LOS and NLOS, it can be seen that a 4×4 MIMO implementing VLC for LOS perform better than the same system with NLOS due to decreasing in the received power resulted from the multipath effect.

Keywords: MIMO; SISO; VLC; Optical; Indoor; Power Distribution.

1- Introduction

Recent developments in lighting industry have heightened the need for Visible Light Communication (VLC) which has been attracting a lot of interest in the short distances wireless communications [1]. There is an urgent need to address license spectrum, electromagnetic interference and security problems for radio frequency (RF) wireless communications; However, VLCs are one of the most promising complementary technologies for RF communications [2].

VLCs have emerged as a powerful solution for indoor high-speed data transmission, where high spectral efficiencies and low latencies are the main requirements for next generation wireless networks. Fig. 1 shows the concept of VLC system [3-4]. Unlike RF signals, VLC modulated signals must be nonnegative and real valued signals. Moreover, intensity modulation and direct detection (IM/DD) schemes may be utilized at the transmitter and the receiver [5].

Due to the characteristics of LEDs, multiple LEDs are popularly employed to provide illuminations as well as translating data because of their higher efficiency, friendly manifest, long life time and better spectrum efficiency in indoor environment.

However, the common white LEDs have a limited bandwidth, which restrict the high data transmission rate [6-8].

*Corresponding Author

MIMO channels where multiple sources and multiple detectors are setting up at transmitter and receiver are predominantly used to combat multipath fading and optimize the data rate. MIMO is fundamental to achieve higher spectral efficiency and link reliability and or diversity [9-10].

Visible light communications implementing MIMO technique is a promising solution for wireless communication systems in beyond 5G networks. However, it provides high energy efficiency, low implementation cost, and high-speed data transmission [11]. Consequently, in a typical indoor VLC system, there are illuminated sources; therefore, it is natural to utilize MIMO technique to have parallel data [12]. On the other hand, due to the highly directional characteristics of light propagation, the communication through VLC channels has mainly relied on the availability of LOS link in addition to NLOS link where the transmitted signal at the receiver through different angles, different time delays and/or different frequency [13].

2- Related Works

More recent attention has focused on the provision of VLC-MIMO communication systems,

A great deal of previous research into 2×2 MIMO-VLC system for indoor environment has focused on the implementation of STBC and Repetition coding assuming LOS and NLOS links.

In their case study, a performance of VLC-MIMO system has been computed and demonstrated. This study indicates that the performance of the proposed system has a good improvement when compared with the system used single PD but they did not take in consideration how the power is distributed in entire room [14]. A number of authors have considered the analysis of a 2×2 VLC-MIMO system employing joint IQ independent component. This analysis involves a novel MIMO detection scheme to decompose the superposed signals. With the help of the proposed machine learning scheme, two received optical signals can be separated into two independent parallel signals. Detailed simulation showed that the unmixing matrix can be quickly converged by iterations.

They evaluated the performance of the algorithm where the Q factor yielded a gain of about 2.5 dB compared with the traditional Alamouti Space Time Block Coding (STBC) scheme [15]. Various studies have assessed the performance of an indoor optical wireless communication system with VLC technology with a spatially random receiver. Considering that the receiver is uniformly distributed on the floor, a 4 light emitting diode (LED) lamps are located at the center of the room. The receiver chooses the best channel link to receive the information from the LED lamps, which depends on the distance between the receiver and each lamp by using stochastic geometry theory [16]. One of the most significant current discussions in VLC-MIMO is the inferiority of BER performance due to the multipath effects in indoor environment. Repetition coding (RC), STBCs, and spatial multiplexing (SMP) had been used to improve the BER performance.

Two different configurations (2×2 and 4×4) are taken into consideration with distinct transmitters spacing. Simulation results and a comparative analysis of their system with an existing system is given mainly in terms of bit error rate (BER), data-rate, and transmission range. The simulation and experimentation results showed that the RC scheme with significant diversity gain provides more robustness as compared to other MIMO schemes [17]. However, in all of the presented woks, the analysis of the VLC-MIMO system for indoor environments has been investigated using either Line of Sight (LOS) or Non LOS (NLOS) propagation models.

In the current work, the power distribution has been simulated for two different propagation modes, LOS, also known as power distribution without reflection) and NLOS, known as power distribution with reflection).

There are two primary aims of this research: 1. To analyse a 4×4 MIMO-VLC system for both LOS and NLOS propagation modes. 2. To measure the power distribution in different cases according to system under study. The system is designed practically using inexpensive electronic circuits for both transmitter and receiver sides.

In the rest of this paper, part II introduces the mathematical model for the VLC-MIMO system. Part III introduces the two different Tx-Rx modules for the proposed system in addition to hardware experiments. In part IV, presents and discuss the MATLAB simulation results.

Notations: We use uppercase bold letters for matrices and lowercase bold-italic letters for vectors. $(\ )^*$ stands for the complex conjugate.

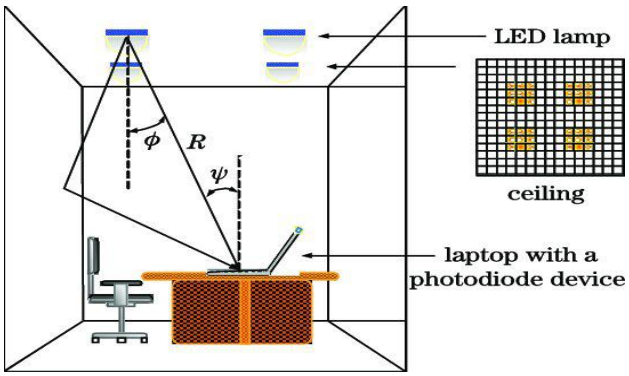

Fig. 1. Application of visible light communication

3- The Proposed Scheme

3-1- Indoor VLC Model

The typical room model for the present work is shown in Fig. 2 with dimensions of 3×3×5 m^3. The location of the receiver is assumed to be put at a height of 2-m from the ground. LOS, L-R1 and L-R1-R2 signals are reaching photodetector. LOS represented by Path d (red line), NLOS has been represented in Fig.2 by path d1d2 (blue line) for L-R1 channel and path d1-d3-d4 (green and blue lines) is for L-R1-R2 channel.

The average transmitted power from the light source is given by

$$P_t = \lim_{T\to\infty} \frac{1}{T}\int_0^T P_i(t)dt \qquad P_i(t) > 0 \tag{1}$$

where P_i is the optical transmitted power.

Through the channel model, the reflectivity of the walls (plastic wall, plaster wall…etc), ceiling, floor differs leading to intersymbol interference (ISI).

The first and second reflections are shown on wall-1 and wall-2 respectively. Thus, the power received at photodetector via direct and non-direct paths is calculated by equation (2)

$$Pr=(\mathbf{H}_{\mathbf{LOS}}(0) + \mathbf{H}_{\mathbf{dif}}(0))\, p_t + \sigma^2{}_{noise} \tag{2}$$

where $\mathbf{H}_{\mathbf{LOS}}(0)$ and $\mathbf{H}_{\mathbf{dif}}(0)$ are the direct gain (DC) of direct path and non-direct paths respectively and $\sigma^2{}_{noise}$ is the noise power.

Angles ϕ, ϕ_1 represent irradiance angles of LOS and diffuse signal respectively, α,ϒ are the incidence angles and β, δ are the exit angles at the surface of the wall. Angles φ, φ_1, φ_2 are the angles of incidence at the detector for direct path, first and second reflections respectively [12-13].

Emitted light intensity via an LED can be represented by Lambert formula and given by [18],

$$s(\varphi) = p_t \frac{m+1}{2\pi} cos^m(\varphi) \tag{3}$$

where m is the Lambertian emission order which is given by

$$m=\frac{\ln(2)}{\ln(cos\varphi_{1/2})} \tag{4}$$

where $\varphi_{1/2}$ is the half power angle of LED.

The channel impulse response of a LOS link due to the transmitted signal from the light source to the photodetector is

$$\mathbf{H}_{\mathbf{LOS}}(0)= \begin{pmatrix} \frac{A_r(ml+1)}{2\pi(d1d2)^2} cos^m(\varphi)\cos(\varphi) g(\varphi).0\le\varphi\le\varphi fov \\ 0. \quad \varphi\ge\varphi fov \end{pmatrix} \tag{5}$$

$$g(\varphi) = \begin{pmatrix} \frac{n^2}{sin^2(\varphi fov)} & 0\le\varphi\le\varphi fov \\ 0 & \varphi>\varphi fov \end{pmatrix} \tag{6}$$

where A_r is the active area at the receiver, φfov is the FOV of the receiver and n is the refractive index.

While, the channel impulse response of the first reflection signal is given by,

$$\mathbf{H}_{\mathbf{1stref}}(0)= \begin{pmatrix} \frac{A_r\Delta AP(ml+1)}{2\pi(d1d2)^2} cos^m(\varphi)\cos(\varphi) g(\varphi).0\le\varphi\le\varphi fov \\ 0. \quad \varphi\ge\varphi fov \end{pmatrix} \tag{7}$$

where Δ_A is the small grids area on the walls surface, ceiling surface and ground, the term P represents the wall's reflection coefficients. Similarly, the channel impulse response of the second reflected signal is given by

$$\mathbf{H}_{\mathbf{2nref}}(0)= \begin{pmatrix} \frac{A_r(\Delta A)^2P^2(ml+1)}{2\pi(d1d2d3d4)^2} cos^m(\varphi)\cos(\varphi) g(\varphi)\cos(\delta)\cos(\Upsilon).0\le\varphi\le\varphi fov \\ 0. \quad \varphi\ge\varphi fov \end{pmatrix} \tag{8}$$

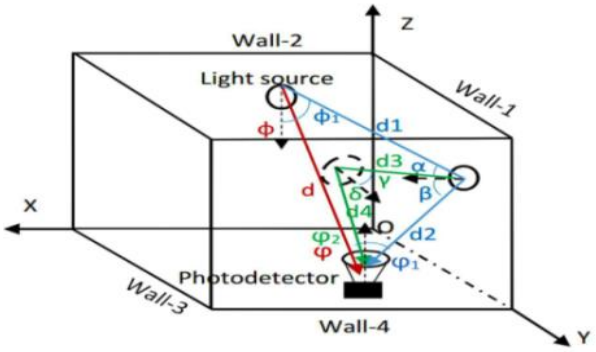

Fig. 2. Typical room model

3-2-VLC-MIMO Model

The case study approach is chosen to investigate the mitigation of multipath reflected signals coming from walls and ceil owing uniform power distribution for entire room environment. In the block diagram of Fig. 3, consider a system of a 4×4 MIMO is applied to transmitter as well as the receiver.

Four symbols s_1,s_2,s_3 and s_4 are transmitted in four consecutive time slots T_{S1}, T_{S2},T_{S3} and T_{S4} using four different arrays of sources at the transmitter and four different detectors at the receiver.

The emitted light signal via an LED is

$$\boldsymbol{x(t)} = 2p_t \sum_{i=0}^{l-1} d_l \tag{9}$$

Where p_t is the transmitted power via an LED and d_l is data symbols. Therefore, at high frequency, the driving circuit modulates the driver current to switch LEDs as ON and OFF. Now, consider a 4×4 matrix for symbols s_1, s_2, s_3 and s_4 are arranged as

$$\begin{bmatrix} s_1 & s_2 & s_3 & s_4 \\ s_2 & -s_1^* & s_4^* & -s_3^* \\ s_3 & -s_4 & -s_1 & s_2 \\ s_4 & s_3^* & -s_2 & -s_1^* \end{bmatrix} \tag{10}$$

The transmitted light signals over four time slots from four arrays of white LEDs are specified in Table 1.

Table 1: light signals transmitted over four time slots of four arrays.

Time	s_1 from $LEDs_1$	s_2 from $LEDs_2$	from s_3 $LEDs_3$	s_4 from $LEDs_4$
$[0.T_s]$	s_1	s_2	s_3	s_4
$[T_s.2T_s]$	s_2	$-s_1^*$	s_4^*	$-s_3^*$
$[2T_s.3T_s]$	s_3	$-s_4$	$-s_1$	s_2
$[3T_s.4T_s]$	s_4	s_3^*	$-s_2$	$-s_1^*$

Once the signals are transmitted via wireless channel with channel gain **H**, the channel matrix between the LEDs and the PDs has been described by;

$$\mathbf{H}=\begin{bmatrix} h_{1.1} & \cdots & h_{1.i} \\ \vdots & \ddots & \vdots \\ h_{j.1} & \cdots & h_{j.i} \end{bmatrix} \quad (11)$$

where $h_{j.i}$ is a channel coefficient between j[th] PD and i[th] LED and the dimension of the MIMO channel matrix ⍰ is ⍰⍰ ×⍰⍰.

The received signals on the Photodetector 1 (PD1) at the time periods $[0.T_s]$, $[T_s.2T_s]$, $[2T_s.3T_s]$ and $[3T_s.4T_s]$ respectively assume the forms,

$$y_{1[0.T_s]}=2P_t^2R[h_{11}s_1x+h_{21}s_2x+h_{31}s_3x+h_{41}s_4x+n_1]$$
$$y_{1[T_s.2T_s]}=2P_t^2R[h_{11}s_2x-h_{21}s_1^*x+h_{31}s_4^*x-h_{41}s_3^*x+n_2]$$
$$y_{1[2T_s.3T_s]}=2P_t^2R[h_{11}s_3x-h_{21}s_4x-h_{31}s_1x+h_{41}s_2x+n_3]$$
$$y_{1[3T_s.4T_s]}=2P_t^2R[h_{11}s_4x+h_{21}s_3^*x-h_{31}s_2x-h_{41}s_1^*x+n_4] \quad (12)$$

Similarly, The received signals on the (PD2) at the time periods $[0.T_s]$, $[T_s.2T_s]$, $[2T_s.3T_s]$ and $[3T_s.4T_s]$ respectively assume the forms,

$$y_{1[0.T_s]}=2P_t^2R[h_{12}s_1x+h_{22}s_2x+h_{32}s_3x+h_{42}s_4x+n_1]$$
$$y_{1[T_s.2T_s]}=2P_t^2R[h_{12}s_2x-h_{22}s_1^*x+h_{32}s_4^*x-h_{42}s_3^*x+n_2]$$
$$y_{1[2T_s.3T_s]}=2P_t^2R[h_{12}s_3x-h_{22}s_4x-h_{32}s_1x+h_{42}s_2x+n_3]$$
$$y_{1[3T_s.4T_s]}=2P_t^2R[h_{12}s_4x+h_{22}s_3^*x-h_{32}s_2x-h_{42}s_1^*x+n_4] \quad (13)$$

The received signals on the (PD3) at the time periods $[0.T_s]$, $[T_s.2T_s]$, $[2T_s.3T_s]$ and $[3T_s.4T_s]$ respectively assume the forms,

$$y_{1[0.T_s]}=2P_t^2R[h_{13}s_1x+h_{23}s_2x+h_{33}s_3x+h_{43}s_4x+n_1]$$
$$y_{1[2T_s.3T_s]}=2P_t^2R[h_{13}s_2x-h_{23}s_1^*x+h_{33}s_4^*x-h_{43}s_3^*x+n_2]$$
$$y_{1[2T_s.3T_s]}=2P_t^2R[h_{13}s_3x-h_{23}s_4x-h_{33}s_1x+h_{43}s_2x+n_3]$$
$$y_{1[3T_s.4T_s]}=2P_t^2R[h_{13}s_4x+h_{23}s_3^*x-h_{33}s_2x-h_{43}s_1^*x+n_4] \quad (14)$$

The received signals on the (PD4) at the time periods $[0.T_s]$, $[T_s.2T_s]$, $[2T_s.3T_s]$ and $[3T_s.4T_s]$ respectively assume the forms,

$$y_{1[0.T_s]}=2P_t^2R[h_{14}s_1x+h_{24}s_2x+h_{34}s_3x+h_{44}s_4x+n_1]$$
$$y_{1[2T_s.3T_s]}=2P_t^2R[h_{14}s_2x-h_{24}s_1^*x+h_{34}s_4^*x-h_{44}s_3^*x+n_2]$$
$$y_{1[2T_s.3T_s]}=2P_t^2R[h_{14}s_3x-h_{24}s_4x-h_{34}s_1x+h_{44}s_2x+n_3]$$
$$y_{1[3T_s.4T_s]}=2P_t^2R[h_{14}s_4x+h_{24}s_3^*x-h_{34}s_2x-h_{44}s_1^*x+n_4] \quad (15)$$

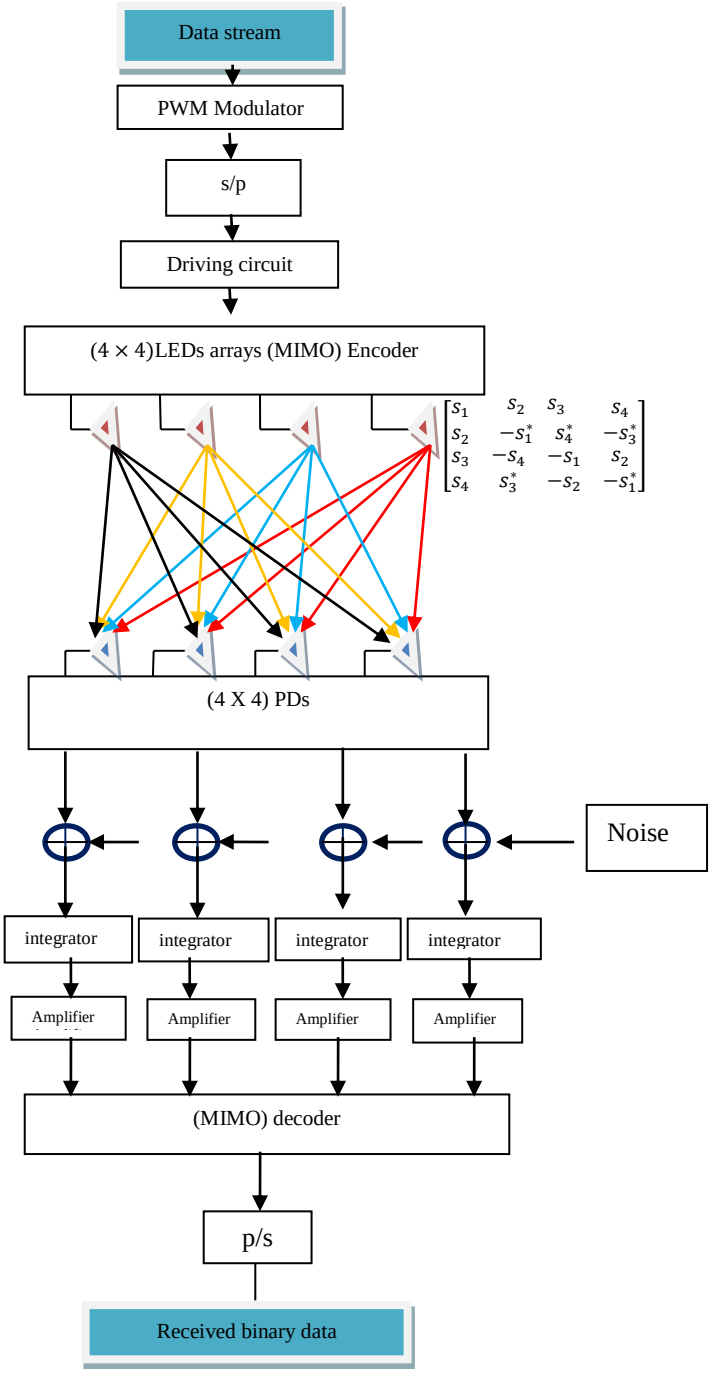

Fig. 3. Block diagram of VLC-MIMO system

where R is the photodetector responsivity and n is the additive white Gaussian noise with zero mean and variance σ_n^2.

3-3-VLC-MIMO System Design

Many researchers have utilized SISO systems in VLC. A major problem with single emitter (LED) and single receiver (photodetector) is the limitation in link range as well as the data throughput.

To increase the reliability of VLC system, multiple input (LEDs) and multiple output (photodetectors) has been proposed offering enhanced range link and data throughput. Fig. 4 shows typical indoor illumination installing MIMO system.

It consists of TX side and RX side. The TX side is setting up in the room ceiling of 3-m altitude above ground like a spot light of 16 white power LEDs.

RX modules could be in any part of the received light spot zone.

The proposed low level of TX-RX modules of 4x4 MIMO systems is shown in Fig. 5.

The system simply consists of 16 power LEDs of 1watt each grouped in 4 groups of 4 LEDs. Each group represents TX module. Each module takes data from TX Arduino (UNO) pins.

The TX Arduino works as data generator in form of 4 metrics as $S_1.S_1^*.S_2$ and S_2^*. The $S_1.S_1^*.S_2$ and S_2^* data elements represented by Arduino pins as pins 7, 8, 12 and pin 13 respectively. These data transmitted using white light by modulate LEDs intensities using PWM modulation.

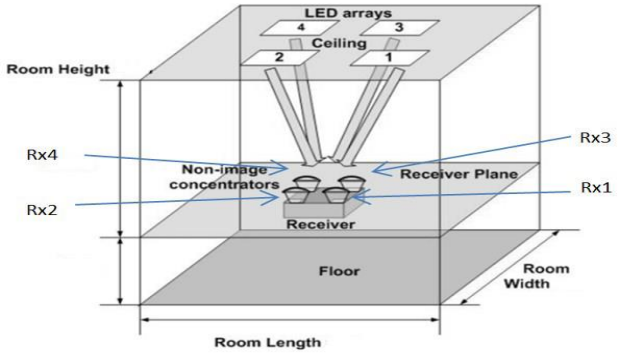

Fig. 4 typical indoor illumination

The RX side consists of 4 RX module, each module simply formed by a photo transistor as photo sensor, PWM demodulator (integrator) and amplifier.

The received signals y_1, y_2, y_3 and y_4 from RX modules is provided to Arduino analogue pins as A_o, A_1, A_2 and A_3 respectively. The Arduino follow the MIMO received algorithm to construct the transmitted data.

3-3-1-TX Module

Fig. 6 shows the TX module, simply consists of LM555 timer IC Q1 as driver and 4 power LEDs. The LEDs work as TX source and spot light.

LM555 IC works as PWM with frequency around 2.5 KHz, the output of the LM555 control the base current of Q1 power transistor which works always to give bias to the 4 LEDs using R1 resistor and the modulation signal is provided to pin 5 of the IC from pin13**.**

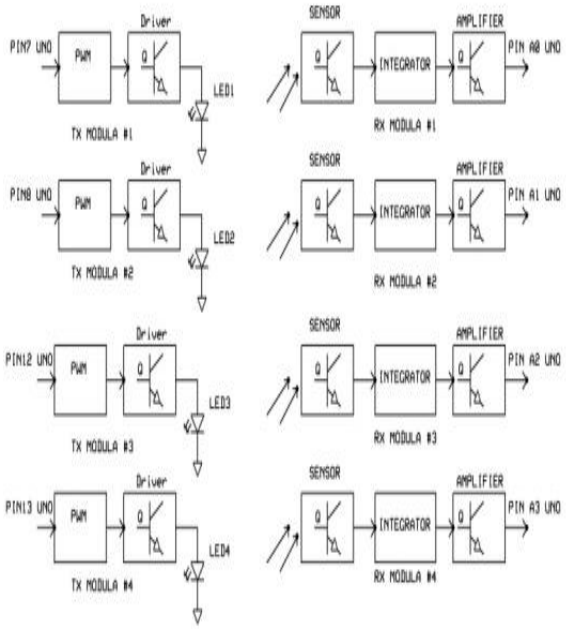

Fig. 5. The low level circuit of TX-RX modules of 4x4 MIMO systems

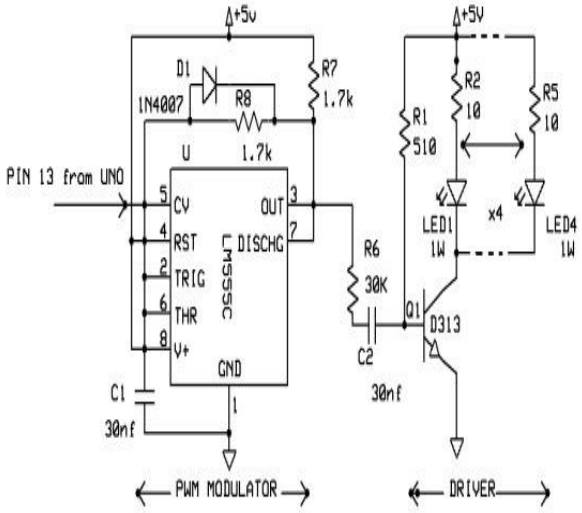

Fig. 6. The transmitter module

3-3-2-RX Module

Fig. 7 shows the RX module, simply constructed from photo sensor like 3DU33 photo transistor, 3 poles passive LPF and 2 stage amplifiers formed by Q2 and Q3.

As mentioned earlier, to get higher power densities the RX module must be near the center zone of the received spotted light as presented in Fig. 8, which shows the received test signal of 2.5KH$_Z$ received for maximum amplitude when the RX module is located near spotted received zone.

If the frequency of the signal is increased, the received signal will be suffered from distortion because of slow time response of the photo sensor. The output of the RX modules lunched to RX Arduino to construct the transmitted data. The proposed VLC circuits implemented MIMO system is set out in Fig. 9.

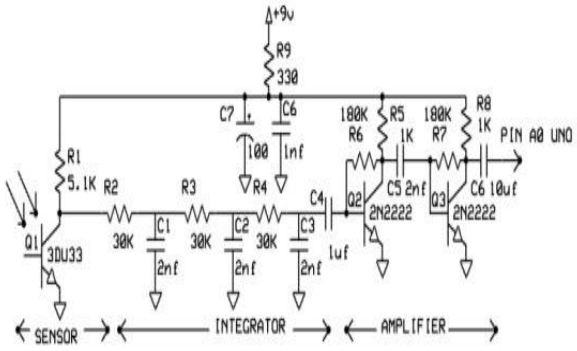

Fig. 7. The receiver module

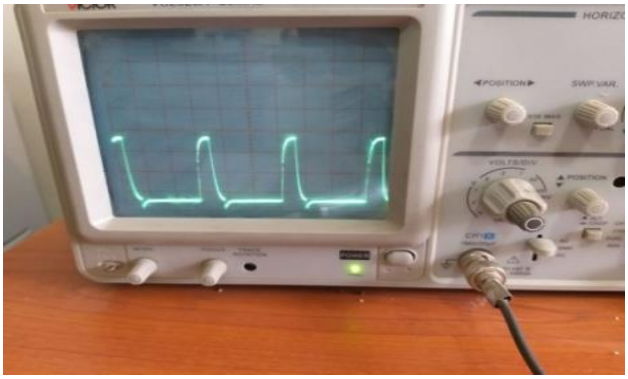

Fig. 8. The received test signal

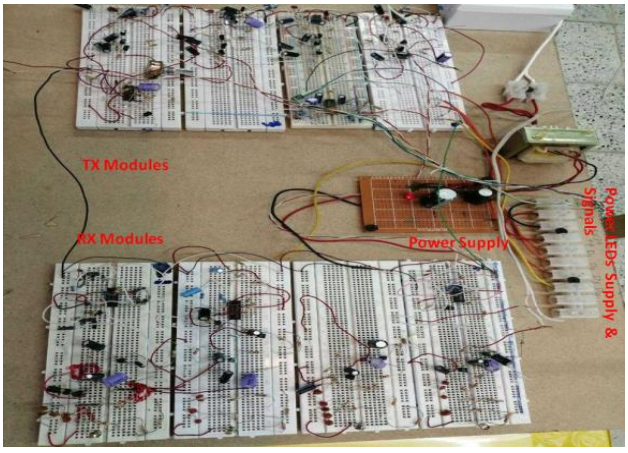

Fig. 9. The proposed VLC system circuits

4- Evaluations

In order to access VLC based MIMO channel, a power distribution of VLC based SISO channel under the specified specifications has been measured.

Table (2) illustrates some of the main parameters of the VLC link.

Table (2) system Parameter of the proposed VLC-MIMO link

Parameters	Value
size of room	3*3*5 m^3
reflection coefficient	0.7
transmitted power	20mW
field of view (FOV)	70^0
Number of LEDs per array	4×4 (16)
Responsivity	0.2

In the case of SISO system considering LOS propagation environment without reflection, the distribution of the optical power is shown in Fig. 10.

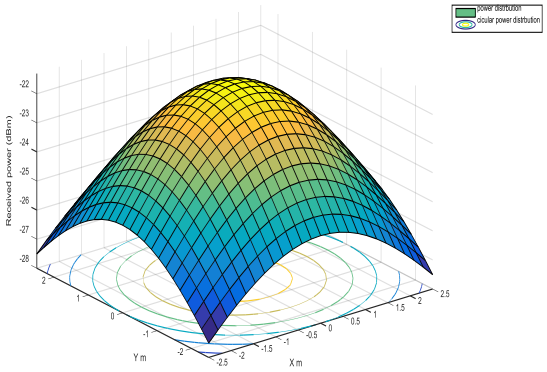

Fig. 10. The optical power distribution of VLC-SISO LOS without reflection.

It can be seen that the optical power is mostly uniform distributed at the center with maximum power at -23.5 dB and minimum at -27.5 dB. Other considering that LOS and NLOS propagation environment where in addition to direct light path, the reflected light from the walls are taken in consecration.

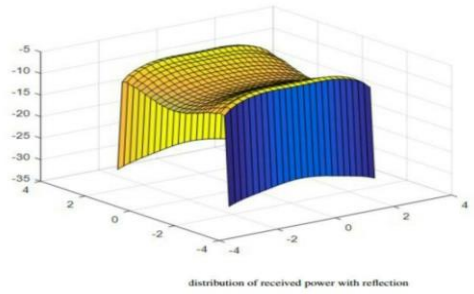

Fig. 11. The optical power distribution of VLC-SISO LOS with reflection.

It can be seen from Fig. 11 that the received optical power distributed non-uniformly due to reflections of light from walls.

As shown in Fig. 12. diverse the sources and detectors at transmitter and receiver respectively reported significantly more distributed for optical power in all directions of the room leading to increasing capacity.

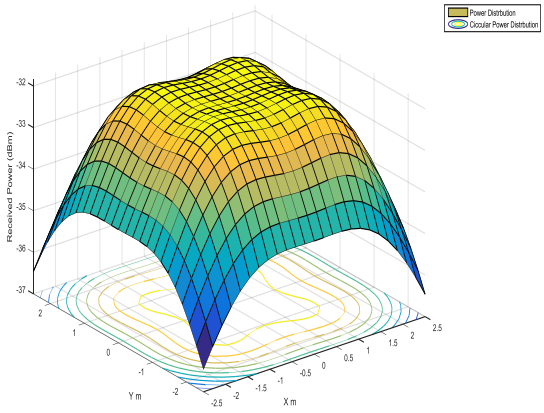

Fig. 12. The optical power distribution of VLC-MIMO reflection

Fig. 13 compares the BER performance against SINR for SISO and MIMO communication systems of LOS propagation mode using OOK modulation scheme. It can be seen that the performance of 4×4 MIMO implemented VLC system has a superior performance as compared to SISO implemented VLC system.

This is due to the ability of MIMO. In Fig. 14, the comparison between the BER performance have been done between SISO and 4×4 MIMO but for NLOS propagation mode for the parameters shown in table (3). 4×4 MIMO implemented VLC system perform better than SISO system. This is due to the ability of MIMO to combat the multipath fading and improve the data rate.

Comparison of the findings with those of other studies confirms that the 4×4 MIMO reported significantly decreased BER performance for NLOS as compared to LOS scenarios.

This is due to decreasing in the power received when the detector in not within the LOS with LEDs. These results reflect those of [14] who also found that the performance of 4×4 MIMO is better than single LED and single PD. These results are consistent with data obtained in [17] that achieves 18 dB in the case of LOS and 22 dB in the case of NLOS at a BER of 10^{-5}.

However, if VLC implemented, MIMO outperforms the SISO at the expensive of more complexity, but in our work, we implemented the VLC-MIMO system with less complexity as explained in section 3.3 as compared to the above study.

The present study was designed to reduce the complexity of the electronic circuit as compared to the circuits designed in the literature. The present implementation is significant in at least two major respects: firstly, the electronic circuit implemented using inexpensive electronic components and available in the markets.

Secondly, the design of the electronic circuit achieved in a simple modality and uncomplicated mathematical

relations. So, to avoid the use of system integration in the circuit design which is limited, we used the Arduino microcontroller which is open source electronic platform, reprogrammable and inexpensive.
However, our design may be considering a real VLC-MIMO communication system.

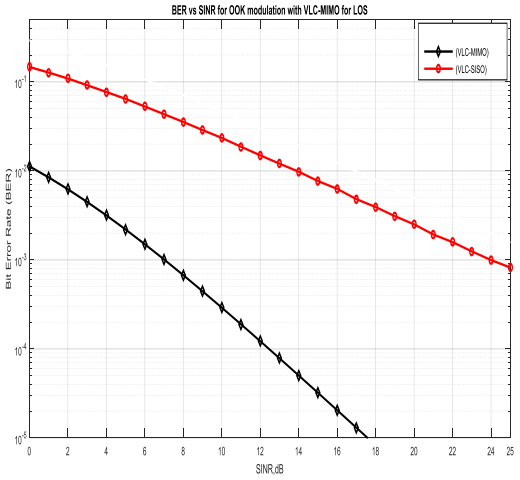

Fig. 13. BER vs. SINR for LOS propagation mode

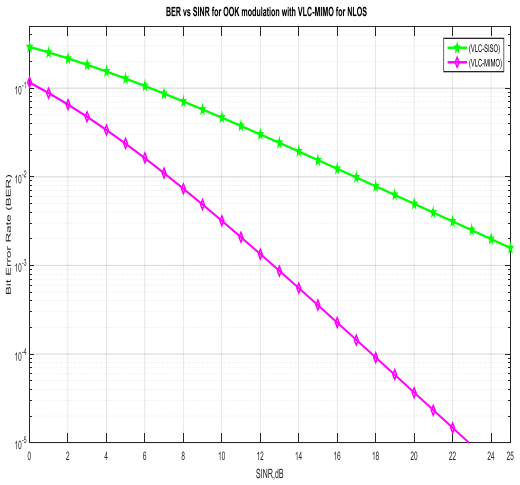

Fig. 14. BER vs. SINR for NLOS propagation mode

5- Conclusions and Future Works

The present work was designed to provide high data rate for VLC by exploiting the benefits of using multiple sources at emitter and multiple detectors at receiver.
The most obvious finding to emerge from this study is that the power is distributed uniformly for entire room using array of 4 × 4 MIMO as compared to SISO systems due to compact the multipath effect and reduces interference of unwanted signals reflected from walls and ceil.
The proposed system is designed practically using inexpensive electronic circuits for both emitter and destination.
In general, therefore, it seems that increasing the number of LEDs as well as PDs for the VLC systems may improve the power distribution and leading to increase the data rate.
The question raised by this study is how the BER can be improved with increasing the number of LEDs and PDs? The study should be repeated using suitable error correction codes such as LDPC code and LT code.

Acknowledgment

This work is partially supported by the Information and Communication Engineering Department at AlKhwarizmi College of Engineering-University of Baghdad.

References

[1] D. Karunatilaka, F. Zafar, V. Kalavally and R. Parthiban, "LED Based Indoor Visible Light Communications: State of the Art", IEEE Communications Surveys & Tutorials, vol. 17, no. 3, pp. 1649-1678, 2015. Available: 10.1109/comst.2015.2417576.

[2] A. Jovicic, J. Li and T. Richardson, "Visible light communication: opportunities, challenges and the path to market", IEEE Communications Magazine, vol. 51, no. 12, pp. 26-32, 2013. Available: 10.1109/mcom.2013.6685754.

[3] M. Chowdhury, M. Hossan, A. Islam and Y. Jang, "A Comparative Survey of Optical Wireless Technologies: Architectures and Applications", IEEE Access, vol. 6, pp. 9819-9840, 2018. Available: 10.1109/access.2018.2792419.

[4] S. Bawazir, P. Sofotasios, S. Muhaidat, Y. Al-Hammadi and G. Karagiannidis, "Multiple Access for Visible Light Communications: Research Challenges and Future Trends", IEEE Access, vol. 6, pp. 26167-26174, 2018. Available: 10.1109/access.2018.2832088.

[5] T. Komine and M. Nakagawa, "Fundamental analysis for visible-light communication system using LED lights", IEEE Transactions on Consumer Electronics, vol. 50, no. 1, pp. 100-107, 2004. Available: 10.1109/tce.2004.1277847.

[6] T. Fath and H. Haas, "Performance Comparison of MIMO Techniques for Optical Wireless Communications in Indoor Environments", IEEE Transactions on Communications, vol. 61, no. 2, pp. 733-742, 2013. Available: 10.1109/tcomm.2012.120512.110578.

[7] Y. Zhang, H. Yu and J. Zhang, "Block Precoding for Peak-Limited MISO Broadcast VLC: Constellation-Optimal Structure and Addition-Unique Designs", IEEE Journal on Selected Areas in Communications, vol. 36, no. 1, pp. 78-90, 2018. Available: 10.1109/jsac.2017.2774480.

[8] M. Uysal, C. Capsoni, Z. Ghassemlooy, A. Boucouvalas and E. Udvary, Optical Wireless Communications. Switzerland: springer, 2016, pp. 107-122.

[9] A. Agarwal and S. Mohammed, "Achievable Rate Region of the Zero-Forcing Precoder in a 2×2 MU-MISO Broadcast VLC Channel With Per-LED Peak Power

Constraint and Dimming Control", Journal of Lightwave Technology, vol. 35, no. 19, pp. 4168-4194, 2017. Available: 10.1109/jlt.2017.2719920.

[10] Y. Zhang, "Intrinsic Robustness of MISO Visible Light Communications: Partial CSIT Can be as Useful as Perfect One", IEEE Transactions on Communications, vol. 67, no. 2, pp. 1297-1312, 2019. Available: 10.1109/tcomm.2018.2874988.

[11] C. Chen, W. Zhong and D. Wu, "On the Coverage of Multiple-Input Multiple-Output Visible Light Communications [Invited]", Journal of Optical Communications and Networking, vol. 9, no. 9, p. D31, 2017. Available: 10.1364/jocn.9.000d31.

[12] S. Nandkeolyar, R. Mohanty and V. Dash, "Management of Time-Flexible Demand to Provide Power System Frequency Response", in IEEE International Conference on Technologies for Smart-City Energy Security and Power, Bhubaneswar, India, 2018, pp. 28-30.

[13] A. Nuwanpriya, S. Ho and C. Chen, "Indoor MIMO Visible Light Communications: Novel Angle Diversity Receivers for Mobile Users", IEEE Journal on Selected Areas in Communications, vol. 33, no. 9, pp. 1780-1792, 2015. Available: 10.1109/jsac.2015.2432514.

[14] A. Alwarafy, M. Alresheedi, A. Abas and A. Alsanie, "Performance Evaluation of Space Time Coding Techniques for Indoor Visible Light Communication Systems", in 2018 International Conference on Optical Network Design and Modeling (ONDM), Dublin, Ireland, 2018, pp. 88-93.

[15] Z. Wang, S. Han and N. Chi, "Performance enhancement based on machine learning scheme for space multiplexing 2×2 MIMO VLC system employing joint IQ independent component analysis", Optics Communications, vol. 458, p. 124733, 2019. Available: 10.1016/j.optcom.2019.124733.

[16] J. Ye, G. Pan, Y. Xie, Q. Feng, Q. Ni, and Z. Ding, "On Indoor Visible Light Communication Systems with Spatially Random Receiver", Optics Communications, Vol. 431,2019 , pp. 29-38.

[17] K. K. Wong, R. D. Murch, and K. Ben Letaief, "Performance enhancement of multiuser MIMO wireless communication systems," IEEE Trans. Commun., vol. 50, no. 12, pp. 1960–1970, 2002, doi: 10.1109/TCOMM.2002.806503.

[18] P. Fahamuel, J. Thompson, and H. Haas, "Improved indoor VLC MIMO channel capacity using mobile receiver with angular diversity detectors"In 2014 IEEE Global Communications Conference. IEEE, Austin, TX, USA,8-12 Dec.2014, p.2060-2065.

Lwaa Faisal Abdulameer is a PhD for Communication Engineering at Information and Communication Dept. - University of Baghdad, Baghdad, Iraq. He graduated in 2004 with an M.Sc degree from University of Technology and acquired his post graduate degree in Communication Engineering in 2004. He was appointed as a Lecturer in the Information and Communication Engineering Department of the Al-Khwarizmi College of Engineering-University of Baghdad in 2006. He acquired a PhD degree in Communication Engineering in 2014 from the National Institute of Technology, India. His areas of research are in the area of Error Control codes, Wireless Communications and Free Space Optics.

Ahmed Kadhim Hassan is an Msc. for Electronic and Communication Engineering at Information and Communication Engineering Dept. - University of Baghdad, Baghdad, Iraq. He is Msc. Holder since 2012 in Electronic and communication Engineering Dept College of Engineering University of Baghdad. He graduated in 2004 with a B.Sc. degree from Department of Information Engineering Al-Khwarizmi College of Engineering University of Baghdad. He was appointed as an Engineer in the Labs of Information and Communication Engineering Department of the Al-Khwarizmi College of Engineering-University of Baghdad since 2004. His areas of research are in the area of Antenna and Propagation, Radio Electronics.

Aliaa Tariq Obeed, obtained a B.Sc in Information and communication Engineering at Information and Communication Dept. - University of Baghdad, Baghdad, Iraq. She is graduated in 2019. Her field of research in wireless optical communication using MIMO technology.

Aya Naeem Dahir obtained a B.Sc. in Information and communication Engineering at Information and Communication Dept. - University of Baghdad, Baghdad, Iraq. She is graduated in 2019. Her area of research are in the area of Wireless Communications and Visible Light Communication Based on MIMO channel.

Providing a Network for Measuring the Dynamics Volatility Connectedness of Oil and Financial Markets

Nasser Gholami*
Faculty of Economics, Allameh Tabataba'i University, Iran
Gholami.nasser@gmail.com
Teymor Mohammadi
Faculty of Economics, Allameh Tabataba'i University, Iran
atmahamadi@gmail.com
Hamid Amadeh
Faculty of Economics, Allameh Tabataba'i University, Iran
amadeh@gmail.com
Morteza Khorsandi
Faculty of Economics, Allameh Tabataba'i University, Iran
Mkhorsandi57@yahoo.com

Received: 04/Jun/2020 Revised: 24/Aug/2020 Accepted: 08/Nov/2020

Abstract

Various studies have shown that markets are not separated and that fluctuations in different markets affect each other. Therefore, awareness of connectedness is needed for investors and policymakers for making appropriate decisions. The aim of this paper is to measure the dynamics connectedness of selected stock markets in the Middle East, oil markets, gold, the dollar index, and euro-dollar and pound-dollar exchange rates during the period February 2007 to August 2019 in networks with different weekly horizons. In this paper, we intend to evaluate the pairwise impact of crude oil and the Middle East stock markets, in particular on the Tehran Stock Exchange, and to analyze this variance using different time horizons. The results show that in all time horizons the variance of forecast error in most markets is due to the shocks themselves. The Saudi Arabian Stock Exchange has the most impact on other Middle Eastern stocks. The dynamics connectedness of the oil markets is remarkable, however, as the time horizon increases, dynamic connectedness between the two markets decreases and they are mostly affected by other markets, especially the Middle East stock exchanges except for Iran. Moreover, Iran stock market is an isolated market. About the gold market, there is a significant connectedness with the pound-dollar exchange rate and gold market; however, the dynamics connectedness of this market with other markets are not significant. Therefore, this market and Iran stock exchange can be used as a tool to hedge risk for investors.

Keywords: Oil Markets; System Design; Volatility; Variance Decomposition Approach; Dynamics Connectedness; Network.

1- Introduction

The expansion of globalization has made the financial markets of different countries more influential than ever before. However, the increasing dynamics connectedness between its financial markets can be seen as a vulnerable factor in hitting any one market because volatility in one market can spread to other financial markets as well. For example, the 2008 financial crisis that began in the US mortgage market spread to most of the world's financial markets, causing a deep recession in many countries. Many studies have cited oil price fluctuations as the external factor causing shocks in the economies of countries, including Hamilton [1], Kilian [2], and Bagheri and Ebrahimi [3]. Oil price shocks affect macroeconomic variables such as stock market, inflation, growth rate, business cycle and dollar equity. These shocks can have a significant impact on many macroeconomic variables such as stock market, inflation, growth rate and business cycle. Given the significant fluctuations in oil prices in recent years and the important role oil plays in the economies of many countries, many researchers and policy makers are looking for evidence that these fluctuations are affecting other financial markets. Since Iran is one of the greatest oil exporters, it is important to measure the dynamics connectedness of the oil market and the Iranian stock market. In addition, many investors tend to trade in markets having less spillover risks of other markets. The purpose of this article is to investigate that how do markets connected to each other in different time horizons? Also this study aimed to present networks in different time horizons to investigate the dynamic connectedness of oil, gold, foreign exchange and stock markets using the variance decomposition method introduced by Diebold & Yilmaz [4] in 2014. The present study is composed in 5 sections. After the introduction in the first

* Corresponding Author

section, we present the background of the research. Then, in the third part, research methodology for measuring the relationships between markets is explained. Section 4 shows the results of applying the research methodology and section 5 provides the conclusions.

2- Review of The Literature

Many researchers have focused on various models in order to investigate the connectedness of markets and companies [5,6,7]. In 2014, Diebold and Yilmaz presented a structure that was based on the analysis of variance of an autoregressive model to accurately measure the dynamics of connectedness among the 13 insurance companies listed on the US Stock Exchange. Then, using this approach in order to present a network based on graphs that show the connectedness of different companies. Jahangiri and Hekmati [8] utilize the variance decomposition and markov switching regime models during April 2002 to September 2014 to examine the dynamics connectedness between Tehran Stock Exchange, currencies, oil markets, gold, US stock market and the European stock markets. The gold and oil markets act as intermediary markets for transmitting shocks between the world's major stock markets and asset markets in Iran respectively. Meghyereh et al. [9] using implied volatility indices and variance decomposition approach, examined the dynamics of connectedness of oil to US securities, euro-dollar exchange rates, precious metals including gold and agricultural commodities. The results showed that there was a significant risk of transmits from oil to stocks and precious metals, but there was a little risk of transmitting to agricultural commodities. The pairwise connectedness of stock was 24.4 percent, while that for wheat, corn and soybeans were 1.6, 1.0 and 2.0 percent. Moreover, the spillover risks from all these markets to oil was low. Mamipour and Feli [10] examine the spillover effects of oil price fluctuations on the returns of selected industries on the Tehran Stock Exchange by using the variance decomposition approach during November 2008 to April 2016. Also, the oil spillover effects of periods of high and low volatility on the stock market were analyzed by using the Markov Switching Model. The results show that the effects of volatility spillover from the oil market to the stock market in the low volatility regime were lower in most industries than the high volatility regime, and spillover fluctuations in the high volatility regime occurred more widely. Singh et al. [11], using the variance decomposition model, examined the dynamic linkage and the path between the dimensions of a given crude oil disorder and the exchange rate of the 9 major currency pairs for a sample period from May 2007 to December 2016. They found that the crude oil market had a significant impact on the currency market. In addition, the bilateral currency pair dynamics between the pair indicated that the euro-dollar was more sensitive to oil price fluctuations than any other major currency pair and was a major currency that transmits specific shocks to other currencies. Husain et al. [12] analyzed the dynamics connectedness of crude oil prices, stock indices, and metal prices for the US economy from 1990 to 2017 using the Diebold & Yilmaz model. Research has shown that palladium, gold, platinum and silver transmitter of the shocks while crude oil, titanium and steel are receiver of the shocks. Alyahyaee et al. [13] analyzed spillover risks between commodity futures (energy and precious metals) and GCC stock markets. By using dynamic correlation models and variance decomposition models, they found significant spillover risks between GCC commodities and stock markets, especially during the global financial crisis. Precious metals (excluding silver) and WTI are net risk transmitters to GCC markets. Moreover, portfolio management analysis shows that a combination of GCC commodities and stocks provides diversification opportunities for different periods of crisis. Fasanya& Akinbowale [14] investigated the dynamics of volatility connectedness between the crude oil market and agricultural commodities in Nigeria using the variance decomposition approach over the period 1997 to 2017. The researchers showed that there were reciprocal relationships between these markets.

Yoon et al. [15] also used the variance decomposition approach to measure the dynamics connectedness of various markets such as crude oil, stocks, gold, currencies and bonds from December 1999 to June 2016. The results showed that the dynamics of the connectedness of markets reached their highest level in the financial crisis of 2008. Furthermore, gold can be chosen as a viable option for hedging investment portfolio risk due to poor connectedness with other markets. Finally, they showed that the US stock market is the most important transmitter of shocks to other markets.

3- Methodology

In this study, we measure the dynamics of volatility connectedness between Iran, Saudi Arabia, Turkey, United Arab Emirates stock markets, crude oil, foreign exchanges and gold market simultaneously across different time horizons. Networks are offered According to the connectedness, and time horizons.

In order to obtain the weekly volatility of markets, the proposed model of Parkinson [16] is used. Therefore, in general, the variables under consideration are calculated as Equation (1), where p_{it}^{max} is the highest weekly price and p_{it}^{min} the lowest weekly price.

$$\sigma_{it}{}^{2} = 0.361[\ln(p_{it}^{max}) - \ln(p_{it}^{min})]^{2} \quad (1)$$

3-1- Variance Decomposition Approach

In 2014, Diebold & Yilmaz introduced the variance decomposition approach with the aim of providing a sized-based network of dynamics connectedness among markets.

They used the "generalized identification" framework of Koop, Pesaran, and Potter [17] and Pesaran and Shin [18], which produces variance decompositions invariant to ordering. To introduce this approach, we first considered an N variable vector that is modeled as a p-order vector regression system:

$$y_t = \sum_{i=1}^{p} \prod_i \; y_{t-1} + \varepsilon_t \qquad \varepsilon_t \sim i.i.d(0, \sum) \tag{2}$$

Here, $\prod_i$ is the $N \times N$ coefficients matrix, ε_t is the vector of disturbed components with uniform and independent distribution and $\sum$ is the variance-covariance matrix.

Equation 3 shows the moving average representation of the p-order vector of the above auto-regressive system:

$$y_t = \sum_{i=1}^{\infty} \Theta_i \varepsilon_t \tag{3}$$

Θ_i represents the moving average coefficient of $N \times N$ identity matrix.

This approach is based on the H-step-ahead forecast-error variance decomposition for each N variable contained in the N variable VAR. In this approach, it is possible to investigate part of the variance of forecast error variable i which can be attributed to the shocks caused by variable j and compute the total dynamics connectedness index by summing these effects.

$$d_{ij}^{g}(H) = \frac{\sigma_{jj}^{-1} \sum_{h=0}^{H-1} (e' \prod_h \sum e_j)^2}{\sum_{h=0}^{H-1} (e' \prod_h \sum \prod_h' e_i)} \tag{4}$$

In the above equation, Σ is the variance matrix of the vector of errors, σ_{jj} denotes the standard deviation of the error term in the jth Equation. e_i is an N × 1 vector with 1 on the ith element.

In the generalized variance decomposition framework, the shocks entered into each variable are not orthogonal necessarily so the sum of each line of variance decomposition matrix will not equal one (i.e $\sum_{j=1}^{N} d_{ij}^{g}(H) \neq 1$)

Therefore, to use the information contained in the variance decomposition matrix to calculate the dynamics connectedness index, each component of this matrix can be normalized by dividing it by the sum of rows such that:

$$= \frac{d_{ij}^{g}(H)}{\sum_{j=1}^{N} d_{ij}^{g}(H)} \; ; \quad \sum_{j=1}^{N} \tilde{d}_{ij}^{g}(H) = 1 \; ; \quad \sum_{i,j=1}^{N} \tilde{d}_{ij}^{g}(H) = N \tag{5}$$

Now $\tilde{d}_{ij}^{g}(H)$ provides a measure of pairwise directional connectedness from j to i at horizon H. As a matter of notation, we change $\tilde{d}_{ij}^{g}(H)$ to $Ci \leftarrow j\,(H)$, which represents the transmission 'To' *i* from *j*.

Using the normalized components of the variance decomposition matrix, we can calculate the total dynamics connectedness index (C). This index calculates the reciprocal spillovers by measuring the spillover of the shocks entered by all N variables into the total variance of forecast error. The total dynamics connectedness index will be as follows:

$$C_{ij}^{g}(H) = \frac{\sum_{\substack{i,j=1 \\ i \neq j}}^{N} d_{ij}^{g}(H)}{\sum_{i,j=1}^{N} \tilde{d}_{ij}^{g}(H)} \times 100 \tag{6}$$

$$= \frac{\sum_{\substack{i,j=1 \\ i \neq j}}^{N} \tilde{d}_{ij}^{g}(H)}{N} \times 100$$

In dynamics connectedness analysis, it would be appropriate to examine the direct effects of (or towards) a particular market. Utilizing the generalized variance decomposition framework allows to measure the directional dynamics connectedness (DC) indices of the spillover effects received in market i from all other j markets:

$$DS_{i \rightarrow j}^{g}(H) = \frac{\sum_{\substack{i=1 \\ i \neq j}}^{N} \tilde{d}_{ij}^{g}(H)}{N} \times 100 \tag{7}$$

An appropriate index that measures the effects of spillover transmitted from market i to all other markets is defined as follows:

$$DS_{i \rightarrow j}^{g}(H) = \frac{\sum_{\substack{i=1 \\ i \neq j}}^{N} \tilde{d}_{ij}^{g}(H)}{N} \times 100 \tag{8}$$

Using the preceding two equations, we can directly calculate the net NC (Net connectedness) index for market i:

$$NC_i^{g}(H) = DS_{i \rightarrow j}^{g}(H) - DS_{i \leftarrow j}^{g}(H) \tag{9}$$

In order to determine whether or not one market is generally more influential than the other markets, we need to obtain the net dynamics connectedness index obtained by equation 9. Positive values of net dynamics connectedness index indicate that spillover effects from i market to other markets and thus have a greater impact on other markets, while negative values indicate that market i receives spillover effects and is more affected by fluctuations in other markets. The results are prepared as a dynamics connectedness table. This table contains N to N components, each of which is a d_{ij} variance decomposition.

Diebold & Yilmaz described this table as a network *adjacency matrix*. The adjacency matrix represents the edges between graph nodes. In other words, the adjacency matrix indicates whether the pairs are adjacent to each other. In addition, in this table *from* and *to* are parallel to *in-degree* and *out-degree* and *total connectedness* is *mean degree*. However, the network is complicated for some reason than the classical network definition. First, the connections are balanced and directional. In addition, these weights can change over time.

4- Results and Discussion

4-1- Data and Summary Statistics

In this research we use weekly data of different markets and generally data was divided into four general sections as follows:

A) Oil markets, including the two top global markets of West Texas Intermediate and Brent.

B) Tehran Stock Exchange Index, Top 100 Istanbul Stock Exchange Companies index, Saudi Stock Exchange Index (Tadawal) and General ADX Index of Abu Dhabi UAE.

C) Currency markets including Euro/ Dollar, Pound / Dollar and Dollar index.

D) Gold market.

This study attempts to analyze the dynamics connectedness of different markets during the period February 2007 to August 2019 in the framework of a generalized vector auto regression model and variance decomposition method. Information from this study was collected from databases including Tehran Stock Exchange, Thomson Reuters and Stooq. The descriptive statistics of the volatility series from February 2007 to August 2019 are shown in Table 1. The reason for choosing this time period is to cover the global financial crisis of 2008, the European financial crisis of 2012 and the sharp fluctuations of oil prices during 2012-2016.

Time series are one of the most important statistical data used in empirical analysis. The first step in estimating time series is to check the stationary of the variables. On the other hand, if the time series variables are not stationary, a problem called spurious regression may occur. Given the Dickey-Fuller test at the 1% level, all variables rejected the null hypothesis that unit root exists, so all variables are stationary at this level.

According to the Jarque-Bera test, the normality of distribution of all variables is rejected at the 1% level. Figure (1) shows the trend of series during the study period. The amount of skewness in each time series indicates the tail is on the right. Given the degree of Kurtosis in each time series, they can be assumed to be fat tail.

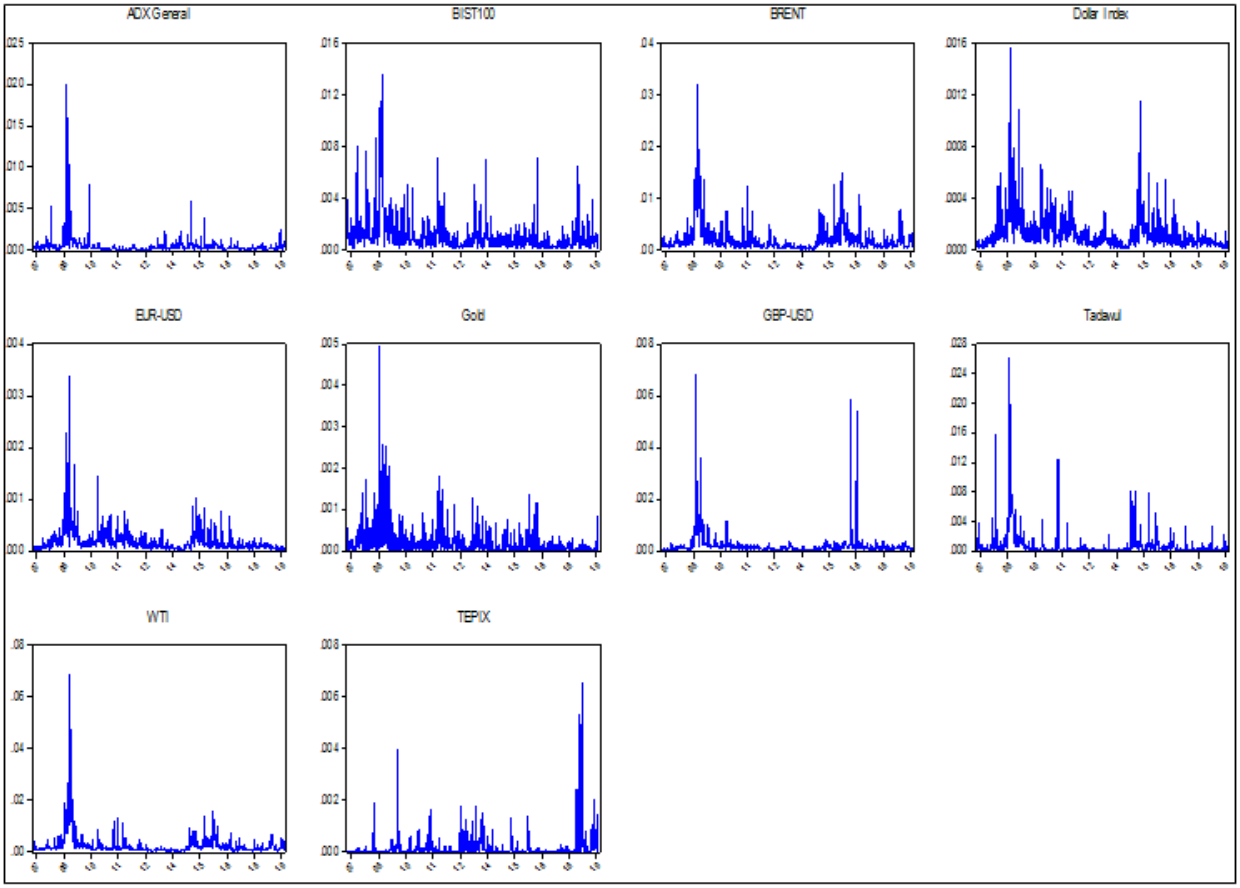

Fig 1. Trend various markets during the period of February 2007 through August 2019

Table 1. Statistical Characteristics of Variable

	Mean	Median	Maximum	Minimum	Skewness	Kurtosis	Jargu bera	Dickey Fuller test
BIST100	0.001126	0.000671	0.013575	1.11E-05	3.94	23.29	12905	-6.5
ADX_GENERAL	0.000494	0.000201	0.020115	5.71E-06	9.413	113.3	341109	-6.09
BRENT	0.001991	0.001121	0.032014	6.73E-05	4.285	31.39	23943	-4.24
GBP_USD	0.000205	0.000113	0.006834	7.98E-06	9.587	111.5	330669	-5.96
EUR_USD	0.000189	0.000117	0.003365	9.53E-06	5.850	56.39	81292	-4.43
DOLLAR_INDEX	0.00013	8.38E-05	0.001567	6.16E-06	3.934	26.86	17181	-4.63
GOLD	0.000216	0.000084	0.004937	1.16E-08	5.10	46.28	53819	-4.99
TADAWUL	0.000776	0.000257	0.026237	0	7.279	77.45	156601	-5.72
TEPIX	0.000156	1.46E-05	0.006539	0	7.8	82.17	177301	-5.75
WTI	0.002535	0.00128	0.068268	0.000145	7.76807	93.23	228095	-4.22

4-2- Estimating Dynamics Connectedness

In this section, we designed a system to measure the dynamics connectedness index and calculate it using the method proposed by Diebold and Yilmaz in three different time horizons. We consider the dynamics connectedness of different markets in the time horizons of 1 week, 10 weeks and 100 weeks is presented in Tables (2), (3) and (4) to consider short-term, medium -term and long-term respectively. In the dynamics connectedness table, which is the adjacency matrix of networks, In fact the (i,j)th element of each table shows the estimated contribution to the forecast-error variance of variable i coming from innovations to market j. The diagonal elements (i = j) are the own variance.

Each row corresponds to a market representing variance of the forecast error of the market itself and other resulting from this market and other market shocks. Each column also represents the market share in the variance of the forecast error of other markets.

Considering Table (2), we find that in the 1-week time horizon, most of the variance of forecast error is due to the shocks that arise from themselves. The Tehran Stock Exchange has the highest rate with 98.52 and the lowest rate belongs to the pound/dollar equaling 46.67%. The Tehran Stock Exchange has little relation to other markets. However, other securities markets in the Middle East have more dynamics connectedness with other financial markets of the world, and there is also a significant relationship between Tadawal and EDX General in the 1-week time horizon.

With regards to oil markets, there is a significant relationship between the West Texas Intermediate market and the Brent market. Among the security markets, the Tadawal and ADX General had the most dynamics connectedness in the short term with the oil markets. The West Texas Intermediate dynamics connectedness Index and the euro/ dollar showed a significant contribution compared to other markets. With regards to the currencies and the dollar index, it is apparent that all of these markets have strong dynamics connectedness to each other. However, the dynamics connectedness of euro-dollar and the dollar index is more impressive. There is a significant relationship between the gold market and the pound-dollar, however, the dynamics connectedness of gold market with other markets was insignificant in the short-term time horizon. Overall, in terms of net dynamics connectedness, the euro-dollar is the most shock transmitter and the pound-dollar receives the most shock from other markets.

Figure (2) shows the short-term dynamics connectedness of different markets across the network.

Considering Table (3), we examined the dynamics connectedness of markets in the 10-week time horizon. Similar to 1-week, the variance of forecast error of most markets arise from the shocks themselves. However, this number was lower than the short-term time horizon. Tehran Stock Exchange had the highest with 95.29% and West Texas Intermediate had the lowest with 29.5%. An examination of the oil market shows that both markets studied in the 10-week time horizon were the biggest recipients of shocks compared to other markets. The strong dynamics connectedness is observed between the West Texas Intermediate and Brent oil markets.

However, the Tadawal and ADX General also have significant impacts on the oil markets, which is greater than the short-term time horizon. Tehran Stock Exchange has no significant relationship with other financial markets like 1-week time horizon. However, among the financial markets, it is more influenced by Istanbul Stock Exchange and the dollar index. By examining other stock markets in the Middle East, it is visible that there are significant dynamics connectedness between these markets, and the Tadawal and ADX General transmit the most shock to other markets and have the most impact. Moreover, compared to the 1-week time horizon, dynamics connectedness among markets have increased. Similar to the short-term time horizon, the dynamics connectedness between the euro-dollar and the dollar index as well as the pound-dollar and gold are remarkable with the difference of a slight decrease over the 1-week time horizon. Figure 3 shows a full view of the dynamics connectedness between these markets.

In terms of the long-term relationships of markets, we find that although most of the variance of forecast error is due to the shocks of those markets, this number declines compared to other time horizons. So we can conclude that in the long run, the time horizon of market shocks has a greater impact on other markets. By examining the oil markets, the impact of

these markets on the stock markets has increased significantly in the long term. The Saudi and UAE stock markets have significant long-term effects on oil markets. However, the share of the Tehran Stock Exchange market is negligible again. Overall, the Tehran Stock Exchange is a market with little dynamics connectedness with other global markets, however, with the Istanbul Stock Exchange, the Dollar Index and the euro-dollar have the most long-term relationships with this market. The dynamics connectedness of other stock markets in the Middle East has increased and, similar to other time horizons, Tadawal and ADX General have more dynamic connectedness than other stock markets. Gold's connectedness with the stock markets has not changed much. However, the market's relationship with the pound-dollar remains significant. Considering currencies, euro-dollar is more influential in these markets and there are significant dynamics connectedness in the 100-week time horizon between the two indices and the euro-dollar. A net dynamics connectedness also shows the that in the long-term oil markets are affected by stock markets. The total dynamics connectedness of these markets also increase with the expansion of time horizon and they are 40.09%, 54.61% and 58.31%, respectively. Figure 4 shows the dynamic connectedness of all markets in the 100-week time horizon.

Table 1. Dynamics volatility connectedness of different markets in 1 week time horizon

	TEPIX	WTI	BRENT	EUR.USD	GBP.USD	GOLD	Dollar Index	ADX General	BIST100	Tadawul	From
TEPIX	98.59	0.02	0	0.58	0.1	0.03	0.27	0.07	0.27	0.07	0.14
WTI	0.04	59.2	21.68	7.32	0.82	0.46	2.87	2.1	1.65	3.87	4.08
BRENT	0.08	22.91	59.46	2.39	0.56	0.1	2.47	3.91	1.58	6.53	4.05
EUR.USD	0.01	5.74	1.72	49.61	4.9	1.8	34.79	0.13	1.08	0.22	5.04
GBP.USD	0.02	0.49	0.65	4.46	46.67	40.82	5.22	0.25	0.78	0.64	5.33
GOLD	0.01	0.17	0.13	1.75	44.7	50.79	1.73	0.11	0.06	0.56	4.92
Dollar Index	0.02	2.07	2.45	35.97	5.68	1.75	49.32	0.1	1.94	0.71	5.07
ADX General	0.11	3.1	3.79	3.93	0.16	0.02	3.13	57.71	4.13	23.92	4.23
BIST100	0.25	1.24	2.32	1.9	1	0.03	2.92	7.88	72.8	9.65	2.72
Tadawul	0.08	3.02	6.01	2.34	0.19	0.06	3.71	21.99	7.72	54.89	4.51
TO	0.06	3.88	3.88	6.06	4.51	4.51	5.71	3.65	1.92	4.62	40.09
NET	**-0.08**	**-0.2**	**-0.17**	**1.02**	**-0.82**	**-0.41**	**0.64**	**-0.58**	**-0.8**	**0.11**	

Table 2. Dynamics volatility connectedness of different markets in 10 weeks time horizon

	TEPIX	WTI	BRENT	EUR.USD	GBP.USD	GOLD	Dollar Index	ADX General	BIST100	Tadawul	FROM
TEPIX	95.29	0.27	0.18	0.9	0.19	0.08	0.76	0.14	1.76	0.44	0.47
WTI	0.14	29.5	17.93	5.9	4.05	2.73	3.72	15.33	5.95	14.76	7.05
BRENT	0.3	16.77	35.11	4.91	1.9	0.96	5.87	12.28	3.73	18.18	6.49
EUR.USD	0.24	5.13	3.64	33.91	5.1	2.25	25.63	9.51	5.44	9.14	6.61
GBP.USD	0.24	3.47	2.28	5.52	32.72	27.85	6.27	8.6	4.24	8.82	6.73
GOLD	0.15	0.76	0.75	2.49	38.89	43.88	2.72	4.37	1.38	4.61	5.61
Dollar Index	0.4	3.57	2.97	28.51	4.39	1.62	38.11	5.56	7.37	7.51	6.19
ADX General	0.37	5.37	4.34	4.67	1.96	1.45	4.51	44.41	10.32	22.59	5.56
BIST100	0.24	2.93	3.26	3.95	2.82	2.07	5.46	11.78	52.22	15.28	4.78
Tadawul	0.26	5.76	5.72	3.48	0.52	0.36	4.47	20.57	10.14	48.71	5.13
TO	0.23	4.4	4.11	6.03	5.98	3.94	5.94	8.81	5.03	10.13	54.61
NET	**-0.24**	**-2.65**	**-2.38**	**-0.58**	**-0.75**	**-1.67**	**-0.25**	**3.25**	**0.25**	**5**	

Table 3. Dynamics volatility connectedness of different markets over 100 weeks time horizon

	TEPIX	WTI	BRENT	EUR.USD	GBP.USD	GOLD	Dollar Index	ADX General	BIST100	Tadawul	FROM
TEPIX	93.16	0.45	0.24	1.38	0.33	0.17	1.24	0.29	1.88	0.86	0.68
WTI	0.37	20.01	12.7	6.66	3.13	1.86	6.86	16.32	11.68	20.41	8
BRENT	0.51	14.02	26.04	4.99	1.54	0.78	6.56	14.48	8.92	22.16	7.4
EUR.USD	0.74	5.74	3.72	30.71	4.18	1.86	24.61	9.27	8.44	10.74	6.93
GBP.USD	0.36	3.94	2.84	6.03	28.73	24.29	6.96	9.7	6.24	10.91	7.13
GOLD	0.19	0.86	0.91	2.61	38.12	42.97	2.88	4.71	1.77	4.99	5.7
Dollar Index	0.92	4.39	3.24	26.61	3.69	1.42	34.6	6.2	9.48	9.46	6.54
ADX General	0.52	5.38	4.31	4.83	1.99	1.49	4.83	42.02	11.72	22.9	5.8
BIST100	0.35	2.96	3.2	4.22	2.84	2.14	5.79	11.72	51.59	15.18	4.84
Tadawul	0.48	5.7	5.53	3.99	0.56	0.42	5.08	20.14	11.01	47.09	5.29
TO	0.44	4.35	3.67	6.13	5.64	3.44	6.48	9.28	7.11	11.76	58.31
NET	**-0.24**	**-3.65**	**-3.73**	**-0.8**	**-1.49**	**-2.26**	**-0.06**	**3.48**	**2.27**	**6.47**	

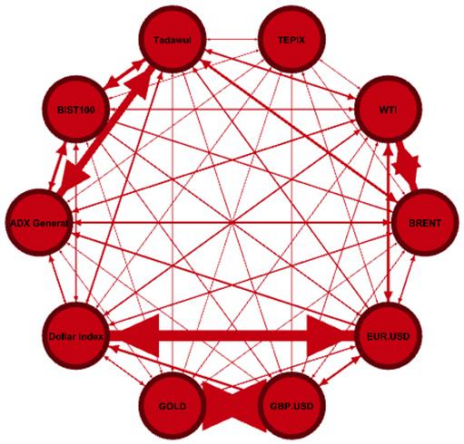

Fig 2. Dynamics volatility connectedness of different markets in 1-week time horizon

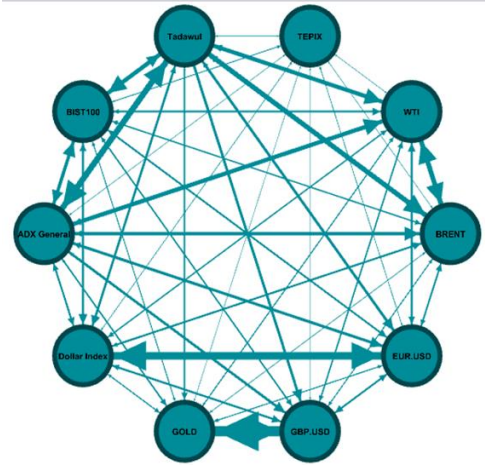

Fig 3. Dynamics volatility connectedness of different markets in time 10-week time horizon

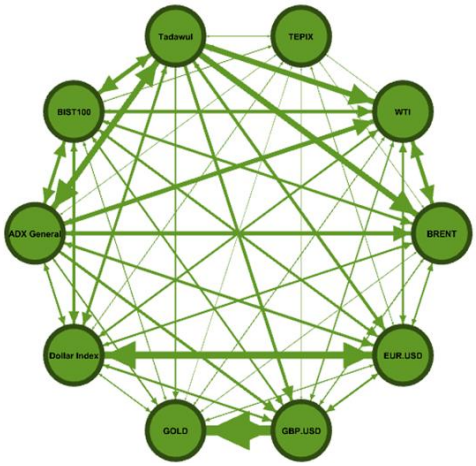

Fig 4. Dynamics volatility connectedness of different markets over a 100- week time horizon

5- Summary and Conclusion

In this study, we provide a system to measure the dynamics connectedness of different global markets from February 2007 to August 2019 in three time horizons of 1 week, 10 weeks and 100 weeks. The results show that most of the variance of forecast error is due to the shocks of those markets themselves, and as the time horizon increases, dynamics connectedness between markets increases. The Tehran Stock Exchange has insignificant dynamics connectedness with other financial markets, while, the dynamics connectedness of other Middle East markets is significant. Since the Tehran Stock Exchange and the Gold Market did not have significant relationships with other global markets, they can be used as suitable investment choices for portfolio managers to hedge their risks. In the long-term time horizon, oil markets mostly receive and the stock markets transmit the most shocks. In the long-term time horizon, shocks from each market have a greater impact on other markets. Due to the significant volatility connectedness in the markets, especially between the Saudi and UAE stock exchanges and the oil markets, it is suggested that investors consider this phenomenon when investing. In addition, considering the impact and the volatility connectedness of some markets and the Tehran Stock Exchange, especially in the long run, the Securities and exchange organization, should carefully monitor the fluctuations of these markets to make decisions effectively preventing potential shocks.

Future research proposes a better analysis of the dynamics connectedness of markets, given the greater number of stock markets around the world and the use of the LASSO (least absolute shrinkage and selection operator) model to more accurately estimate vector auto regression (VAR).

References

[1] Hamilton, J. D. "What is an oil shock?". Journal of econometrics, 113(2), 363-398. 2003

[2] Kilian, L. "The economic effects of energy price shocks". Journal of Economic Literature, 46(4), 871-909. 2008.

[3] Bagheri, E., & Ebrahimi, S. B., "Estimating Network Connectedness of Financial Markets and Commodities". Journal of Systems Science and Systems Engineering, 29(5), 572-589. 2020

[4] Diebold, F. X., & Yılmaz, K. "On the network topology of variance decompositions: Measuring the connectedness of financial firms". Journal of Econometrics, 182(1), 119-134. 2014.

[5] Billio, M. A.W., and Pelizzon, L. "Econometric measures of connectedness and systemic risk in the finance and insurance sectors". Journal of financial economics, 104(3), pp. 535-559. 2012.

[6] Acharya, V. Philippon, T., & Richardson, M. "Measuring systemic risk". Review of Financial Studies, 30(1), pp. 2–47. 2017.
[7] Adrian, T. "CoVaR". The American Economic Review, 106(7), pp. 1705-1741. 2016.
[8] Jahangiri, Khalil and Hekmati Farid, Samad. "Studying the effects of spillover volatility on stock markets, gold, oil and foreign exchange". Journal of Economic Research, p. 194-161. 2015. (In Persian)
[9] Maghyereh, A. I., Awartani, B., & Bouri, E. "The directional volatility connectedness between crude oil and equity markets: New evidence from implied volatility indexes". Energy Economics, 57, 78-93. 2016.
[10] Mimipour, Sayab and Feli, Atefeh. "Investigation of spillover volatility of oil prices on yields of selected industries in Tehran Stock Exchange: variance decomposition approach". Monetary Economics Research. 2017. (In Persian)
[11] Singh, V. K., Nishant, S., & Kumar, P. "Dynamic and directional network connectedness of crude oil and currencies: Evidence from implied volatility". Energy Economics, 76, 48-63. 2018.
[12] Husain, S., Tiwari, A. K., Sohag, K., & Shahbaz, M. "Connectedness among crude oil prices, stock index and metal prices: An application of network approach in the USA". Resources Policy, 62, 57-65. 2019.
[13] Al-Yahyaee, K. H., Mensi, W., Sensoy, A., & Kang, S. H. "Energy, precious metals, and GCC stock markets: Is there any risk spillover?". Pacific-Basin Finance Journal, 56, 45-70. 2019.
[14] Fasanya, I., & Akinbowale, S. "Modelling the return and volatility spillovers of crude oil and food prices in Nigeria". Energy, 169, 186-205. 2019.
[15] Yoon, S. M., Al Mamun, M., Uddin, G. S., & Kang, S. H. "Network connectedness and net spillover between financial and commodity markets". The North American Journal of Economics and Finance, 48, 801-818. 2019.
[16] Parkinson, M. "The extreme value method for estimating the variance of the rate of return". Journal of business, 61-65. 1980.
[17] Koop, G., Pesaran, M. H., & Potter, S. M. "Impulse response analysis in nonlinear multivariate models". Journal of econometrics, 74(1), 119-147. 1996.
[18] Pesaran, H. H., & Shin, Y. "Generalized impulse response analysis in linear multivariate models". Economics letters, 58(1), 17-29. 1998.

Nasser Gholami is a Ph.D. Candidate in Allameh Tabataba'i University. He Received his B.Sc. in Industrial management and M.Sc. in Economics. Moreover, he has been lecturer of economics at Payame Noor University. His research interests include Econometrics and Microeconomics.

Morteza Khorsandi is an associate professor of Economics at Allameh Tabataba'i University. He received his B.Sc. and M.Sc. in Economics at Shiraz university and his PhD in theoretical economics at this university too. His research is focused on Energy Economics, International Economics and Monetary Economics..

Teymor Mohammadi is an associate professor of Economics at Allameh Tabataba'i University. He received his B.Sc. and M.Sc. in Economics at Tehran University and his PhD at Allameh Tabataba'i University. Also, he is Editor-in-Chief of Insurance Research and published several books. His research is focused on energy economic and macroeconomics.

Hamid Amadeh is an associate professor of Economics at Allameh Tabataba'i University. conducting research activities in the areas of microeconomics and global economy. Moreover, he published several books related to economics.

Localization of Blockchain and E-Currency Model for E-Government Services

Maryam Niknezhad *
Department of Information Technology Management, Central Tehran Branch, Islamic Azad University, Tehran, Iran
Maryam.Niknezhad@gmail.com
Sajjad Shokouhyar
Department of management, Shahid Beheshti University, Tehran, Iran
s_shokouhyar@sbu.ac.ir
Mehrzad Minouei
Department of management, Central Tehran Branch, Islamic Azad University, Tehran, Iran
meh.minouei@iauctb.ac.ir

Received: 04/Mar/2020 Revised: 24/Jul/2020 Accepted: 08/Sep/2020

Abstract

Blockchain can reduce bureaucracy and increase the efficiency and performance of administrative processes through a platform possessing features and attributes such as storing and exchanging electronic messages in a decentralized environment and executing high level of security transactions and transparency, if used in government public service delivery. Many scholars believe that this distributed technology can bring new utilizations to a variety of industries and fields, including finance and banking, economics, supply chain, and authentication and increase economic productivity and efficiency dramatically by transforming many industries in the context of today's economy. The present study, presents the characteristics of the localized blockchain and e-currency conceptual model for the evolution of e-government services. It also examines the impact of the blockchain and e-currency model on the economy and electronic financial transactions as a viable, practical and constructive solution (rather than blocking and filtering of e-currency and blockchain). Ultimately designing a localized block chain and e-currency model, has played an effective role in exploit its high potential to speed up the administrative processes and reduce costs related to electronic transactions and payments in e-government and increase e-government revenues and ultimately it can speed up the customer service delivery and increase their satisfaction with the government.

Keywords: Blockchain; E-Currency; E-Government; Distributed Ledger Technology; Artificial Intelligence.

1- Introduction

Today, society and the global economy are governed by the trust we have on intermediaries such as banks, governments, and big Internet companies like Google and Facebook. Some of the largest corporations and the greatest wealth come from becoming an intermediary in the business world. Intermediaries accomplish a transaction and take their share. Such intermediaries do a great job but have their own limitations: "they are costly and slow down everything. Anything that becomes central is vulnerable." But above all, they "make a disproportionate profit" of what they have provided. Simply put: for the little value they add, they make a lot of money. Their best product is trust, and that trust is built on the notion of their perpetual existence [1].

Decentralized systems face major problems, including scalability and issues related to privacy and multi-identity. So, experts are trying to design decentralized protocols that are attack resistance in addition to being scalable and optimized. Analyzing such protocols requires extensive knowledge in areas such as distributed systems, cryptography, game theory, and concepts of information theory. Blockchain technology basically could be regarded as a public ledger and all of committed transactions or digital events are stored in a list of blocks. This chain grows as new blocks are appended to it continuously. Asymmetric cryptography and distributed consensus algorithms have been implemented for user security and ledger consistency. The blockchain technology generally has key characteristics of decentralization, persistency, anonymity and auditability. With these traits, blockchain can greatly save the cost and improve the efficiency [2], [3] and facilitate the move to a more equitable and flat society. Today, more than 100 blockchain projects created to transform government systems are being conducted in more than 30 countries. What leads countries rapidly initiate blockchain projects? It is because blockchain is a technology directly related to social organization; unlike other technologies, a consensus mechanism form the core

* Corresponding Author

of blockchain. Traditionally, consensus is not the domain of machines but rather humankind. However, blockchain operates through a consensus algorithm with human intervention; once that consensus is made, it cannot be modified or forged [4].

There are two different perspectives for governments in relation to the rise of blockchain architectures and applications. On the one hand the perspective of governance by blockchain, in which public organizations adopt blockchain technology for their own processes, like service provisioning, and in which blockchain technology is used to govern transactions. The other perspective is termed governance of blockchain, or blockchain Governance, which determines how blockchain should look like, how to adapt to changes and should ensure that public values and societal needs are fulfilled. Both require in-depth knowledge of the blockchain technology and the situation at hand [5].

In traditional e-government model Just as a common transaction, for example, need to experience more government audit and the corresponding archive, subsequent department needs through internal data query platform of leading department database data, and combining with affairs to deal with the data submitted to the department, offer certain audit opinion. Although the whole process has realized information, the system has the shortcomings like long business time between departments, low efficiency, lack of multiple levels of permissions on the laws and regulations, among database data redundancy is serious, the lack of unified update management, failure to ensure data security and high cost. But the e-government system based on blockchain government affair has the advantages like high efficiency, build a multi-level laws and regulations of the authority, unified database and data security guaranteed. The application of blockchain technology to e-government also can reconfigure public resources, improve government efficiency, save cost, improve the basic income of people, and promote the construction of harmonious social relations [6].

With the increasing number of e-users in Iran and the increasing use of e-government services throughout the country, banking networks traffic as well as e-service centers are gradually increasing due to the use of traditional protocols and methods for money transfer and service provision. The use of blockchain and e-currency services can play a very effective role in accelerating and reducing the cost of financial transactions and electronic payment transfers in e-government, increasing e-government revenues, reducing banking traffic, and speeding up delivery of service to customers. Providing a localized blockchain and e-currency model can also ensure security of service delivery and greatly prevent subversive attacks and theft of customer information and accounts. Obviously, to achieve this, the culture of using e-currency and e-services must be created and developed for the society and people, also trust and necessary substrates must be made.

Finally, the problem statement of this research can be the fatigue of decision-makers of E-Currency and E-Government services due to the combination of different methods of reducing e-government relocation expenditure, Enhancing the security of e-government services, Blockchain capabilities to reduce the breakdown of the consensus protocol, increasing e-revenues of the government, and the use of e-currency based on consensus algorithms; in improving payment of e-government services. On the other hand, the need for using an intelligent system is in order to increasing confidence and reliability in decision making, as well as the need for multiple expertise by simultaneously utilizing the expertise of different field specialists to solving problems of research.

2- Related Work

According a study that analyses seven pilot blockchain deployments in the public sector in Europe, Significant incremental benefits can be realized in some areas through the utilization of blockchain technologies for the provision of public services. The two main groups of are increased security (enhancement of data integrity, immutability and data consistency between organizations) and efficiency gains (such as reduced processing time and lower costs). At this stage of the technology life cycle, the continuation of experimentation with different technical designs is vital. Prior to the scale-up, technical and governance standards need to be developed, in order ensure interoperability of different designs and facilitate operative services. Incompatibility between blockchain-based solutions and existing legal and organizational frameworks is a major barrier to unlock the transformative potential of blockchain. Hence, the major policy objective should be to increase the technological and ecosystem maturity of distributed ledgers. Policy actions should aim not only at adaption of the technology to existing ecosystems but also at transformation of existing processes, organizations and structures using the disruptive potential of blockchain [7].

There are several working groups and pilot projects (in all stages of work ranging from proposed, to under development, to deploy) focused on applying blockchain within the U.S. government. The most common trends evaluated by federal agencies include: financial management, procurement, supply chain management, smart contracts, government-issued credentials, Federal personnel workforce data, Federal assistance programs, foreign aid delivery, health records and biometric data. But Increase technical understanding of blockchain within government by developing familiarity with the

decentralized and distributed paradigms of DLT [1] , Develop an internal blockchain subject matter expert workforce, Participate in the stewardship of blockchain and DLT by entering collaborative relationships with institutions like the World Economic Forum's Center for the Fourth Industrial Revolution, Increase government awareness of malign crypto-financial activity, Consider and study privacy & legality implications especially regarding the intentional "right to be forgotten" and accidental private key destruction and Amplify knowledge of potential blockchain-based national security threats, particularly in intelligence, critical infrastructure, and the Internet of Things must be considered [8].

Blockchain technology as a type of decentralized transaction and data management technologies, provide trust, obscurity, security and data integrity without having to use any third party controlling organization. The literature review identify three groups of factors, namely institutional (norms and culture, regulations and legislations, governance), market (market structure, contracts and agreements, business process) and technical (information exchange and transactions, distributed ledges, shared infrastructure) those are needed for organizational adoption of blockchain. Factors presented in this framework (institutional factors, market factors and technical factors) interact and mutually influence each other. The way how different factors will interact with each other depends on the context in which blockchain will be adopted. Additionally, factors which influence the adoption of blockchain technologies depend on its intended use [9].

2-1- Theoretical Framework and Variables

Based on the evaluations and critical reviews of the books and articles related to the research model, at first, variables, indices, and measures are identified. The initial research model, the relationship between variables, and localization of the blockchain and e-currency model via this relationship for e-government payment are following specified:

2-1-1- E-government Component [4], [10], [11], [12]:

2-1-1-1-Reducing e-government relocation expenditure:
- Reducing e-government expenditure on hardware
- Reducing e-government expenditure on software
- Reducing e-government expenditure on human resources

2-1-1-2- Enhancing the security of e-payment services of e-government:
- Protecting user information of personal accounts
- Improving the security level of users' accounts
- Preventing hacking and intrusion into the e-service system network of the e-government

2-1-1-3- Increasing e-revenues of the government:
- Increase of government e-revenues in G2B transactions
- Increase of government e-revenues in G2G transactions
- Increase of government e-revenues in G2C transactions

2-1-2- E-Currency Application Component [10], [13], [3], [14]:

2-1-2-1- The international value of e-currency:
- International consensus on the value of currency
- The value of currency based on the reduction of Internet banking network traffic
- The value of currency based on the type

2-1-2-2- The volume of e-currency:
- The volume of currency available to individuals
- The volume of currency available to businesses
- The volume of currency available to governments

2-1-2-3- E-currency rules:
- Managing the implementation of contracts related to the selection and qualification of supervisory and operating parties
- Developing and communicating the technical architecture of e-services through blockchain and e-currency
- Management of providing consulting, educational, and cultural services to the executives

2-1-3- Blockchain Capabilities Component [4], [3], [15], [16]:

2-1-3-1- Decentralization capability:
- Distributed data logging
- Distributed data storage
- Updating data as distributed

2-1-3-2- Open-source capability:
- Developing of applications by people
- Evaluating the data publicly
- Transparency of data and applications for people

2-1-3-3- Anonymity capability:
- Anonymity of data transfer
- Anonymity of transaction
- Increase of trust between nodes

2-1-3-4- Independence capability:
- Independent data transfer
- Independent data updating
- Protection and immutability of all records forever

Figure 1 shows the initial model of research and the relationship between variables.

After reviewing the theoretical foundations of the research and investigating the literature history of the research, it was determined that considering the research gaps in the knowledge domains of "reducing e-government relocation expenditure, Enhancing the security of e-government

[1] Distributed Ledger Technology

services, Blockchain capabilities to reduce the breakdown of the consensus protocol, increasing e-revenues of the government, and the use of e-currency based on consensus algorithms; in improving payment of e-government services", as well as the lack of an intelligent system to provide guidance to the managers for decision making, the research innovations are localizing and realized in solving those research gaps.

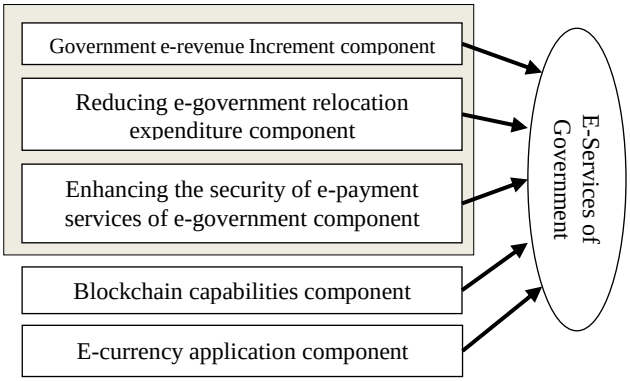

Fig. 1 Initial model of research and the variables.

2-2- Data Analysis Method

After reviewing the research background and theoretical foundations of the research, it was found that no similar research has been carried out to localize the blockchain and e-currency model for e-government services based on the documentation of e-government services of the country, employing a combined methodology of statistical analysis and artificial intelligence in MATLAB.

Figure 2 illustrates the research steps as following. A descriptive-modeling and exploratory (qualitative, quantitative) type of research was conducted. Due to the use of articles and documentation related to the research subject from a variety of sources, the method of data collection in this research is a "case-study of documentation". To evaluate the rules of artificial intelligence system based on the artificial neural network to localize the model extracted from expert opinions, the tools of determining the variables of decision-making model and interview have been utilized.

The study population consisted of professors, specialists, and experts working in the Iranian Blockchain Association and the Blockchain Laboratory of the Sharif University of Technology in Iran or similar positions. The sampling method is a combination of two methods of non-probability purposive sampling (judgmental) and snowball sampling. Due to the nature of the sampling method, the sample size of the study will be equal to the number of available and collaborative experts.

Consensus algorithms (especially Proof-of-Work (POW) and Proof-of-Stake (POS)) are used to present and evaluate the localized model. Also, breakdown analysis was used to investigate the intrusion and weaknesses of the localized model. In addition, to investigate the security of the proposed model against hackers and subversive attacks, the randomly chosen nodes analysis method in the network is used to create blocks by exploiting both Nakamoto and voting methods.

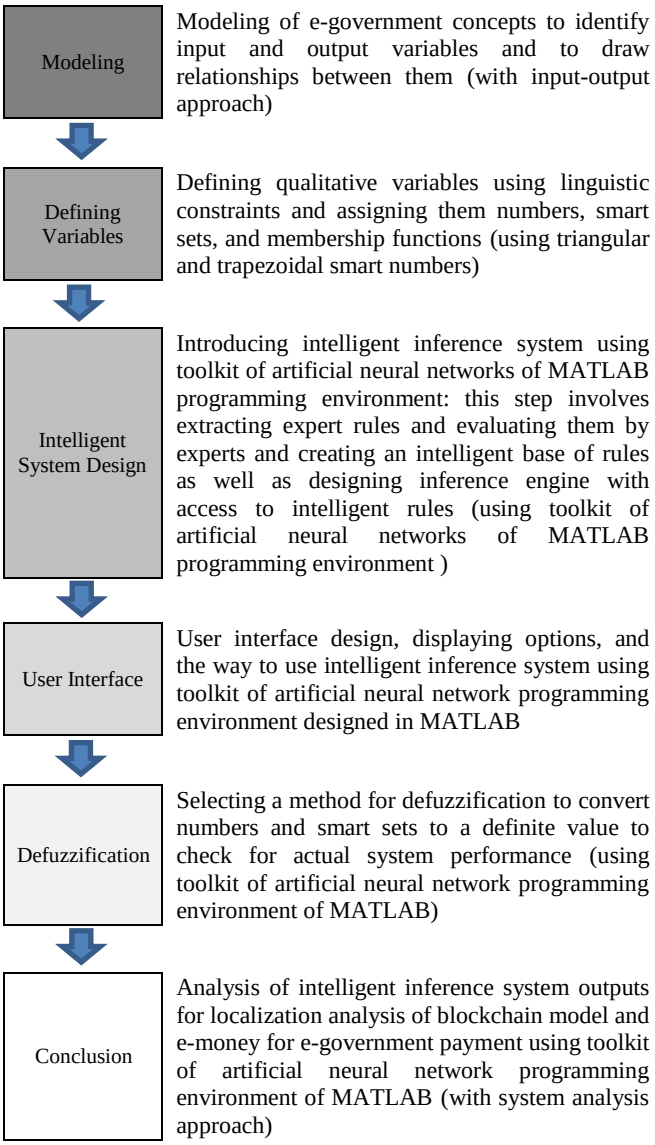

Fig. 2 Flowchart of research steps

3- Research Methodology: Intelligent System Design Based on Artificial Neural Networks

The methodology of this article is applied-modeling because it aims to accurately describe the concepts and rules related to the Blockchain and E-Currency model for E-Government services. On the other hand, the

relationship between these concepts and rules is assessed and evaluated by the experts. Indeed, Statistical Analysis is the study of the effect of input variables on the output variable at a statistical model.

The Research technique of this article is Artificial Neural Networks in Matlab software. One of the most important reasons for using artificial neural networks and fuzzy systems in this research is that real world issues typically have a complex structure, which implies ambiguity and uncertainty in their definition and understanding [17], [18]. Ever since it has been able to think, it has always been ambiguous in various social, technical and economic issues. The human brain defines and evaluates sentences by considering various factors based on inferential thinking, whose pattern in mathematical language and formulas, if not impossible, will be very complicated [17], [19]. Linguistics variables are expressed on the basis of language (spoken) values that are in the phrase set (words / terms), and language expressions are attributes for linguistic variables. Here, linguistic variables are said to be variables that words, and sentences of human and machine languages are acceptable values for them instead of numbers. A fuzzy number is a special fuzzy set in which x denotes the true values of the member of the set of R and its membership function $\mu_{\tilde{A}}(x)$ as it is Eq. (1) [17], [18]:

$$A' = \{(x, \mu_{\tilde{A}}(x)) \mid x \in X\} \quad (1)$$

In fact, the dividing below describes how the relationship between fuzzy logic and the artificial neural network is expressed in terms of this view [17], [18], [19]:

Symmetric Neuro-Fuzzy models: The neural network and the fuzzy system work on one single operation, but they do not affect each other. None of them are used to determine another parameter. Usually, in this model, the neural network is used to pre-process the input or output of the fuzzy system.

Artificial Neural Network based Fuzzy Inference Systems: Some of these systems are considered as Cooperative models. These models are used to expand fuzzy rules.

Combined Neuro-Fuzzy models: Artificial neural network and fuzzy system combine in a coordinated structure. This pattern can be considered as a neural network with a fuzzy parameter or a distributed learning fuzzy system. ANFIS and ANNBFIS are examples of this model.

Finally, the five steps of designing an intelligent system based on artificial neural networks to localize the blockchain and e-currency model for payment of e-government services according to Figure 3 are as follows:

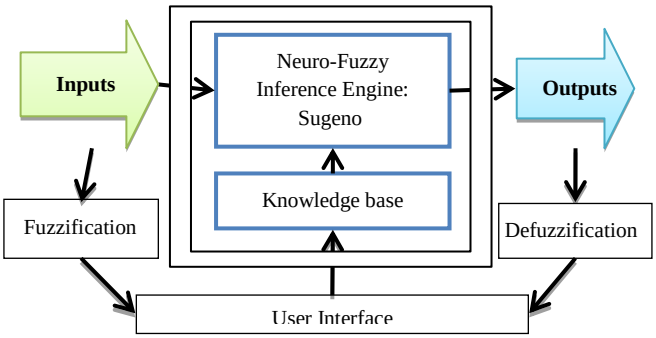

Fig. 3 Intelligent System Structure Based on artificial neural networks

Step 1: Modeling of the field concepts to identify input and output variables and to draw relationships between them

Step 2: Defining qualitative variables, exploiting linguistic constraints and assigning them numbers, fuzzy sets, and membership functions

Step 3: Designing an intelligent system based on artificial neural networks including the extraction of expert rules, their evaluation by experts, the creation of fuzzy rules database, and designing inference engine with access to fuzzy rules.

Step 4: Designing user interface, displaying options, and using the designed intelligent system

Step 5: Selecting a method for defuzzification to convert fuzzy numbers to a definite value to verify the actual performance of the system.

The sample and population of this research can be divided into two general groups: the first group consists of University Professors (Academic Experts), the second group includes experts working in e-government services or similar positions (Industrial Experts).

4- Results

After distributing 100 questionnaires, the sample size of this study is 96 available and cooperative experts who were selected by a combination of two methods: non-probability purposive (judgmental) sampling and snowball sampling. The data related to measure 1 (localization tool of blockchain model and e-currency for paying e-government services) and measure 2 (validation tool of the intelligent system) were collected in the fall of 2019. Table 1 shows the descriptive information of the research variables and indicators, based on the number of data and mean, and standard deviation, indicating that the data in this study are in good condition in terms of symmetry and aggregation. The most important criteria for the variables are outlined in the table.

Table 1: descriptive information of the research variables and indicators

Variables and Indicators	*Ideal*		*Functional status*	
	Data	*Mean*	*Data*	*Mean*
Reducing e-government relocation expenditure (X1)	96	5.47	92	4.90
Reducing e-government expenditure on human resources	92	5.65	96	4.21
Reducing e-government expenditure on infrastructure	96	5.63	96	4.66
Reducing e-government expenditure on media	96	5.68	92	4.59
Reducing e-government expenditure on hardware	96	5.80	96	4.76
Reducing e-government expenditure on software	96	5.91	96	4.25
Enhancing the security of e-government services (X2)	96	5.79	96	5.05
Preventing hacking and intrusion into the e-service system network of the e-government	96	5.51	94	4.61
Information Security Management System	96	5.67	92	4.79
Protecting user information of personal accounts	92	5.93	96	4.48
Improving the security level of users' accounts	96	5.92	94	4.67
Encryption of e-payment services	96	5.77	96	4.91
Blockchain capabilities to reduce the breakdown of the consensus protocol (X3)	96	5.73	90	5.31
Anonymity capability	96	5.91	96	5.01
Decentralization capability	92	5.95	94	4.76
Independence capability	96	5.51	92	4.90
Open-source capability	96	5.62	92	4.52
Immutability capability	96	5.66	96	4.95
Increasing e-revenues of the government (X4)	96	5.56	92	4.95
Increase of government e-avenues in G2G transactions	96	5.67	92	4.39
Increase of government e-avenues in G2B transactions	96	5.83	96	4.42
Increase of government e-avenues in B2B transactions	96	5.68	96	4.58
Increase of government e-avenues in G2C transactions	96	5.76	92	4.30
Increase of government e-avenues in B2C transactions	96	5.59	96	4.82
use of e-currency based on consensus algorithms (X5)	96	5.73	96	4.63
e-currency rules based on PoW	96	5.52	96	4.76
Type of e-currency based on PoS	96	5.51	94	4.61
Liquidity based on PoW	96	5.64	92	4.46
International Value of e-currency Based on PoW	96	5.91	96	4.76
Volume of e-currency based on PoS	96	5.91	94	4.88

Following are the five steps of designing and implementing of the intelligent system for localizing the model:

Step one: input and output variables are defined. Input variables of the intelligent system involve reducing e-government relocation expenditure (X1), Enhancing the security of e-government services (X2), Blockchain capabilities to reduce the breakdown of the consensus protocol (X3), increasing e-revenues of the government (X4), and the use of e-currency based on consensus algorithms (X5); the output variable of the intelligent system is the status of "improving payment of e-government services."

Step two: qualitative variables are defined by linguistic constraints and assigning them numbers, fuzzy sets, and membership function. Table 2 illustrate the linguistic variables, fuzzy values, and membership functions of triangular and trapezoidal numbers associated with the input and output variables of the intelligent system within three- and five-spectra.

Table 2: linguistic variables associated with the input and output variables of the intelligent system

Linguistic variables	*Membership functions of triangular and trapezoidal numbers*
Low	(0.3 0.15 0)
Medium	(0.7 0.5 0.3)
High	(1 0.85 0.7)
Training Data (ANFIS)	
0,0,0,0,0,0	
0-0.025,0-0.025,0-0.025,0-0.025,0-0.025,0.05	

0.025-0.05,0.025-0.05,0.025-0.05,0.025-0.05,0.025-0.05,0.1
0.05-0.075,0.05-0.075,0.05-0.075,0.05-0.075,0.05-0.075,0.15
0.075-0.10,0.075-0.10,0.075-0.10,0.075-0.10,0.075-0.10,0.2
0.10-0.15,0.10-0.15,0.10-0.15,0.10-0.15,0.10-0.15,0.25
0.15-0.25,0.15-0.25,0.15-0.25,0.15-0.25,0.15-0.25,0.3
0.25-0.30,0.25-0.30,0.25-0.30,0.25-0.30,0.25-0.30,0.35
0.30-0.35,0.30-0.35,0.30-0.35,0.30-0.35,0.30-0.35,0.4
0.35-0.4,0.35-0.4,0.35-0.4,0.35-0.4,0.35-0.4,0.45
0.40-0.45,0.40-0.45,0.40-0.45,0.40-0.45,0.40-0.45,0.5
0.45-0.5,0.45-0.5,0.45-0.5,0.45-0.5,0.45-0.5,0.55
0.50-0.55,0.50-0.55,0.50-0.55,0.50-0.55,0.50-0.55,0.6
0.55-0.6,0.55-0.6,0.55-0.6,0.55-0.6,0.55-0.6,0.65
0.60-0.65,0.60-0.65,0.60-0.65,0.60-0.65,0.60-0.65,0.7
0.65-0.7,0.65-0.7,0.65-0.7,0.65-0.7,0.65-0.7,0.75
0.70-0.75,0.70-0.75,0.70-0.75,0.70-0.75,0.70-0.75,0.8
0.75-0.80,0.75-0.80,0.75-0.80,0.75-0.80,0.75-0.80,0.85
0.8-0.85,0.8-0.85,0.8-0.85,0.8-0.85,0.8-0.85,0.9
0.85-0.9,0.85-0.9,0.85-0.9,0.85-0.9,0.85-0.9,0.925
0.90-0.95,0.90-0.95,0.90-0.95,0.90-0.95,0.90-0.95,0.95
0.95-1,0.95-1,0.95-1,0.95-1,0.95-1,0.975
1,1,1,1,1,1

Step three: a knowledge base of intelligent system is designed, which involves extracting expert rules, evaluating them by experts, and creating fuzzy rules database. The starting point of building a rule-based knowledge base is to obtain a set of rules when a phase of expert knowledge or the field of knowledge being examined and the subsequent step are a combination of these rules into a single system. Finally, the number of fuzzy rules of the module "improving the payment of e-government services in the country" of the intelligent system is equal to 243 because of the five main variables, each of which has three states. Figure 4 shows how to generate fuzzy rules within the knowledge base.

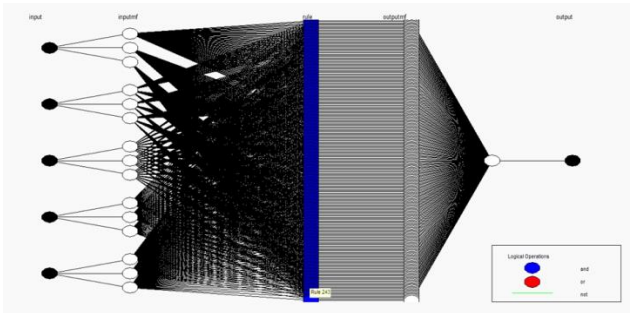

Fig. 4 How to generate fuzzy rules inside the knowledge base

Step four: an inference engine of intelligent system is designed (Figure 5). In this step, the wtaver method is used for defuzzification to convert fuzzy numbers and sets to a definite value for actual evaluation of the system performance

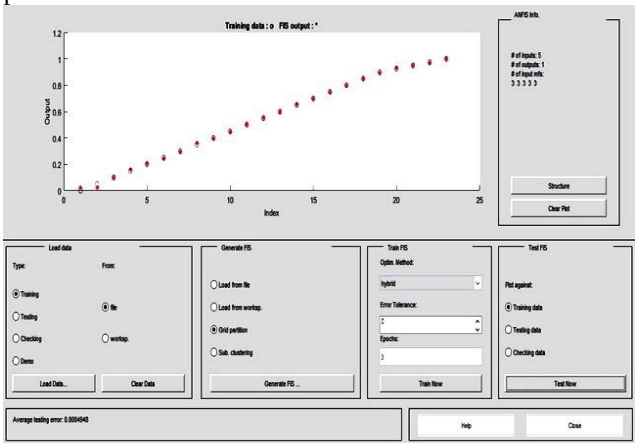

Fig. 5 System Inference Engine

The mean error of the test data was calculated 0.0085 (less than 1%) in the inference engine of the intelligent system for "localization of blockchain and e-currency model for the payment of e-government services", which shows the high accuracy of the calculations of artificial neural networks of the research. The defuzzification in the intelligent system converts the fuzzy output to a definite number.

Step five: this step explains how to exploit the intelligent system and analyze its outputs numerically (accurate) and linguistically to analyze the behavior of system's output variable. In order to determine the weight of the input values of the system, information about the ideal and functional weight of each of the main variables of the research is presented in Table 3.

Table 3: Ideal weight and functional weight of main variables

Variables	***Ideal weight***		***Functional weight***	
	Weighted average	***Fuzzy Weight***	***Weighted average***	***Fuzzy Weight***
(X1)	5.690	0.813	4.562	0.652
(X2)	5.765	0.824	4.752	0.679
(X3)	5.730	0.819	4.903	0.701
(X4)	5.**682**	0.812	4.577	0.654
(X5)	5.703	0.815	4.683	0.669

According to the rules of knowledge base of the main module of the intelligent system and based on the calculation of the weight of each main variable using the expert opinions and also taking advantage of the intelligent system based on designed artificial neural networks, it is

possible to numerically and more precisely examine the status of "improving the payment of e-government services in the country"

The main findings of research based on localized model is utilizing intelligent system outputs, the status of "improving the payment of e-government services of the country" can be analyzed on the basis of variables such as "Blockchain capabilities to reduce breakdown of consensus protocol (X3)", "Increasing e-revenues of the government (X4)", "Enhancing the security of e-government services (X2)", "Use of e-currency based on consensus algorithms (X5)", and "Reducing e-government relocation expenditure (X1)" because, as outlined in the E-Government Foresight Framework, the services should at least be provided through only one single port. Or, in the most optimistic way, log-in should be via a port, and then the user transfer operation should be done.

In fact, according to the rules of knowledge base of the main module of the intelligent system based on the calculation of the weight of each main variable using the expert opinions and utilizing the intelligent system designed in this research, the status of "improving the payment of e-government services of the country" can be investigated numerically and more precisely: Ideally, if the status of "Reducing e-government relocation expenditure (X1)" is good, i.e. exactly 0.813, and "Enhancing the security of e-government services (X2)" is good, i.e. exactly 0.824, and "blockchain capabilities to reduce breakdown of consensus protocol (X3)" is good, i.e. exactly 0.819, and "Increasing e-revenues of the government (X4)" is good, i.e. exactly 0.812, and "Use of e-currency based on consensus algorithms (X5)" is good, i.e. exactly 0.815, then, "improvement of e-government services payment" is excellent (fifth level)", i.e. exactly 0.952. Considering the membership functions of linguistic variables provided by the experts in the previous tables, the value of 4.76 within a 5-value spectrum is calculated in a defined range for the linguistic variable "excellent", i.e. the improvement of the country's e-government payment services, with programming code of [0.815; 0.812; 0.819; 0.824; 0.813] exactly 0.952 (95% objective function optimality). On the other hand, in terms of performance status, if the status of "Reducing e-government relocation expenditure (X1)" is average, i.e. exactly 0.652, and "Enhancing the security of e-government services (X2)" is average, i.e. exactly 0.679, and "Blockchain capacity to reduce breakdown of consensus protocol (X3)" is good, i.e. exactly 0.701, and "Increasing e-revenues of the government (X4)" is average, i.e. exactly 0.654, and "Use of e-currency based on consensus algorithms (X5)" is average, i.e. exactly 0.669, then, the status of "improvement of e-government services payment" is average (third level)", i.e. exactly 0.468. According to the membership functions of linguistic variables provided by the experts in the previous tables, the value of 2.34 within a 5-value spectrum is calculated exactly 0.468 in a defined range for the linguistic variable "average", i.e. the status of the improvement of the country's e-government payment services, with programming code of [0.669; 0.654; 0.701; 0.679; 0.652].

After designing, the outputs and responses of the intelligent system were compared in a separate measurement tool with the opinions of 18 so-called experts, the results of which can be seen in Table 4 based on the intelligent system rules and the mean of expert responses. Since experts' opinions are expressed based on the spectrum of five membership functions, to test the hypothesis above, we can exploit the discrepancy percentage between the outputs of the intelligent system of this research and the mean of expert opinions.

Hence, the final difference between the outputs of the intelligent system and the mean of expert opinions was not significant and was equal to 0.065. Since there is not a sufficient reason to accept the null hypothesis, the opposite hypothesis is accepted, i.e. there is no significant difference between the mean of expert opinions and the outputs of the "intelligent system".

Table 4: Comparison of "intelligent system" outputs with the mean of expert responses

Intelligent system rules	***Intelligent system outputs***	***Mean of expert responses***	***Difference ratio***
Rule. 3	1	1.22	0.055=0.22/4
Rule. 45	3	2.72	0.0675=0.28/4
Rule. 79	3	2.78	0.055=0.22/4
Rule. 86	2	1.67	0.0825=0.22/4
Rule. 103	2	1.67	0.0825=0.22/4
Rule. 140	3	2.78	0.055=0.22/4
Rule. 157	3	3	0=0/4
Rule. 219	2	2.94	0.015=0.06/4
Rule. 224	2	2.39	0.1525=0.61/4
Rule. 235	2	2.67	0.0825=0.33/4
Final Difference			0.065

5- Conclusions

One of the most important results of the research is that in improving the payment of e-government, blockchain technology has the ability to facilitate direct interaction between government agencies, citizens and economic actors, which at the basic level means improving public services in registration and information exchange processes.

Finally, utilizing the results of the present study, we may contribute to the removal of existing barriers to improvement of the payment of e-government services.

The following solutions can facilitate the achievement of e-government's goals:

- Making Citizens' Digital Authentication more secure, for Enhancing the security of e-government services.
- Increasing citizens' ownership and control over economic processes, for increasing e-revenues of the government.
- Using smart contracts in process automation or registering economic documents in official government offices, for reducing e-government relocation expenditure.
- Implementing the Blockchain capabilities to reduce the breakdown of the consensus protocol, for the use of e-currency based on consensus algorithms.
- Supporting administrative agency to accelerate the electrification of their services.
- Using the potentials of the private enterprises to increase citizens' satisfaction with services.
- Reducing the duties of the government and transferring them to non-state sectors through the capabilities of information technology.
- Accelerate and facilitate the receipt of citizens and business's services from the executive apparatus.
- Creating a comprehensive and scientific model based on local solutions in e-services.
- Increasing the productivity of government agencies and reducing the cost of service exposition.

Also the most important recommendations and suggestions for future research can be stated as:

- Utilization of Data envelopment analysis (DEA) Methodology for measuring the efficiency of multiple decision-making units (DMUs) in the model.
- Using System Dynamic Methodology (Vensim) for relationship building modeling,
- Utilization of fuzzy Multiple Criteria Decision Making (MCDM) techniques for relationship network ranking in the model
- Employment of Fuzzy Ontology for the comprehensive modeling of relationships in the model.

References

[1] D. Tapscott and A. Tapscott, "Block chain revolution", Portfolio: Reprint edition, 2018, ISBN-10: 1101980141.

[2] Z. Zheng, S. Xie, H. Dai, X. Chen and H. Wang, "An overview of blockchain technology: Architecture, consensus, and future trends", in 2017 IEEE International Congress on Big Data (BigData Congress), 2017, DOI: 10.1109/ BigDataCongress .2017.85, pp. 557-564.

[3] W. Petersz, E. Panayiy, and A. Chapelley, "Trends in crypto-currencies and blockchain technologies: A monetary theory and regulation perspective Gareth", arXiv: 1508.04364v1, [cs.CR], 2015.

[4] M. Jun, "Blockchain government - a next form of infrastructure for the twenty-first century", CreateSpace Independent Publishing Platform; 1 edition, 2018, ISBN-10: 171912714X, pp. 2-6.

[5] S. Olnes, J. U-b.acht and M. Janssen, "Blockchain in government: Benefits and implications of distributed ledger technology for information sharing", Government Information Quarterly, 34, Issue 3, 2017, pp. 355-364.

[6] H. Chen, "An E-government Model Design Based on Block Chain", in International Conference on Manufacturing Construction and Energy Engineering, 2017, ISBN: 978-1-60595-483-7, pp. 176-179.

[7] D. Allessie, M. Sobolewski and L. Vaccari, "Blockchain for digital government", Science for Policy report by the Joint Research Centre (JRC), the European Commission's science and knowledge service, 2019, ISBN 978-92-76-00582-7, doi:10.2760/93808. pp. 65-67.

[8] G. Mark, N. Melinda, P. Lisa, G. Bell, J. Downing, K. Rahbari and M. Kilani, "Blockchain and Suitability for Government Applications", PUBLIC-PRIVATE ANALYTIC EXCHANGE PROGRAM, 2018, pp. 27-31.

[9] M. Janssen, V. Weerakkody, E. Ismagilova, U. Sivarajah and Z. Irani, "A framework for analysing blockchain technology adoption: Integrating institutional, market and technical factorsInternational Journal of Information Management, 50, 2020, ISBN 0268-4012, pp.302–309.

[10] R. Böhme, N. Christin, B. Edelman, and T. Moore, "Bitcoin: Economics, Technology, and Governance", Journal of Economic Perspectives, 29, Number 2, 2015, pp. 213–238.

[11] E. Shahghasemi, B. Tafazzoli, M. Akhavan, G. Mirani and T. Khairkhah, "Electronic Government in Iran: A Case Study", Online Journal of Social Sciences Research. ISSN 2277-0844; Volume 2, Issue 9, 2013, pp. 254-262.

[12] A. Jahangiri, and N. Alavi, "Creating the Groundwork for an Electronic Government", Journal of Management and Development Process, 20 (3 and 4): 42-53, 2006. [In Persian]

[13] S. Barber, X. Boyen, E. Shi, and E.Uzun, "Bitter to Better—How to Make Bitcoin a Better Currency", 16 th International Conference on Financial Cryptography and Data Security, 2012, pp. 399-414.

[14] E. Rasolinejad "Factors affecting the use of e-money: The Case of Saderat Bank", Journal of New Economy and Commerce, Volume 3, Issue 10, 2009, pp. 131-153. [In Persian]

[15] T. Aste, P. Tasca, and T.D. Matteo, "Blockchain Technologies: foreseeable impact on industry and society", COMPUTER, 50(9), 2017, pp. 18-28.

[16] I. Lin and T. Liao, "A Survey of Blockchain Security Issues and Challenges", International Journal of Network Security, Vol.19, No 5, 2017, pp. 653-659.
[17] C. T. Lin and C. S. George Lee, Neural Fuzzy Systems: A Neuro-Fuzzy Synergism to Intelligent Systems, Hardcover – Publisher: Prentice Hall; Har/Dskt edition, ISBN 10: 0132351692ISBN 13: 9780132351690, 1996.
[18] R. N. Mishra and K. Mohanty, "Real time implementation of an ANFIS-based induction motor drive via feedback linearization for performance enhancement", Engineering Science and Technology an International Journal, 2016, 19(4) DOI: 10.1016/j.jestch.2016.09.014
[19] S. Moayer and P. A. Bahri, "Hybrid intelligent scenario generator for business strategic planning by using ANFIS" Expert Systems with Applications, 2009, Volume 36, Issue 4, May 2009, pp. 7729-7737.

Maryam Niknezhad received the B.Sc. degree in computer engineering from Alzahra University of Tehran, Iran, in 2004. She received the M.Sc. degree in Information Technology engineering from Shiraz University, Iran, in 2012. Currently she is Ph.D. Candidate in Islamic Azad University, Central Tehran Branch, Iran. She works in Ministry of Economic Affairs and Finance, Iran. Her area research interests include Data mining, Social Commerce, Blockchain, Social Networking, and Deep Learning.

Sajjad Shokouhyar is an Assistant Professor of industrial management and information system at Shahid Beheshti University. He earned his doctoral degree in industrial engineering from Polytechnic University of Tehran and completed his M.S. in systems engineering at Polytechnic University. His research is focused on developing decision analytic tools that can be implemented in supply chain management, logistic, Transportation and supplier evaluation systems.

Mehrzad Minouei is an Assistant Professor of Financial Management at Central Tehran Branch, Islamic Azad University, Tehran, Iran. He received his Ph.D. degree in Financial Management from Science and Research Branch, Islamic Azad University, Iran. He is conducting research activities in the areas of Financial Management and Capital Market.

Reliability Analysis of the Sum-Product Decoding Algorithm for the PSK Modulation Scheme

Hadi Khodaei Jooshin
Faculty of Electrical and Computer Engineering,University of Tabriz, Tabriz, Iran
hadikhodaei.j@gmail.com
Mahdi Nangir *
Faculty of Electrical and Computer Engineering,University of Tabriz, Tabriz, Iran
nangir@tabrizu.ac.ir

Received: 04/Apr/2020 Revised: 24/Aug/2020 Accepted: 08/Oct/2020

Abstract
Iteratively decoding and reconstruction of encoded data has been considered in recent decades. Most of these iterative schemes are based on graphical codes. Messages are passed through space graphs to reach a reliable belief of the original data. This paper presents a performance analysis of the Low-Density Parity-Check (LDPC) code design method which approach the capacity of the Additive White Gaussian Noise (AWGN) model for communication channels. We investigate the reliability of the system under Phase Shift Keying (PSK) modulation. We study the effects and advantages of variation in the codeword length, the rate of parity-check matrix of the LDPC codes, and the number of iterations in the Sum-Product Algorithm (SPA). By employing an LDPC encoder prior to the PSK modulation block and the SPA in the decoding part, the Bit Error Rate (BER) performance of the PSK modulation system can improve significantly. The BER performance improvement of a point-to-point communication system is measured in different cases. Our analysis is capable for applying any other iterative message-passing algorithm. The code design process of the communication systems and parameter selection of the encoding and decoding algorithms are accomplished by considering hardware limitations in a communication system. Our results help to design and select paramours efficiently.

Keywords: LDPC Codes; BER Performance; SPA; Channel Decoding Algorithm; Rate; Channel Capacity.

1- Introduction

Berrou et al. introduced Turbo Codes in 1993 and made it possible that by utilizing these error correction codes, one can approach the Shannon limit of the channel capacity [1-2]. A few years later in 1996, Mackay and Neal rediscovered the Shannon limit performance of the Low-Density Parity-Check (LDPC) codes [3-5], that were introduced by Gallager in 1963 [6]. The LDPC codes could compete with the Turbo Codes successfully. Nowadays, there is an increasing demand for the reliable communication systems, which can handle a large amount of data rate with high-speed equipment. It requires cheap, fast, and very small size communication and storage devices.

The performance of all communication and storage systems has some limitations. One of these limitations is the channel capacity concept that has been introduced by Claude Shannon in 1948. Channel Capacity is the maximum possible value of rate, which can be achieved by using a specific communication system with an arbitrary small enough BER value.

Some applicable error correction codes are the Hamming codes, the LDPC codes, the Turbo codes, and Polar codes, which have been employed in the real world communication systems. The LDPC codes are a kind of linear block codes that strongly contrasts the channel noise effect. The LDPC code is one of the hot research topics in the coding and information theory due to its high speed encoding and decoding algorithms, it's capability to achieve the channel capacity providing a reliable communication for an arbitrary transmission rate. It is a progressive coding scheme and is proper in a wide range of applications such as signal processing, cryptography, compressed sensing, wireless communications, and data compression.

The LDPC codes utilize a parity-check matrix H, in which the proportion of ones to zeros is very low; in other words, the matrix H is sparse. These codes are classified into the regular and the irregular codes. A code is regular if the number of ones in each column (say w_c) and the number of ones in each row (say w_r) in the parity-check matrix H are

* Corresponding Author

fixed values. Obviously, if a code is not regular, then it is irregular code. An LDPC code of length n can be indicated with (n,w_c,w_r), where w_c and w_r are generally two vectors, respectively showing the degree of the variable nodes and the check nodes of H. Thus, each information bit in a variable node is involved with w_c check bits, and similarly each check bit in a check node is involved with w_r information bits. The decoder in the receiver side employs the parity-check matrix H for accomplishing its task. It reconstruct the original data with a BER utilizing a decoding algorithm.

In this work, we consider SPA and evaluate its reliability. The LDPC codes are very efficient codes in several communication scenarios, such as wireless communications [7], optical communication systems [8], satellite communication systems [9], digital video broadcast (DVB) systems [10], and terrestrial multimedia broadcasting (TMB) systems [11]. Furthermore, it's applications in high-density data storage systems, such as digital electronic memories are now considerable. These codes have capacity-approaching performance and can be achieved using practical and implementable iterative decoding algorithms. The LDPC codes have been adopted to use in the next generation of communication systems [12-13] such as 5G due to the low BER. As an example, BER=10^{-13} is achievable with an acceptable complexity of encoding and decoding schemes.

In this paper, we investigate SPA, which is one of the fast, implementable, and simple iterative message-passing algorithms that have been utilized for decoding of the LDPC codes [14-16].

Through this paper, we follow three main goals for a designed parity-check matrix H. First, we show that by increasing the size of parity-check matrix H, the performance improves and BER value decreases. Second, we illustrate that the BER performance improves by increasing the iteration numbers in the SPA. Our third finding is that the performance or BER decreases by decreasing the rate of parity-check matrix H. For instance, for the LDPC code with parity-check matrix H (768, 1024, irregular), rate=1/4, and iteration=10 in the SPA, we achieve BER≈10^{-9} for Eb/N0=6dB, while for the LDPC code with H (384, 512, irregular), rate=1/4, and iteration=10, we achieve BER≈10^{-7} for Eb/N0=6dB. Hence, the advantage of increasing the size of the parity-check matrix H is concluded. The effect of parameter variations is desirable in this work.

The rest of this paper is organized as follows: In section II, the system model and definitions are proposed. Furthermore, the details of the encoding and decoding schemes are provided in this section. Simulation results and discussions are presented in section III. Finally, section IV concludes this paper.

2- System Model and Definitions

In this section we present system model and provide some fundamental tools for iterative decoding schemes. Specifically, we study the SPA because it can be simply modified and extended to get other message-passing algorithms for other communication system tasks.

2-1-System model

The task of a point-to-point communication system is conveying information from a source to a destination. In Fig. 1, a simplified block diagram a point-to-point communication system is depicted. A brief description of each block is presented.

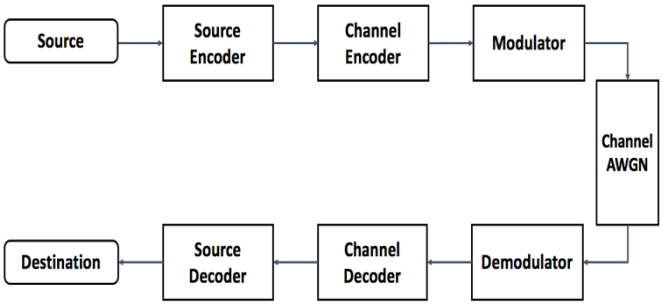

Fig. 1: Block Diagram of Communication System.

In the source encoder, the information symbols of the source are mapped to codewords. The main reasons of using a source encoder is reduction of redundancy from information symbols, which can significantly reduce the size of transmitted data. For instance, the Lempel-Ziv 77 (LZ77), the Lempel-Ziv 78 (LZ78), and the LZ-Storer-Szymanski (LZSS) are some source encoding algorithms based on text compression algorithms. They use a sliding window over the sequence of symbols, with two sub-windows for the source coding [17-19].

If source information can be completely recovered from codewords, this coding is called *lossless compression*, otherwise it is called *lossy compression*. For the sources with unknown distributions, we use universal source coding algorithms [20]. Furthermore, multi-terminal source coding algorithms can be applied for the case of single binary source [21].

The second block is a channel encoder. Some intentional redundancy is added to the vector of the information symbols to increase reliability of the transmission via the noisy channel, which causes a rate reduction [22].

The channel coding methods can be categorized into two main classes. First, the *linear block codes* maps a sequence of m information bits into a codeword with n bits ($n>m$). The Hamming codes, LDPC codes, BCH codes, and cyclic

codes are some examples of this category. Second, the *convolutional codes* which maps a vector of *m* information bits into a codeword with *n* bits, depending on the current and previous information bits. For instance, the turbo codes is in this category. In this work, the LDPC codes and the SPA are exploited for the channel encoding and the channel decoding, respectively. Finally, the third block is modulator, which prepares the encoded data to send via communication channel.

Modulation superimposes data on a carrier signal, which its frequency is higher than the bandwidth of the information signal [23]. The *M*-PSK (phase-shift keying), the *M*-FSK (frequency-shift keying), and *M*-ASK (amplitude-shift keying) are fundamental digital modulation schemes. In this paper, the BPSK (*M*=2) is exploited for accomplishing the modulation.

The modulated data is transmitted by noisy channel such as a wire, an antenna, an optical fiber, etc. In this paper, the channel noise is assumed to be the Adaptive White Gaussian Noise (AWGN). Furthermore, an amplification of the modulated data is done before transmitting over the noisy channel due to channel debilitation and fading phenomena.

In the receiver side, all performed operations at the transmitter should be accomplished on the received data reversely. Therefore, first, data is being demodulated then the demodulated data is being decoded by the SPA to get source codewords. Finally, these codewords are being decoded to obtain the information source symbols. All of the methods and procedures for the encoding in transmitter and the decoding in receiver should be the same, and they should be done in a reverse order.

2-2- Graphical Representation of The LDPC Codes

A bipartite Tanner graph that has been illustrated in Fig .2 is a graphical representation of the parity-check matrix *H*, made of two types of nodes, the variable nodes (VN) denoted by v_j and the check nodes (CN) denoted by c_i [24]. The *j*-th VN (v_j) and *i*-th CN (c_i) in the Tanner graph are connected with each other if and only if $h_{i,j}$=1, in the matrix *H*. The following matrix is a parity-check matrix *H* (5,10,regular). It's corresponding Tanner graph is shown in Fig. 2.

$$H=\begin{pmatrix}1&1&1&1&0&0&0&0&0&0\\1&0&0&0&1&1&1&0&0&0\\0&1&0&0&1&0&0&1&1&0\\0&0&1&0&0&1&0&1&0&1\\0&0&0&1&0&0&1&0&1&1\end{pmatrix}$$

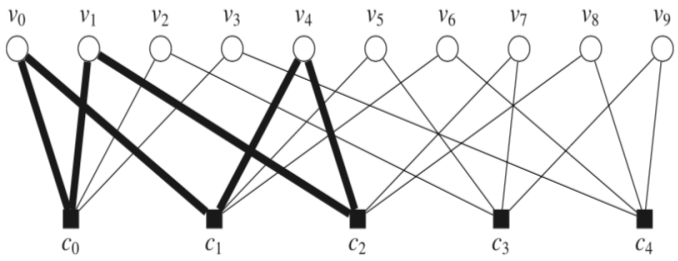

Fig. 2: Graphical representation (Tanner graph) of *H* (5,10, regular) with w_c=2, w_r=4 .

A loop or cycle is a close path of nodes that crosses over the edges of the Tanner graph. The shortest cycle in a Tanner graph is called the *girth* of graph. A cycle of the length 6 is illustrated in Fig. 2, by the bold edges. Hence, there is no cycle of length 4 in this graph, the length of its girth is 6. We investigate the BER performance of LDPC codes over AWGN channels from different points of view caused by the parameter variation.

We implement and decode the noisy corrupted codewords by utilizing iterative belief propagation decoding algorithm based on LDPC codes, which its performance strongly depends on the length of girth. As the length of girth increases, the computability of decoding algorithm increases. Furthermore, the BER performance can be improved by removing lower length cycles (i.e., increasing the length of girth). In our implementations, the minimum length of girth is assumed to be 6.

2-3- The LDPC Encoding Algorithm

A sequence of blocks each of them having *k* information bits are encoded by using the generator matrix *G*, which can be derived from the parity-check matrix *H* in different ways. Reader can refer to [25] for further explanation about deriving generator matrix *G*. For the obtained generator matrix *G*, we have GH^T=0.

Let consider *C* is the codeword of length *n* obtained from multiplying the information bit of length *k* and the generator matrix *G* with the size of $k\times n$. Thus, *C* forms the data that is modulated before transmission. *C* is a valid codeword if and only if CH^T=0. Therefore, the *C* is as follows,

$$C_{1,n} = D_{1,k}G_{k,n}\ , \tag{1}$$

where,

$$D= \{d_1\ d_2\ d_3 \ldots d_k\},$$

and

$$C= \{c_1\ c_2\ c_3 \ldots c_n\}.$$

Furthermore, k and n are respectively the length of the information packet bits and the length of the codeword C. Note that, n-k is the length of the redundancy which is added to the information bits for providing protection.

Besides, there is another encoding algorithm using LDPC codes which is called syndrome generation method. This method has a source coding and compression goal. A syndrome generated by using the parity-check matrix of an LDPC code is sent to the decoder as a lossless compressed data. Thus, for data n-tuple u, we send $s=uH^T$ to the decoder.

In this method, the decoder finds an estimation of u based on the received syndrome s by utilizing a syndrome decoding scheme. An efficient scheme for the syndrome decoding is SPA algorithm. In this scheme, in addition to the syndrome, a side information is needed. Actually, side information is a corrupted version of the original data u affected by the channel noise. Here, we briefly describe syndrome decoding scheme based on the SPA.

In this scheme, first the syndrome s is located in the CNs and the side information is located in VNs. Then, the message-passing SPA is run. For a given number of iterations, Log-Likelihood-Ratio (LLR) values are calculated and passed between CNs and VNs. The VN values are updated in each iteration based on the calculated LLR values. Finally, one can find the decoded data which are located in the VNs of the Tanner graph of the LDPC code with parity-check matrix H.

2-4- The Sum-Product Decoding Algorithm

The message-passing algorithms are iterative decoding procedures, in which some messages are passed back and forward between the VNs and CNs until the process is stopped. The bit-flipping decoding algorithm is one of the message-passing algorithms in which the received symbols are hard decoded into 1's and 0's.

The SPA is similar to the bit-flipping algorithm, but the bit-flipping decoding is a kind of hard decisions while the SPA is a soft decision message-passing algorithm that utilizes the probability of each bit instead of its value. The extrinsic data between j-th CN and i-th VN which is the probability of c_i=1 is denoted by $E_{j,i}$ as the j-th parity check equation is satisfied.

The probability that a parity-check equation is established for the bit c_i to be 1 is represented by P that is calculated as follows:

$$P_{j,i}^{ext} = \frac{1}{2} - \frac{1}{2}\prod_{i' \in B_j, i' \neq i}(1 - 2P_{j,i'}), \quad (2)$$

where B_j is the set of VNs which is connected to j-th CN.

LLR is a metric for a binary variable that is represented by L and is as follows:

$$L(\mathrm{c}) = \log \frac{P(\mathrm{c}=0)}{P(\mathrm{c}=1)}. \quad (3)$$

The sign of $L(\mathrm{c})$ makes a hard decision on c and its magnitude $|L(\mathrm{c})|$ shows the reliability of the decision rule. Thus, the probability of c can be obtained from LLR as follows:

$$p(\mathrm{c}=1) = \frac{e^{-L(c)}}{1+e^{-L(c)}}, \quad (4)$$

$$p(\mathrm{c}=0) = \frac{1}{1+e^{-L(c)}}, \quad (5)$$

the main reason of exploiting LLR metric is that when probabilities need to be multiplied to each other, then logarithms just need to be added, hence, the complexity of calculations decreases. The information that are transferred from j-th CN to i-th VN is expressed as a LLR that it's value is as follows:

$$E_{j,i} = L(P_{j,i}^{ext}) = \log \frac{1-P_{j,i}^{ext}}{P_{j,i}^{ext}}. \quad (6)$$

Hence,

$$\begin{aligned} E_{j,i} &= \log \frac{\frac{1}{2} + \frac{1}{2}\prod_{i' \in B_j, i' \neq i}(1-2P_{j,i'})}{\frac{1}{2} - \frac{1}{2}\prod_{i' \in B_j, i' \neq i}(1-2P_{j,i'})} \\ &= \log \frac{1 + \prod_{i' \in B_j, i' \neq i}(1 - 2\frac{e^{-L(P_{j,i'})}}{1+e^{-L(P_{j,i'})}})}{1 - \prod_{i' \in B_j, i' \neq i}(1 - 2\frac{e^{-L(P_{j,i'})}}{1+e^{-L(P_{j,i'})}})} \\ &= \log \frac{1 + \prod_{i' \in B_j, i' \neq i}(\frac{1 - e^{-L(P_{j,i'})}}{1 + e^{-L(P_{j,i'})}})}{1 - \prod_{i' \in B_j, i' \neq i}(\frac{1 - e^{-L(P_{j,i'})}}{1 + e^{-L(P_{j,i'})}})}. \end{aligned} \quad (7)$$

By using the following relation,

$$\tanh\{\frac{1}{2}\log(\frac{1-P}{P})\} = 1-2P, \quad (8)$$

it can be concluded that,

$$E_{j,i} = \log \frac{1 + \prod_{i' \in B_j, i' \neq i} \tanh(L(P_{j,i'})/2)}{1 - \prod_{i' \in B_j, i' \neq i} \tanh(L(P_{j,i'})/2)}, \quad (9)$$

and by using the relation,

$$2\tanh^{-1} p = \log \frac{1+p}{1-p}, \quad (10)$$

we can write,

$$E_{j,i} = 2\tanh^{-1} \prod_{i' \in B_j, i' \neq i} \tanh(L(P_{j,i'})/2). \quad (11)$$

The value of $L(P_{j,i'})$ can be separated to its sign and its magnitude as follows:

$$L(P_{j,i'}) = S_{j,i'} M_{j,i'} , \quad (12)$$

where,

$$S_{j,i'} = \text{sign}(L(P_{j,i'})) , \quad (13)$$

$$M_{j,i'} = |L(P_{j,i'})| . \quad (14)$$

Thus, equation (11) can be rewritten as

$$\tanh\left(\frac{1}{2}L(P_{j,i'})\right) = \prod_{i' \in B_j, i' \neq i} S_{j,i'} . \prod_{i' \in B_j, i' \neq i} \tanh(\frac{1}{2} M_{j,i'}) . \quad (15)$$

Therefore,

$$E_{j,i} = \prod_{i'} S_{j,i'} . 2\tanh^{-1}(\prod_{i'} \tanh(\frac{1}{2} M_{j,i'}))$$

$$= \prod_{i'} S_{j,i'} . 2\tanh^{-1} \log^{-1}\log(\prod_{i'} \tanh(\frac{1}{2} M_{j,i'}))$$

$$= \prod_{i'} S_{j,i'} . 2\tanh^{-1} \log^{-1} \sum_{i'} \log(\tanh(\frac{1}{2} M_{j,i'}))$$

$$= \prod_{i'} S_{j,i'} . \emptyset(\sum_{i'} \emptyset(M_{j,i'})) , \quad (16)$$

where $\emptyset(x)$ is defined as follows:

$$\emptyset(x) = -\log(\tanh(x/2)) = \log(\frac{e^x + 1}{e^x - 1}) . \quad (17)$$

In the SPA each VN has access to the initial LLR and LLRs from connected CNs because probability passes between nodes. The total LLR of the i-th bit is as follows:

$$L_i^{\text{total}} = L_i + \sum_{j \in A_i} E_{j,i} , \quad (18)$$

where A_i is the set of CNs connected to i-th VN.

The decoder is initialized by setting VN information $L(P_{j,i})$, for which $h_{i,j}$=1, as follows:

$$L_i = L(c_i|y_i) = \log(\frac{P(c_i=0|y_i)}{P(c_i=1|y_i)}) , \quad (19)$$

where y_i is the i-th information bit value that has been received. L_i can be calculated for the binary input AWGN channel as follows:

$$P(x_i = x|y_i) = \frac{1}{1+\exp(-4y_i x/N_0)} , \quad (20)$$

from equation (20),

$$L_i = L(c_i|y_i) = - 4y_i/N_0 , \quad (21)$$

where N_0 is the noise power spectrum density.

After calculating total LLR for every VN, $\hat{C}$ is obtained as follows:

$$\hat{C}_i = \begin{cases} 1 & \text{if } L_i^{total} < 0 \\ 0 & \text{else,} \end{cases} \text{ , for } i=1, 2, \ldots, N; \quad (22)$$

where N is the length of codewords.

The accuracy of decoded data $\hat{C}$ can be obtained by multiplying $\hat{C}$ and H^T. If $\hat{C}H^T = 0$, then the decoded data is correct, else LLRs should update as follows:

$$L(P_{j,i'}) = \sum_{j' \in A_i, j' \neq j} E_{j',i} + L_i . \quad (23)$$

These operations continue until the parity-check equations are satisfied ($\hat{C}H^T = 0$), or the number of iteration equals the maximum limit which has been considered.

3- Simulation Results

In this section, we report some simulation results which are obtained from implementation of the described communication system. All BER values are averaged over 50 tests for randomly generated binary sequences as an information source.

The BER performance of a PSK modulated communication is presented with respect to the number of iterations, the code length, and coding rate. A fair comparison is done for various values of the signal to noise ratio.

After decoding received data in receiver the number of bits that have not received correctly can be simply obtained by comparing the received bits in the receiver and transmitted bits of the transmitter. The BER is calculated by dividing the number of incorrect received bits to the number of total received bits.

In Fig. 3, it is depicted that the BER decreases by increasing the number of iterations in the SPA with a same parity-check matrix H (384,512,irregular) with the rate of $\frac{1}{4}$. This observation is because of increasing the number of runs in update equations of the SPA.

For instance, the BER is 5.46×10-6, 3.91×10-6, and 2.8×10-6 respectively for the cases of iteration=10, iteration=20, and iteration=50 in SNR=6db.

Based on the results, which is reported in Fig. 4, it is obvious that the BER decreases by increasing the size of the parity-check matrix H. This fact stems from the direct effect of increasing length. Note that, by increasing the size of H, complexity of implementations increases. For example, the BER is 3.91×10-6 and 1.17×10-8 respectively for H(384,512,irregular) and H(768,1024,irreglar), with the rate of $\frac{1}{4}$ and iteration=20 in SNR=6db.

The effect of increasing the number of added redundancy to a same information block with a constant length to the BER performance is presented in Fig. 5. As it is seen, the BER value decreases by increasing redundancy or equivalently by decreasing coding rate.

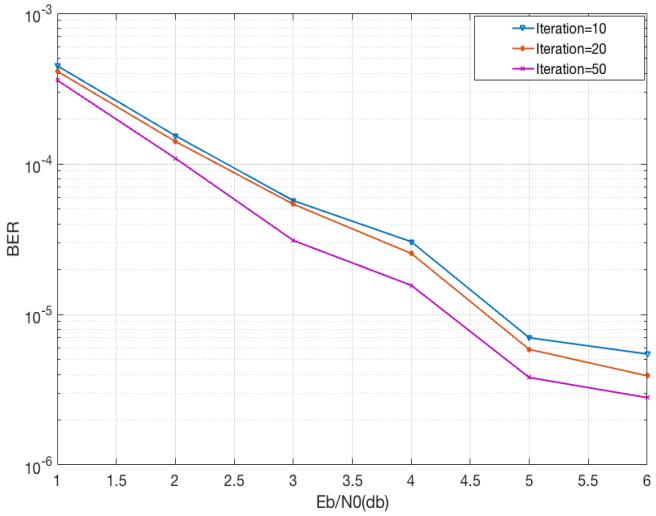

Fig. 3: The BER performance of code H (384,512,irregular).

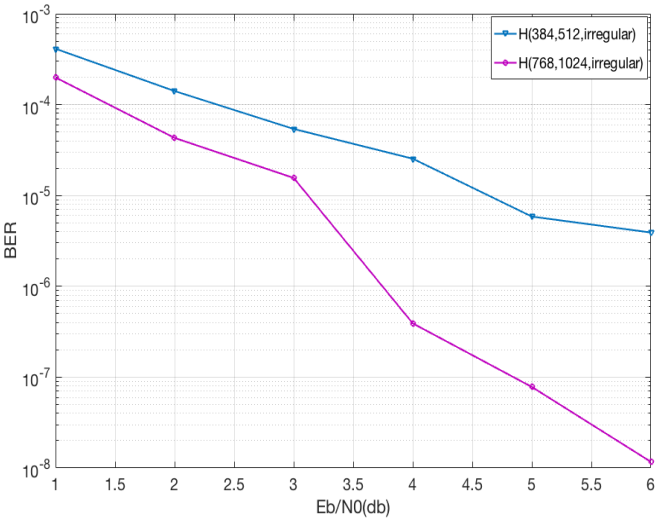

Fig. 4: The BER performance of H(384,512,irregular) and H(768,1024,irreglar). Rate is 0.25 and the number of iterations is 20.

As an example, the BER is 2.97×10^{-3}, 6.72×10^{-4}, 8×10^{-7}, and 8×10^{-11} respectively for rate= $\frac{2}{3}$, rate= $\frac{1}{2}$, rate= $\frac{1}{4}$, and rate= $\frac{1}{8}$ in SNR=7db.

Based on the reported results, it is seen that the SPA is reliable with respect to parameter changes and can be utilized for the BPSK modulation scheme with an acceptable performance. In the design process, one can choose proper rate, number of iterations and length to reach a required quality of service.

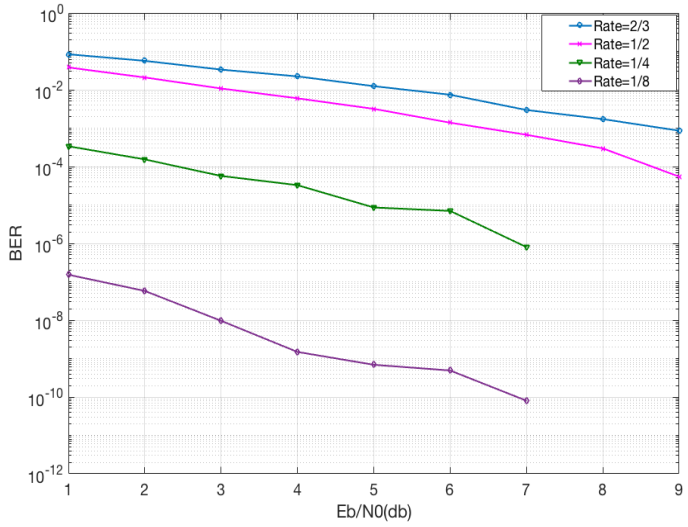

Fig. 5: The BER performance for four LDPC codes H_1(64,192,irregular), H_2(128,256,irregular), H_3(384,512,irregular), and H_4(896,1024,irregular) with iteration=10.

4- Conclusions

In this paper, a point-to-point communication system is investigated. Our focus is on the channel encoder and the channel decoder blocks and their BER performances. The LDPC codes are employed for the channel encoder block and the SPA with the same parity-check matrix of encoder are exploited for the channel decoding. The BER performance of the system under AWGN communication channel model with PSK modulation scheme is derived from implementations for various cases. Our simulation results show the effect of the parameter changes in order to achieve lower BER values. This provide the direction of parameter changes to a system designer to improve the performance.

Appendix

Here, we present the degree distributions of the parity-check matrices, which have been used in our implementations for some rates. Note that the parity-check matrices are obtained from these degree distributions by using progressive edge growth method with some approximations.

For the rate of 0.75, we have:

$\lambda(x) = 0.2911x + 0.1892x^2 + 0.0408x^4 + 0.0873x^5 + 0.0074x^6 + 0.1126x^7 + 0.0925x^{15} + 0.0186x^{20} + 0.124x^{32} + 0.016x^{39} + 0.0202x^{44}$,

and

$\rho(x) = 0.8x^4 + 0.2x^5$.

For the rate of 0.66, we have:

$\lambda(x) = 0.2177x + 0.1634x^2 + 0.098x^5 + 0.1018x^6 + 0.0538x^{13} + 0.0301x^{16} + 0.0566x^{20} + 0.0109x^{26} + 0.0809x^{30} + 0.1863x^{99}$,

and

$\rho(x) = 0.9x^6 + 0.1x^7$.

For the rate of 0.5, we have:

$\lambda(x) = 0.1528x + 0.2825x^2 + 0.0062x^3 + 0.5586x^{19}$,

and

$\rho(x) = x^9$.

For the rate of 0.25, we have:

$\lambda(x) = 0.1118x + 0.1479x^2 + 0.0721x^5 + 0.2464x^6 + 0.0021x^8 + 0.4195x^{29}$,

and

$\rho(x) = x^{23}$.

For the rate of 0.125, we have:

$\lambda(x) = 0.1154x + 0.1846x^2 + 0.1872x^6 + 0.0107x^7 + 0.0107x^8 + 0.0298x^9 + 0.0676x^{17} + 0.0713x^{21} + 0.0311x^{22} + 0.0523x^{25} + 0.194x^{65} + 0.0148x^{69} + 0.0192x^{72} + 0.0021x^{89} + 0.0086x^{99}$,

and

$\rho(x) = 0.5x^{45} + 0.5x^{46}$.

References

[1] C. Berrou, A. Glavieux, and P. Thitimajshima, "Near Shannon limit error-correcting coding and decoding : Turbo-codes," In Communications, 1993. ICC '93 Geneva. Technical Program, Conference Record, IEEE International Conference on,, vol. 2, pp. 1064–1070.

[2] C. E. Shannon, "A mathematical theory of communication," Bell System Technical Journal, vol. 27, 1948, pp. 379–423 and 623–656.

[3] D. J. C. MacKay and R. M. Neal, "Near Shannon limit performance of low density parity check codes," IEEE electronics letters 32, no. 18 ,1996, pp. 1645-1646.

[4] D. J. C. MacKay, "Good error-correcting codes based on very sparse matrices," IEEE Transactions on Information Theory, vol. 45, no. 2, Aug 1999, pp. 399–431.

[5] H. Hatami, DG. Mitchell, DJ. Costello, TE. Fuja. "Performance bounds and estimates for quantized LDPC decoders". IEEE Transactions on Communications. 2019 Nov 13;68(2):683-96.

[6] R.G. Gallager, "Low-density parity-check codes," IRE Trans. Inf. Theory, 1962, IT-8, pp. 21–28.

[7] B. Rong, Y. Wu and G. Gagnon, "Multi -Layer Iterative LDPC Decoding for Broadband Wireless Access Networks: A Recursive Shortening Algorithm," IEEE Transactions on Wireless Communications, vol. 12, no. 3, March 2013, pp. 1320–1327.

[8] T. Koike-Akino, K. Kojima, D.S. Millar, K. Parsons, T. Yoshida and T. Sugihara, "Pareto Optimization of Adaptive Modulation and Coding Set in Nonlinear Fiber-Optic Systems," Journal of Lightwave Technology, Vol. 35, no. 4, February 2017, pp.1041–1049.

[9] R. Xue, H. Yu and Q. Cheng, "Adaptive Coded Modulation Based on Continuous Phase Modulation for Inter-Satellite Links of Global Navigation Satellite Systems," IEEE Access, vol. 6, April 2018, pp. 20652–20662.

[10] S. Chen, K. Peng, J. Song and Y. Zhang, "Performance Analysis of Practical QC-LDPC Codes: From DVB-S2 to ATSC 3.0," IEEE Transactions on Broadcasting, vol. 65, no. 1, March 2019, pp. 172–178.

[11] J. Song, C. Zhang, K. Peng, J. Wang, C. Pan, F. Yang, J. Wang, H. Yang, Y. Xue, Y. Zhang, and Z. Yang, "Key Technologies and Measurements for DTMB-A System," IEEE Transactions on Broadcasting, vol. 65, no. 1, March 2019, pp. 53–64.

[12] S.-K. Ahn, K.-J. Kim, S. Myung, S.I. Park and K. Yang, "Comparison of Low-Density Parity-Check Codes in ATSC 3.0 and 5G Standards," IEEE Transactions on Broadcasting, vol. 65, no. 3, September 2019, pp. 489-495.

[13] KS. Chan, A. James, S. Rahardja. "Evaluation of a Joint Detector Demodulator Decoder (JDDD) Performance With Modulation Schemes Specified in the DVB-S2 Standard". IEEE Access. 2019 Jun 19;7:86217-25.

[14] S. Papaharalabos and P. T. Mathiopoulos, "Simplified sum-product algorithm for decoding LDPC codes with optimal performance," Electronics Letters, vol. 45, no. 2, January 2009, pp. 116-117.

[15] IB. de Almeida, GP. Aquino, LL. Mendes. "Iterative Receiver for Non-Orthogonal Waveforms Based on the Sum-Product Algorithm". In 16th International Symposium on Wireless Communication Systems (ISWCS) 2019 Aug 27, pp. 38-42.

[16] F. Vatta, A. Soranzo, F. Babich. "More accurate analysis of sum-product decoding of LDPC codes using a Gaussian approximation". IEEE Communications Letters. 2018 Dec 11;23(2):230-3.

[17] J. Ziv and A. Lempel, "A Universal Algorithm for Sequential Data Compression," IEEE Transactions on Information Theory, vol. 23, no. 3, May 1997, pp. 337–343.

[18] J. Ziv and A. Lempel, "Compression of Individual Sequences via Variable-Rate Coding," IEEE Transactions on Information Theory, vol. 24, no. 5, September 1978, pp. 530–536.

[19] J. A. Storer and T. G. Szymanski, "Data Compression via Textual Substitution," Journal of the ACM, vol. 29, no. 4, October 1982, pp. 928–951.

[20] M. Nangir, H. Behroozi, and M. R. Aref, "A new recursive algorithm for universal coding of integers". Journal of Information Systems and Telecommunication (JIST), vol. 3, no. 1, Jan 2015, pp. 1–6.
[21] M. Nangir, R. Asvadi, M. Ahmadian-Attari, and J. Chen, "Binary CEO problem under log-loss with BSC test-channel model", In 2018 29th Biennial Symposium on Communications (BSC), IEEE, Jun 2018, pp. 1–5.
[22] D. Harita, KP. Rajan. "Reliability Variance based Weighted Bit Flipping Algorithms for LDPC". In 9th International Conference on Cloud Computing, Data Science & Engineering (Confluence), 2019 Jan 10, pp. 593-595.
[23] J. Liu, J. Yuan, J. Sha. "Symbol-Based Algorithms for Decoding Binary LDPC Codes with Higher-Order Modulations". In IEEE International Symposium on Circuits and Systems (ISCAS) 2019 May 26, pp. 1-5.
[24] R. Tanner, "A recursive approach to low complexity codes," IEEE Transactions on Information Theory, vol. 27, no. 5, 1981, pp. 533–547.
[25] T. Richardson and R. Urbanke, "Efficient encoding of low-density parity-check codes," IEEE Transactions on Information Theory, vol. 47, no. 2, Feb 2000, pp. 638–656.

Hadi Khodaei Jooshin received the B.S. degree in Telecommunication, Electrical Engineering from University of Tabriz, Tabriz, Iran in 2020. Currently he is working on extending iterative channel decoding algorithms for special applications. His area research interests include Channel Coding and Information Systems, Image Processing, Machine Learning and Signal Processing.

Mahdi Nangir received the B.Sc. degree with first rank in Electrical Engineering from University of Tabriz and M.Sc. degree in Communication System Engineering from Sharif University of Technology, Tehran, Iran, in 2010 and 2012, respectively. He received the Ph.D. degree from K. N. Toosi University of Technology, Tehran, Iran, in 2018. He was a finalist of the Mathematics Olympiad and owner of bronze medal in 2005 from Young Scholar Club. He received high ranks in Iranian National Electrical Engineering Student Olympiads of 2009 and 2010. In 2017, he joined McMaster University, Hamilton, Ontario, Canada as a research visiting student. He is now an assistance professor in Faculty of Electrical and Computer Engineering, University of Tabriz, Tabriz, Iran. His research interests include coding and information theory, distributed source coding, data compression algorithms and optimization.

Sailor Localization in Oceans Beds using Genetic and Firefly Algorithm

Shruti Gupta*
Student, Amity University
Shrutigupta.it@gmail.com
Dr Ajay Rana
Professor, Amity University
ajay_rana@amity.edu
Dr Vineet Kansal
Pro Vice Chancellor - Dr. A.P.J. Abdul Kalam
vineetkansal@ietlucknow.ac.in

Received: 23/July/2019 Revised: 28/Sept/2020 Accepted: 08/Nov/2020

Abstract
The Localization is the core element in Wireless Sensor Network WSN, especially for those nodes without GPS or BDS; leaning towards improvement, based on its effective and increased use in the past decade. Localization methods are thus very important for estimating the position of relative nodes in the network allowing a better and effective network for increasing the efficiency and thus increasing the lifeline of the network. Determining the current limitations in FA that are applied for solving different optimization problems is poor exploitation capability when the randomization factor is taken large during firefly changing position. This poor exploitation may lead to skip the most optimal solution even present in the vicinity of the current solution which results in poor local convergence rate that ultimately degrades the solution quality. This paper presents GEFIR (GenFire) algorithm to calculate position of unknown nodes for the fishermen in the ocean. The proposed approach calculates the position of unknown nodes, the proposed method effectively selects the anchor node in the cluster head to reduce the energy dissipation. Major benefits over other similar localization algorithms are a better positioning of nodes is provided and average localization error is reduced which eventually leads to better efficiency thus optimize the lifetime of the network for sailors. The obtained results depict that the proposed model surpasses the previous generation of localization algorithm in terms of energy dispersion and location estimation which is suitable for fishermen on the ocean bed.

Keywords:. Wireless Sensor Network; localization; firefly; Genetic Algorithm.

1- Introduction

By the symphony of the wind carrying the burden of the IOT technology that is transposing the means by which individuals strive, a huge deprivation leads to more utilization thus leading to a better solution. IOT having the similar case requiring node positioning for various real life application[1-7], our work revolves around the requirement of node localization and positioning in WSN (backbone of IOT) ; as depicted by various leaflet about 80% of the contingent information is related to location [2].WSN(Wireless Sensor network) is a substantial unit of IOT and is defined as a group of sensor network that are randomly distributed over a particular area that tends to provide different information in an orderly fashion [1-3].Upon diagnosing the problem with GPS and BDS: the cost of installation, the energy required to run them and the space that the technology occupy, a better approach of providing GPS/BDS for the few of the nodes (beacon nodes) are used and others are positioned using localization algorithm. Therefore, a better and more suitable localization algorithm for bettr positioning the nodes is required.

Location has been an important aspect in practical usage of any wireless sensor network thus localization is important, making it important to construct various localization algorithms based on the needs.

Localization algorithms can be defined as a group of algorithms which are used by the WSN to make decisions in real time based on local and limited knowledge unlike global network knowledge. Thus, 'locality' is often referred to as the knowledge processed by the WSN in its area of reach.[8]

Localization thus consists of the problem of finding the geographical location of a node in a WSN, which can be calculated either by a central WSN that contains the global network knowledge or a more practical approach in which

WSN are spread in a distributed manner. [9,10,11,12,13,14]

Localization can be broadly classified into two categories: Ranged based and Range free algorithms.

Range based algorithms shine in accurate positioning of the WSN in a specific distance but at the high cost of deployment and need high end hardware. Range based algorithms efficiently use ranging techniques and operate on the distance measurement between different internodes for calculating location of nodes. Some of the range-based algorithms are Received Signal Strength Indicator (RSSI), Time of Arrival (ToA), and Time Difference of Arrival (TDoA) [15]. Due to the high cost of deployment and taking into account the efficiency, Range free algorithms are used as they don't require high tier hardware and rather are operated on connectivity, multi-hop routing and other real time-shared information for calculating the distance between the nodes. Range free algorithms have their research oriented towards hop-count estimation that is based on the probability that there exists a function which can be mapped such that the physical distance between the nodes is somewhat related to the smallest hop-counts. But due to the deployment of sensor nodes in complex scenarios, mapping function can no longer be defined accurately resulting in blunders which yield errors. Another major problem with multi-hop is ambiguity. Another example is Centroid localization algorithm which computes the position of nodes based on supported close sensors among a pre outlined radio range. The main advantage is its low computational complexity but it has a high location estimation error that is dependent on the node density (The number of nodes located in a particular range respective to the centroid node) [16].

Table1 : The chosen method depends upon the application requirement and scenario

Algorithm for Distance computation	***Correctness***	***Range of communication***	***Additional Hardware***	***Challenging Encounters***
Received Signal Strength Indicator: RSSI	2 meter - 6 meters	Few inches to 40-50 meter	None	Interference due to environment
Time Difference of Arrival: TDoA	2 centimeter – 4 centimeters	2 meter-15 meters	Ultrasound Transmitter	Maximum distance of deployment
Time of Arrival: ToA	2 centimeter – 4 centimeters	Communication range	None	Synchronization
Angle of Arrival: AoA	A few degree (6˚)	Communication range	Receivers set	Limited to small sensor nodes
Communication range	Half the distance of communication range	Communication range	None	None

The choice of computational algorithm to use to estimate the distance between to nodes in a wireless sensor network majorly affects the final performance of the system; but we can't simply take into account the final performance rather other factors like size of hardware and cost is equally important for the sake of which the position estimation method is chosen wisely. Table 1 compares each one of the range free distance computational algorithms. The chosen method of computation solely depends upon the available resources and requirements.Due to unsatisfactory processing of both range free and range-based algorithms and the need for more accurate positioning and better lifetime several proposals have been made which consist of artificial intelligence techniques which use soft computing algorithms, optimization techniques etc. and because of their ability to solve the optimization problem in uncertain scenarios and provide better results.

Artificial intelligence localization techniques have been used in previous research, including Artificial Neural Network (ANN) [17], Neural Fuzzy Inference System (ANFIS) [18], Fuzzy logic [19], and optimization algorithms, such as Genetic Algorithms [20], Particle Swarm Optimization (PSO) [21], Bacterial Foraging Algorithm (BFA) [22], and Gravitational Search Algorithm (GSA) [23].

These Artificial intelligence localization techniques are generally combined with baseline algorithms that are range based and range free algorithms which provide some degree of betterment but still unsatisfactory results are obtained.

1-1- Paper Organization

The flow of paper is organized as follows in section 2 the literature review gives the details about various implementations of localization algorithm, A and firefly and identification of gap in same. Section 3 describes the methodology of GEFIR algorithm that gives the detailed description of implementing the proposed algorithm, Section 4 gives the simulation and result of GA Firefly and GEFIR and comparison between them based on different parameters.

2- Related work

Localization holds a major aspect in WSN and is thus optimized by various entities across the globe in different fashion [24,25].

Localization is in this way required as about 13.7% of streamlining includes localization angle [26].There are numerous calculation, for example, Localization-network, bionics restriction calculation centroid confinement calculation, district cover confinement calculation, bionics confinement calculation, checklimitation calculation, milestone arrangement limitation calculation, milestone overhaul limitation calculation, limitation calculation, geometric limitation calculation, way arranging limitation calculation, time confinement calculation and likelihood circulation confinement calculation that are talked about and future examination bearings in limitation are suggested.[26] The proposition talked about above spotlights just on one procedure to improve the outcomes while a few substances have even delivered half and half models conveying more than one enhancement calculations.A cross breed approach including Fuzzy Logic and GAs was distributed by Yun et al. [27], who incorporated a half and half model along these lines ad-libbing his past working [28], which utilized just a FL approach, by joining those two techniques to determine the correct loads. At first, GA algo was utilized to alter the participation capacity of FL (utilizing an iterative process) for edge loads dependent on RSSI data. In any case, this technique has restrictions like the GA-based confinement strategy: it accepts that the real position is realized while figuring the mean square mistake. Additionally, an in half and half methodology including NNs and GAs was assessed and talked about by Chagas et al. [29], in which the GA was utilized to determine ideal boundaries preceding contribution to at that point, yet once more, these techniques include an exchange among precision and multifaceted nature. Rather than applying FL to determine the weight legitimately, Huan Xiang Et al. [30] integrated GAs to alter the weighted centroid estimation to accomplish higher exactness dependent on signal quality sources of info and restriction reference data. Additionally, Yang et al. [31] applied GAs utilizing a channel recharging methodology to deliver better combination—a procedure that can be utilized with enormous scope WSNs. Here, the wellness work was gotten from the genuine area of the assessment.

Table 2 : Methods for position estimation

Method	Rfes	Distance required for computation?	Angle required for computation?	Complexity	Challenging Encounters
Trilateration	3	Yes	No	F(1)	Vulnerable to wrong distance
Multiliterate	a≥3	Yes	No	F(a3)	Computational complexity
Triangulation	3	No	Yes	F(1)	Extra Hardware required
Probabilistic	a≥3	Yes	No	F3d2 (d=grid)	Space and Computational complexity
Bounding box	a≥2	Yes	No	F(a)	Final position error
Central Position	a≥1	No	No	F(a)	Final position error

For the algorithms to work distance estimation (as answered in table 1) and position estimation is required. Position estimation is based on the strategic deployment of different method which uses the distance estimated from the algorithms explained in table 1 and deploy them to estimate accurate and correct position using methods – Trilateration,Multiliterate,Triangulation,Probabilistic, bounding box, Central position as depicted in Table 2.

2-1- Motivation

Upon studying the annual rate of sailor deaths due to weather hazards and unable to reach the shore on time the idea of deploying WSN onto this particular problem statement was developed. Being aware that the node position would be the key issue in order to locate precisely the sailors, a new algorithm was proposed keeping the challenges of the Sailors in mind. Thus, a new GEFIR algorithm was proposed and deployed. The lives of sailors are constantly endangered due to the abnormal weather aspects shown over the past few years in different parts of the

world. Working on the same problem and trying to get a way out of it a wireless sensor network deployment was introduced on the sailors that are deployed on the sea bed. A new algorithm was considered to be introduced that would consider mobile beacon nodes and anchor nodes that would help the sailors (small fishermen) to be easily located and can be rescued in case of an emergency. The proposed WSN is built and tweaked keeping the problem statement of the sailors in mind and thus the algorithm is capable of both optimizing the large area and accurately finding the relative accurate position of the sailors.

3- Methodology and Implementation

3-1- Proposed Mechanism for Node localization

The proposed gear for routing data based on the localization is based on the natural selection as done in firefly algorithm [31] by creating a newly developed algorithm for estimating nearly exact location of the sailors. The proposed algorithm
helps to achieve better accuracy in a cost effective and energy efficient manner.
The localization system can be divided into 3 distinct parts that are distance estimation, position computation and then the most important phase localization algorithm. As figure 1 shows the complete description of implementing GEFIR algorithm. As in the paper to obtain the results we started with initialization of the parameter for both GA and FA. Then we have generated the random population and on the random population we applied the objective function. For each iteration calculate the distance then we update all the positions in firefly for all the offspring. We are applying GA to populate more offspring of best fireflies. We will compute till either we reached our results or till the maximum iterations. As the implementation approach divides in three stages. In the bottom of the paper each stage describing their own working.

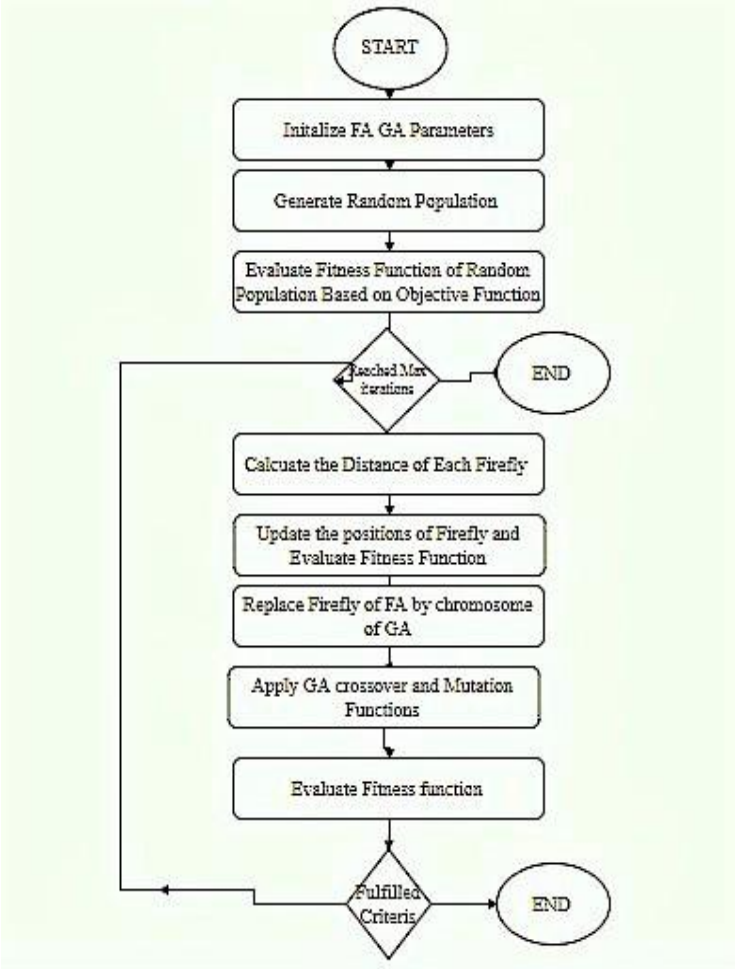

Fig 1: Implementation Methodology for Gefir Algorithm

3-2- Stage 1: Initialization

Deployment scheme: Distance and Position estimation

Action: This type of estimation constitutes of 2 steps

i. Distance calculation

ii. Position estimation for the nodes.

Distance estimation component is accountable for computing the distance between the two nodes which can serve as valuable information

The System of equation is described as below

$$x - \varkappa i2 + y - yi2 = i2 - \varepsilon \quad (1)$$

$$x - \varkappa n2 + y - yn2 = n2 - \varepsilon \quad (2)$$

The distance of unknown nodes is calculated using the RSSI value as it doesn't require any additional hardware and most radios can receive it directly. Firstly, the anchors diffuse their neighbor traditional nodes then receive the transmitted beacon from links and measure the strength. Then position is calculated on the basis of RSSI by the beacon nodes. The method used for computing the position is multilateration.This method was initially developed for the military as then it didn't want to be seen. In this case scenario we opted this method as there won't be the possibility of clear visibility on the sea bed.

I=1to N

ε is the random variable with 0 mean

The above system can be linearized and can be solved using the standard method like least square [33,34]The computed position using this method is defined as:

$$f(x, y) = i = 1nx - \varkappa i2 + y - yi2 - di22 \quad (3)$$

Where, xi and yi are the position coordinates of the ith reference node, di is the estimated distance.

Table3 : Pseudo code for Genetic Algorithm

Genetic Algorithm
1. Encrypt the solution space
2. set Pop Size, MaximumGen and Gen=0
a. set CrossRate
b. set MutationRate
Initialize population
while MaximumGen>=Gen
. Compute fitness
a. for 1 to PopSize
i. select Parent1 and Parent2
ii. if (rand (0,1) <CrossRate)
1. child=crossover (Parent1, Parent2)
iii. if(rand (0,1) <MutationRate)
1. child=Mutation (Chromosome)
b. end for
c. add OffSpring to the new generation
d. Gen=Gen+1
end while
return best Chromosome.

3-3- Stage2: Deployment Scheme: Genetic Algorithm

Action: This type of algorithm is used to obtain a better optimized result over a huge space. Nature selects what's best for the world and going by this principle of selecting the most optimized path is the purpose of this algorithm as devised by John Holland in 1960 based on Darwin's theory of evolution this algorithm was proposed[35].They are mostly used to generate high quality optimization results over a larger data set by going through the tunnel of processes like natural selection, mutation and crossover[36].Major advantage and the basic purpose to select this particular algorithm is that It doesn't have the need for derivative information which in this case may or may not be available at first glance. Other features include the optimization ability of the algorithm to optimize both continuous and discrete functions depending upon the function deployed on the problem statement. Basic terminology is described as below

i. Population: The total number of nodes constitutes the population

ii. Chromosomes: Defines the set of coordinated i.e. a chromosome contains 2 genes; the 1st gene defining the x coordinate of the node and the 2nd gene defining the y coordinate of the node.

iii. Gene: A gene is one element position of a chromosome; for this particular set it contains 2 genes-x and y coordinate

iv. Allele: The numeric value of a gene.[18]

A genetic algorithm initializes with an initial population which is made up of a set of solutions. This population then evolves into a different population as generation passes and lastly the best individual is returned as the solution of the problem. For each generation the evolution is preceded by a fixed set of rules [36]. The two parents from the population are chosen and based on some traits they are allowed to be a crossover operator to produce a new generation offspring containing traits of both the parents. The offspring is then modified by mutation operators to generate an unexplored search space to the population thus enhancing the diversity. After a while the offspring replace the entire population and thus evolution is met and it is continued until desired condition is met.

3-4- Stage 3: Localization Algorithm Using FA

Deployment scheme: Firefly Algorithm

Action: This algorithm shines out in fine tuning but in a small space.

Firefly algorithm was constructed and implemented by Dr.Xin She Yang in 2008 and is based on the mating behavior of fireflies [32]. Fireflies use their ability to produce natural light to lure their mate or prey. Also known as the lightning bug there are around 2000 species which have the capability to generate short and rhythmic flashes. Flashes from these bugs even so often appear to be in a particular pattern and generate an amazing sight among the tropical areas throughout summer. If a firefly is starving or looking for a mate its light-weight glows brighter to make the attraction of mates additionally sensible. The brightness of the light-weight depends on the accessible quantity of a pigment referred to as 'luciferin', and tons of pigment suggests that tons of light-weight

Table 4 : Pseudo Code for Firefly Algorithm

Firefly Algorithm

```
        for i = 1:N
Randomly generate xi within the range
        End for i
        Estimate the function values of the firefly population
        do while (criteria for terminating is not accomplished)
.       for i = 1: N
                    i.    for variable j = 1: N
                      1.  If ObjectiveFunction(xj) <ObjectiveFunction(xi)
                      2.  If (Ij>Ii), move firefly i towards j
                      3.  End if
                      4.  Calculate new solutions and keep posted the light intensity;
                    ii.   end for j
end for i
Compute the new population
Note the best solution generated
        end while
```

Based on the above mention communication phenomenon of fireflies, the SFA consists of set rules:

firefly will be engrossed by other fireflies regardless of their gender. Attractiveness is proportional to their light-weight(brightness) and diminution occurs as the distance among them surges.

The landscape of the objective function determines the brightness of a firefly [20] Instead of old firefly algorithm a new modified firefly algorithm is deployed which would reduce the issue of formulation of attractiveness and irregularity due to variation in intensity.[11] The construction of firefly algorithm for the proposed problem is defined as follows. Initially the brightness is calculated using the function(x,y) is computed using equation 3Next attractiveness between the firefly is calculated using eq3. Attractiveness refers to the movement of the ith firefly to the brighter jth firefly.

$$qr = q0e - r2 \quad (4)$$

Where,q0 is the attractiveness at r=0; is the absorption factor; r is the distance between the two fireflies Where distance function ribest is defined by the equation:

ribest = ϰi − ϰgb2 + yi − ygb2 (5)

Depending upon the values obtained by the above-mentioned equation movement is given by the equation:

xi = ϰi + (q0e − ρrij2(ϰj − ϰi) + q0e − ρrib2(ϰgb − ϰi)) + □Ƶ + ℝƵ (ϰi − gb) (6)

Where $q0e - \rho rij2(\varkappa j - \varkappa i) + q0e - \rho rib2(\varkappa gb - \varkappa i)$ is the attractiveness module;

□ - randomizing parameter.

In this algorithm the randomizing parameter is not kept fixed rather than a changing parameter which is linearly decreasing as the iteration gradually increases. This particularly helps in finding the balance between exploration and exploitation.

gb – represents the current global best which is used to redefine the measure and movement of the firefly. The above-mentioned algorithm is run for 100 iteration or till convergence is obtained. The position of the brightest firefly is the ideal location of the sensor node as calculated. Firefly algorithm.

3-5- Stage 4: Proposed Algorithm-GEFIR:

The GEFIR algorithm provides accurate and more timely information to the WSN as deployed for the sailors. GEFIR; it accomplishes path tuning to estimate unknown nodes and then by the fine-tuning capabilities nodes positions are estimated. The proposed algorithm as defined below outperforms GA and FA in almost every possible way. A total of 50 nodes include anchor and beacon nodes were taken which includes 10 nodes are the anchor nodes(nodes knowing their respective position) and the rest 40 are mobile beacon nodes whose location has to be formed .In real case scenario our beacon nodes get up to 100-200 nodes consisting of the fishermen whose location is to be estimated and the anchor nodes are the fixed landmark location on the shore and on the surface sea.

Table 5 : Pseudo Code for (GEFIR) GenFire Algorithm

Start algorithm GEFIR

Initialization:
Let ꝑ be the solution space.
Let n be the number of chromosomes in ꝑ which represents the total population ranging from 1 to n.
Each chromosome contains the coordinates of the fishermen in the sea; X coordinate and Y coordinate.
For nodes n; n∈ꝑ
For individual j; u=(u1,u2,u3un) ∈n
ji(1≤i≤n,1≤j≤n)
For range (xp,yp)
xp=0≤xp100 ;yp= 0≤yp≤100
Initial Round:

1. Tournament selection is deployed to find mating parents among the np.
2. Mating pool for fittest parents is to be calculated using the fitness function

Fitness function is defined as f1=ƶ Ø
Where
Ø=i,j=1 i,j∈n n(â ij-aij)2
f1=ƶ i,j=1 i,j∈n nâ ij-aij2

3. Partially mapped crossover is done on the parent chromosomes in the mating pool.
   Elite selection strategy: At the same instance of time the best fitted offspring is retained in the next generation without any changes or mutation.
4. Mutation of genes in the np is done on the basis of mutation probability.
   GA performs course tune to estimate unknown nodes.
5. Deploying steps 2 to 4 repeatedly up until it reaches maximum number of iterations.

The final population of evolution created by GA becomes initial population of firefly algorithm.
Fine tuning:

6. Brightness (f (x^ ,y^))is estimated using equation 1
7. Attractiveness is calculated using equation 2
8. Distance of attraction is calculated using equation 3
9. Firefly movement towards brighter firefly is then calculated using equation 4
10. Select the global most light weight among the fireflies
11. Until stopping criterion repeat steps 6 to 11.
12. Location value of sensor node is estimated.

Stop algorithm GEFIR

Parameter estimation problem of the presented non-linear dynamic system of identifying sailor boats (nodes) on the ocean bed is stated as the minimization of the distance measure J between the experimental and the model predicted values of the considered state variables:

$$J = \sum_{i=1}^{n} \quad \sum_{j=1}^{m} \quad \left(Y_{exp}\ (i) - y_{mod}{}^{j}\right)^2 \qquad (7)$$

where m is the number of experimental data; n is the number of state variables; yexp is the known vector of experimental data; ymod is the vector of model predictions with a given set of parameters.

3-6- Tuning of The Parameters for Sailor Specific Problem

Each algorithm has its set of defined parameters that affect its performance in terms of solution space of sailor and execution time. To use FA and GA at their best in terms of network efficiency, it is necessary to provide the modifications of the parameters depending on the domain. With the appropriate choice of the algorithm parameters the accuracy of the algorithms and the execution time can be optimized. Parameters of the FA and GA are tuned based on many pre-tests.

4- Experiment and Simulation Result

4-1- Simulation Setup

This section simulation experiments are deployed on the derived algorithm for the sailor problem and accuracy is calculated based on Matlab R2019a deployed on Windows 10 i9-9000k. We set up and deploy the GA, FA and GEFIR algorithm and thus results were obtained. Note that 50 nodes were placed in a solution space of 100*100 m. The simulation results were calculated several times in a random fashion. On account of the FA-GA calculation, the unadulterated FA begins from arbitrarily produced introductory arrangements (population) which can be very apart from the ideal one. The FA is executed for 10 cycles just and in this way the underlying population for GA, which are nearer to the ideal, is produced. The GA begins from arrangements which are not passage from the ideal and subsequently the convergence of the calculation is expanded. Progressively over crossover plots the population(chromosomes and fireflies) are little, just 20 (versus 100 individuals in unadulterated GA and FA). Such little populace extensively diminishes the pre-owned memory. A graphical portrayal of the union of the target work J (mean estimations of the 30 runs) for both unadulterated GA and FA calculations with time is appeared (in logarithmic scale) in Fig.2 The outcomes about the half breed GA-FA and FA-GA are appeared (in logarithmic scale) in Fig. 3.As the structure from Fig.2 the FA calculation shows somewhat better intermingling execution in the start of the streamlining procedure, contrasted with the GA. The FA meets quicker than the GA and accomplishes lower value for J toward the finish of the advancement. The FA better execution is much clearer in the half breed calculations (see Fig.3). For the half and half FA-GA it is unmistakably noticeable that FA unites quicker than the GA for the initial 10 emphases (10 cycles and 20 chromosomes/fireflies – 250 objective capacity assessments). At that point GA with starting population – FA last arrangement. In the other case, hybrid GA-FA, even the more inaccurate initial population FA convergence fast and achieved similar to FA-GA hybrid solution – JGA−F A = 6.0502 vs. JF A−GA = 6.0479. Total running time for the hybrid algorithms is about 25–30 s vs. about 220 s for pure GA and FA. Total objective function evaluations are 1250 for the hybrid schemes vs. 10000 for the pure GA and FA. Thus, the presented hybrid algorithms have two advantages - much less running time and much less memory usage.

Keeping this in mind and comparing the values obtained for J from the equation 7 we have opted to implement the GA- FA structure as our method for identifying the nodes on the ocean bed in the form of sailor nodes.

Table 6 summarizes the parameters that were used in GEFIR Algorithm and sequentially the output was obtained fig 4 and Fig 5 depicts the global optimal value of the objective function against the transmission radius.

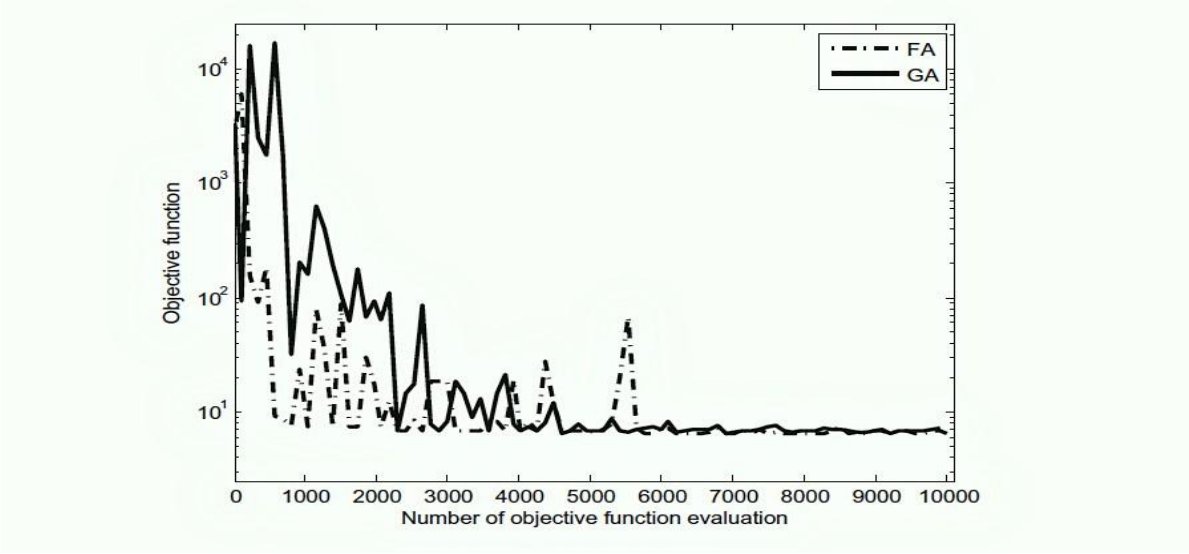

Fig 2: Output graph for objective function evaluation (no. of rounds) to their respective objective function

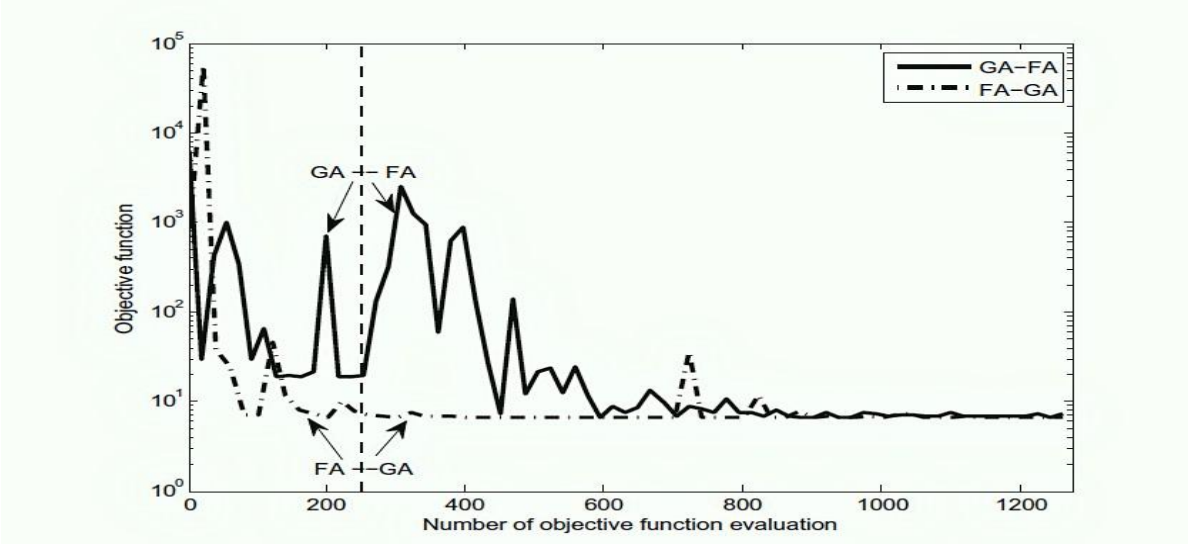

Fig 3: Output graph for objective function evaluation (no. of rounds) to their respective objective function for gefir vs firge

Table 6: The Parameters are used for GenFire (GEFIR) Algorithm

Parameters Used in GEFIR algorithm	***Tweaked Values***
Maximum number of iterations	100
Space Size ꝑ	99
Number of landmarks: Anchor nodes	10
Number of unknown nodes: Beacon nodes	40
Total number of nodes	50
Crossover constant: GA	0.6
Mutation constant: GA	0.1
Number of fireflies	20
Random coefficient (initial value): □	0.2
Attractiveness at r=0: q0	1
Absorption factor:	0.95

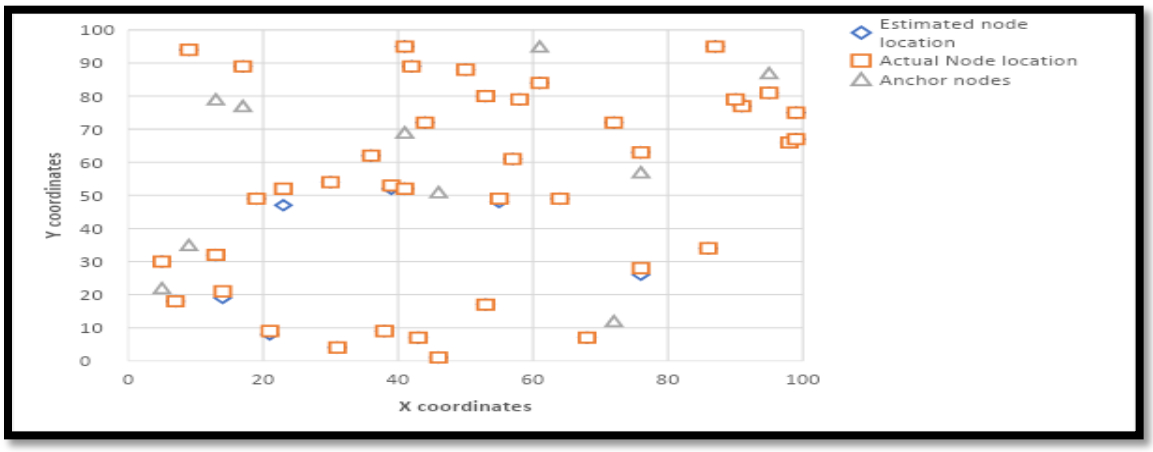

Fig 4: Output for 20 fireflies as obtained by deploying GEFIR

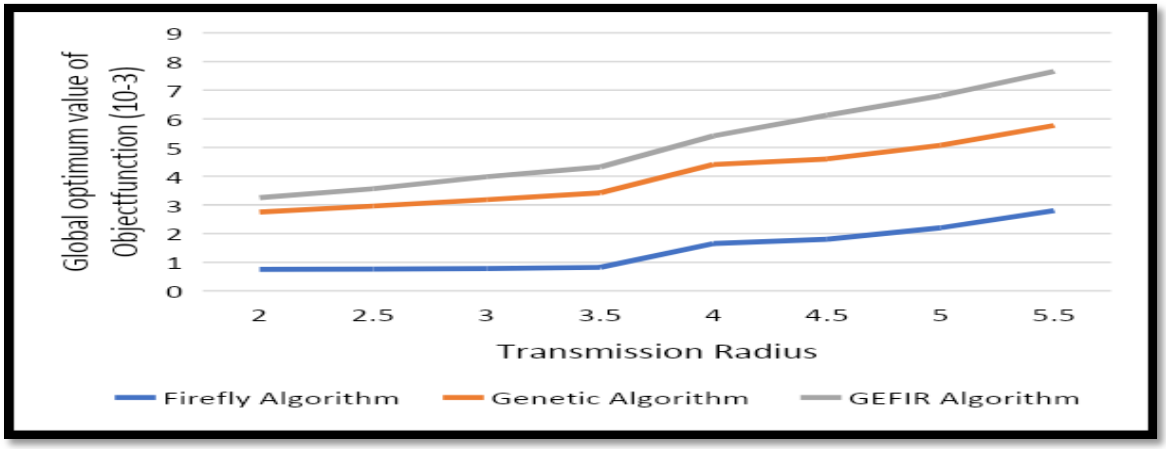

Fig 5:Global optimum value of object function

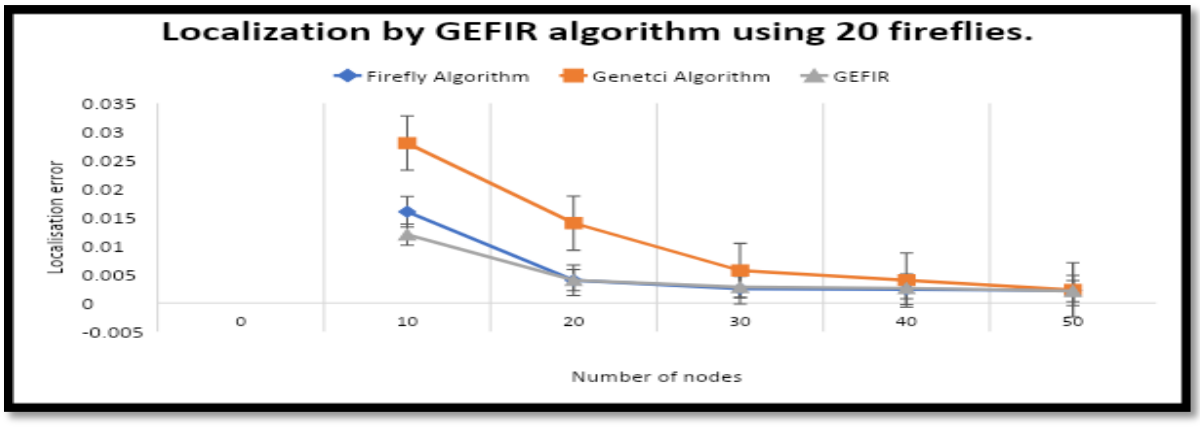

Fig 6: Number of nodes vs Localization error

Performance of the proposed GEFIR algorithm was analyzed and compared with existing firefly and genetic algorithm on the problem statement defined above. The generated results show that the GEFIR algorithm is best suited in terms of time complexity as well as accuracy in table 7

Table 7: Comparison between in GA ,FA AND GEFIR

Localization Algorithm	***Genetic Algorithm***	***Firefly Algorithm***	***GEFIR Algorithm***
Time complexity	Medium	Worst	Best
Accuracy	Good for optimization	Good for error removal	Best for both optimization and error removal
Number of Iteration	Medium	More	Less

5- Conclusion:

GEFIR calculation was built and executed on the issue of the mariners on the seabed and expected outcomes were obtained. The calculation was utilized to advance the limitation blunder and to accomplish the generally exact situation of the sensor hub on the ocean bed. The proposed calculation was tried for several fireflies and were modified to accomplish better accuracy. Though many have proposed the same arrangement for the calculation our relational work was explicitlystreamlined remembering theissue proclamation. A future arrangement of this calculation would send it on a real sensor and develop an engineering of a similar model. Being cornered by the irregular factors of the condition the proposed calculation was as yet ready to beat the current calculation for the mariners on the ocean bed and had the option to moderately discover the area and along these lines a stage towards progressively situating was taken. This framework was all around forced however experienced irregular condition factors which caused interruption and accordingly nearly low speed of correspondence.

References

[1] B Abbas, A Benslimane, and K.D. Singh "Dynamic anchor points selection for mobility management in Software Defined Networks" Journal of Network and Computer Applications, 57, 1-11.

[2] Meguerdichian, S., Slijepcevic, S., Karayan, V., &Potkonjak, M. (2001, October). "Localized algorithms in wireless ad-hoc networks: location discovery and sensor exposure". In Proceedings of the 2nd ACM international symposium on Mobile ad hoc networking & computing (pp. 106-116).

[3] J.S Lee and WL Cheng" Fuzzy-logic-based clustering approach for wireless sensor networks using energy predication", IEEE Sensors Journal, 12(9), 2891-2897..

[4] RV Kulkarni, A Förster and GK Venayagamoorthy "Computational intelligence in wireless sensor networks: A survey". IEEE communications surveys & tutorials, 13(1), 68-96.

[5] S Kumar, DK Lobiyal "Power efficient range-free localization algorithm for wireless sensor networks. Wireless networks", 20(4), 681-694.

[6] S Kumar, DK Lobiyal "Novel DV-Hop localization algorithm for wireless sensor networks", Telecommun. Syst. 64 (3) (2017) 509–524.

[7] S Kumar, DK Lobiyal"An advanced DV-Hop localization algorithm for wireless sensor networks," Wireless personal communications, 71(2), 1365-1385.

[8] I.Mohammad, and I.Mahgoub, Handbook of sensor networks: compact wireless and wired sensing systems. CRC press, 2004.

[9] N.Dragos, and B.Nath. "Ad hoc positioning system (APS)." GLOBECOM'01. IEEE Global Telecommunications Conference (Cat. No. 01CH37270). Vol. 5. IEEE, 2001.

[10] S.Chris, J.M. Rabaey, and J.Beutel. "Location in distributed ad-hoc wireless sensor networks." 2001 IEEE international conference on acoustics, speech, and signal processing. proceedings (Cat. No. 01CH37221). Vol. 4. IEEE, 2001.

[11] Savvides, Andreas, H.Park, and M.B. Srivastava. "The bits and flops of the n-hop multilateration primitive for node localization problems." Proceedings of the 1st ACM international workshop on Wireless sensor networks and applications. 2002.

[12] Savvides, Andreas, H.Park, and M.B. Srivastava. "The n-hop multilateration primitive for node localization problems." Mobile Networks and Applications 8.4 (2003): 443-451.

[13] Hu, Lingxuan, and D.Evans. "Localization for mobile sensor networks." Proceedings of the 10th annual international conference on Mobile computing and networking. 2004.

[14] D.Oliveira, H.ABF, . F., Loureiro, A. A. F., &, A Boukerche. "Directed position estimation: A recursive localization approach for wireless sensor networks." Proceedings. 14th International Conference on Computer Communications and Networks, 2005. ICCCN 2005.. IEEE, 2005.

[15] D.Oliveira, H.ABF, . F., Loureiro, A. A. F., &, A Boukerche. "Directed position estimation: A recursive localization approach for wireless sensor networks. In Proceedings" 14th International Conference on Computer Communications and Networks, 2005. ICCCN 2005. (pp. 557-562). IEEE.

[16] B.Nirupama, J.Heidemann, and D.Estrin. "GPS-less low-cost outdoor localization for very small devices." IEEE personal communications 7.5 (2000): 28-34.

[17] Zhao, Lin-zhe, Xian-bin Wen, and Dan Li. "Amorphous localization algorithm based on BP artificial neural network." (2014): 178-183.

[18] Lin, Chih-Min, "ANFIS-based indoor location awareness system for the position monitoring of patients." Acta Polytech. Hung 11.1 (2014): 37-48.

[19] S.Velimirovic, Andrija Fuzzy ring-overlapping range-free (FRORF) localization method for wireless sensor networks." Computer Communications 35.13 (2012): 1590-1600.

[20] H.Stephan, JB. Martins, and L.Oliveira. "An approach to localization scheme of wireless sensor networks based on artificial neural networks and genetic algorithms." 10th IEEE international NEWCAS conference. IEEE, 2012.

[21] Z-kLiu, and L.Zhong. "Node self-localization algorithm for wireless sensor networks based on modified particle swarm optimization." The 27th Chinese Control and Decision Conference (2015 CCDC). IEEE, 2015.

[22] R.Kulkarni, and G.K.Venayagamoorthy. "Bio-inspired algorithms for autonomous deployment and localization of sensor nodes." IEEE Transactions on Systems, Man, and Cybernetics, Part C (Applications and Reviews) 40.6 (2010): 663-675.

[23] S K Gharghan, R.Nordin, and M.Ismail. "A wireless sensor network with soft computing localization techniques for track cycling applications." Sensors 16.8 (2016): 1043.

[24] G Aloor, and L.Jacob. "Performance of some metaheuristic algorithms for localization in wireless sensor networks." International journal of network management 19.5 (2009): 355-373.

[25] V.Kumar, A.Kumar, and S. Soni. "A combined Mamdani-Sugeno fuzzy approach for localization in wireless sensor networks." Proceedings of the International Conference & Workshop on Emerging Trends in Technology. 2011.

[26] S.Kazem, D.Minoli, and T.Znati. Wireless sensor networks: technology, protocols, and applications. John wiley & sons, 2007.

[27] Yun, Sukhyun, et al. "A soft computing approach to localization in wireless sensor networks." Expert Systems with Applications 36.4 (2009): 7552-7561.

[28] Yun, Sukhyun, et al. "Centroid localization method in wireless sensor networks using TSK fuzzy modeling." Proc. 6th Int'l Symps. On Advanced Intelligent System (ISIS) (2005): 971-974.

[29] A.Tran, Duc ., and T.Nguyen. "Localization in wireless sensor networks based on support vector machines." IEEE Transactions on Parallel and Distributed Systems 19.7 (2008): 981-994..

[30] H.Jia, W.Yong, and T.Xiaoling. "Localization algorithm for mobile anchor node based on genetic algorithm in wireless sensor network." 2010 international conference on intelligent computing and integrated systems. IEEE, 2010.

[31] S.Ali, Y.Zhu, and M.Musavi. "Localization using neural networks in wireless sensor networks." Proceedings of the 1st international conference on MOBILe Wireless MiddleWARE, Operating Systems, and Applications. 2008.

[32] Yang, Xin-She. "Firefly algorithms for multimodal optimization." International symposium on stochastic algorithms. Springer, Berlin, Heidelberg, 2009.

[33] G.Gene., and C.F. Van Loan. "Matrix Computations Johns Hopkins University Press." Baltimore and London (1996).

[34] Bukh, Per D.Nikolaj. "The art of computer systems performance analysis, techniques for experimental design, measurement, simulation and modeling." (1992): 113-115.

[35] M.Melanie. "An introduction to genetic algorithms mit press." Cambridge, Massachusetts. London, England 1996 (1996).[36] S.Javad, S.Sadeghi, and S.Taghi A. Niaki. "Optimizing a hybrid vendor-managed inventory and transportation problem with fuzzy demand: an improved particle swarm optimization algorithm." Information Sciences 272 (2014): 126-144.

[36] S P Ponmalar,V. J.S. Kumar, and R. Harikrishnan. "Hybrid firefly variants algorithm for localization optimization in WSN." International Journal of Computational Intelligence Systems 10.1 (2017): 1263-1271.

[37] H.Subir, and A.Ghosal. "A survey on mobility-assisted localization techniques in wireless sensor networks." Journal of Network and Computer Applications 60 (2016): 82-94.

[38] SP Singh, and S. C. Sharma. "Range free localization techniques in wireless sensor networks: A review." Procedia Computer Science 57.7-16 (2015): 3rd.

[39] S Gupta, A.Rana, and V.Kansal "Comparison of Heuristic techniques: A case of TSP." 2020 10th International Conference on Cloud Computing, Data Science & Engineering (Confluence). IEEE, 2020.

[40] K.Fard, Abdollah, H.Samet, and F.Marzbani. "A new hybrid modified firefly algorithm and support vector regression model for accurate short term load forecasting." Expert systems with applications 41.13 (2014): 6047-6056.

[41] Pandey, P.Kumar, A.Swaroop, and V.Kansal.. "Vehicular Ad Hoc Networks (VANETs): Architecture, Challenges, and Applications." Handling Priority Inversion in Time-Constrained Distributed Databases. IGI Global, 2020. 224-239.

[42] Pandey, P.Kumar, A.Swaroop, and V.Kansal. "A Concise Survey on Recent Routing Protocols for Vehicular Ad hoc Networks (VANETs)." 2019 International Conference on Computing, Communication, and Intelligent Systems (ICCCIS). IEEE, 2019.

[43] S Gupta, A.Rana, and V.Kansal. "Optimization in Wireless Sensor Network Using Soft Computing." Proceedings of the Third International Conference on Computational Intelligence and Informatics. Springer, Singapore, 2020.

Shruti Gupta received the B.Tech. degree in IT UPTU University 2011, and M.S. degree in Computer Science from Amity University,, in 2013. Currently she is Ph.D. Candidate in Amity School of Engineering and Technology India. Her research interests include Computer Networking, Wireless Sensor Network, ,Cloud Concepts, Artificial Intelligence.

Prof. (Dr.) Ajay Rana is Professor of Computer Science and Engineering. He is currently working in the capacity of Dean and Director in Amity University. He has a rich experience spanning over two decades now in academics and industry. He also owns the additional responsibility, as Senior Vice President, RBEF – trust of Amity. He is part of the Board of Directors and also serving as Advisor to the Management of Amity Group. Dr Ajay Rana completed his M. Tech. and Ph.D. in Computer Science and Engineering from reputed institutes of India. He has 22 patents under his name in the field of IoT, Network and Sensors. He has published more than 265 Research Papers in reputed Journals and International and National Conferences, Co-authored 06 Books and co-edited 36 Conference Proceedings. He has undertaken 30 Sponsored Research Projects and 09 major systems based Management/HRD Consultancies in a number of reputed organizations both public and private, in India and abroad. 16 students have completed their PhD under him and currently 6 students are working on their doctorate under him. He is senior member of the Academic Council and the Executive Council of Amity University and is also the chairman of DRC and NTCC board. He has organized more than 150 conferences, workshops, and faculty development programs.

Prof.(Dr.) Vineet Kansal, is working Pro Vice Chancellor at Dr. A.P.J. Abdul Kalam Technical University, Having more than 25 years of rich experience as academician and administrator at various government and non-government organizations in different capacities. He has earned his Ph.D. Degree in the area of Information systems from IIT Delhi, M.Tech. Information System and B.Tech.(CSE). His expertise is in the area of Software Engineering, Data Sciences, Machine learning Artificial Intelligence, Requirements Analysis Software Project Management Team Management.

Farsi Font Detection using the Adaptive RKEM-SURF Algorithm

Zahra Hossein-Nejad
Department of Electrical Engineering, Shiraz Branch, Islamic Azad University, Shiraz, Iran.
hoseinnejad.zahra@yahoo.com
Hamed Agahi*
Department of Electrical Engineering, Shiraz Branch, Islamic Azad University, Shiraz, Iran.
agahi@iaushiraz.ac.ir
Azar Mahmoodzadeh
Department of Electrical Engineering, Shiraz Branch, Islamic Azad University, Shiraz, Iran.
mahmoodzadeh@iaushiraz.ac.ir

Received: 29/Feb/2020 Revised: 24/Aug/2020 Accepted: 01/Sep/2020

Abstract
Farsi font detection is considered as the first stage in the Farsi optical character recognition (FOCR) of scanned printed texts. To this aim, this paper proposes an improved version of the speeded-up robust features (SURF) algorithm, as the feature detector in the font recognition process. The SURF algorithm suffers from creation of several redundant features during the detection phase. Thus, the presented version employs the redundant keypoint elimination method (RKEM) to enhance the matching performance of the SURF by reducing unnecessary keypoints. Although the performance of the RKEM is acceptable in this task, it exploits a fixed experimental threshold value which has a detrimental impact on the results. In this paper, an Adaptive RKEM is proposed for the SURF algorithm which considers image type and distortion, when adjusting the threshold value. Then, this improved version is applied to recognize Farsi fonts in texts. To do this, the proposed Adaptive RKEM-SURF detects the keypoints and then SURF is used as the descriptor for the features. Finally, the matching process is done using the nearest neighbor distance ratio. The proposed approach is compared with recently published algorithms for FOCR to confirm its superiority. This method has the capability to be generalized to other languages such as Arabic and English.

Keywords: Adaptivity; Feature Extraction; Font Detection; Redundant Keypoint Elimination Method (RKEM); Speeded-Up Robust Features (SURF).

1- Introduction

Farsi is the official language of Iran, Tajikistan and Afghanistan. Farsi is among the first three languages of the world in terms of the number and variety of proverbs [1]. With vocabulary coming from Arabic (and other languages like Greek, Aramaic, Turkish, etc.) into Farsi, it has become one of the richest languages in terms of the word count [2]. Farsi is the ninth most widely used language in web content, and higher than Arabic, Turkish and other Middle Eastern languages [3]. To understand written Farsi texts by computers, new particular algorithms should be generated.

Optical character recognition (OCR) is a process by which printed documents or scanned pages are converted to recognizable characters. OCR is one of the most important sectors of e-government. Most of the work done in the field of OCR is related to English, Chinese, and Japanese texts with dramatic improvements in recent years. While, Farsi OCR has continued to thrive despite the relatively high volume of academic research and the urgent need for government agencies. Farsi OCR has still a long way from its intended desire, and yet no completely acceptable system has been developed. In other words, the aim is to generate Farsi systems that are comparable in accuracy and performance to the English OCRs.

Font detection is one of the most useful pre-processing steps in improving the OCR performance for systems which deal with typeset-printed-scanned texts consisting several different fonts [4, 5]. Font detection is the process through which text language and font type, size and style could be identified. Although many methods can be found in the literature for font detection, most of them are composed of two major stages, i.e., feature extraction and font recognition [6, 7]. In general, feature extraction phase of font detection methods is categorized into two approaches including typographical and textural features [8]. In typographical features extraction methods, character weights and space widths are used to analyze textual images [9, 10]. While, in textural feature extraction methods, local and global features are used to describe textural images [6]. Overall, textural based methods are more accurate compared to the typographical ones, with more applications in OCR software [11, 12]. Gabor filter,

*Corresponding Author

wavelet transform and local detectors are examples of textural features widely used in font detection [13].

Although many studies have been conducted to detect English, Chinese and Japanese fonts, few ones have been done for Farsi font detection [14-16]. Due to the complexities in Farsi texts including continuous writing, the variations of the letters with respect to their relative position in words and the difference in the shape of the characters in different fonts, direct application of English-font detection methods for Farsi fonts is not possible. On the other hand, no effective method has been developed for Farsi font detection which is comparable to those for English in terms of recognition accuracy. Given the importance and wide spread use of OCR and low accuracy of existing methods, proposing operative Farsi OCRs is mandatory and challenging. This paves the ground for the motivation to propose approaches which improve the Farsi font detection system so that it reaches acceptable detection rates.

One of the most common feature extraction methods in the font detection applications is the scale-invariant feature transform (SIFT). This algorithm is robust against scale and rotation changes and also intensity variations, affine distortion and noise [17]. These advantages have made this algorithm significant and widely used in the image processing tasks. Meanwhile, the imperative problem of the SIFT is the creation of redundant points, which lead to similar descriptors and consequently possible interference in the matching process. Recently, the RKEM has been proposed by Hossein-Nejad and Nasri [18], which aims to identify and eliminate redundant points in the SIFT using a redundancy index. The RKEM-SIFT could well remove useless keypoints and result in very good attainments in the image registration. Applying the RKEM to problems such as image registration [18], copy-move forgery detection [19] and image mosaicking [20] validated that this algorithm identifies important features and removes unnecessary ones.

This paper proposes an approach for Farsi font detection, which works based on an improved version of the SURF algorithm. For this purpose, first an Adaptive RKEM (A.RKEM) is presented to eliminate redundant keypoints of the SURF algorithm. The proposed method operates based on the adaptive calculation of the threshold in the RKEM-SURF method. In fact, the threshold value is determined based on the amount of dispersion (variance) of keypoints distances. Hence, the type of the images and the between distortions are considered. These points can lead to the improvement in the RKEM-SURF efficiency via eliminating redundant points and consequently enhancing the image matching performance. Another improvement with respect to the RKEM-SURF is that the threshold value in the input and pattern images are found separately, again leading to a more successful image matching process. Afterwards, feature descriptors are extracted using the SURF algorithm. This descriptor is robust against rotation, scale and brightness. It gives vectors of length 64 and has high processing speed. Finally, the matching process is done using the nearest neighbor distance ratio (NNDR) to assign a font type to a query text. Simulation results on a database provided by the authors and standard databases demonstrated that the proposed method achieves higher recognition rates compared to the RKEM-SIFT [18], SURF [21] and also recently published algorithms.

The organization of the rest of paper is as follows. In Section II, review of literature and research method are described. Section III introduces the proposed A.RKEM-SURF algorithm, adapted to the font detection problem. Experimental results and comparisons are presented in Section IV. Finally, the paper is concluded in Section V.

2- Review of Literature and Research Method

In this section, related works is described briefly, and then the RKEM-SIFT algorithm and its problems in font detection are investigated.

2-1- Related Work

In recent years, there has been an increasing interest in the font detection. A considerable amount of literature has been published on this issue, some of which are referred to in this section. In [6], the statistical analysis of edge pixels relationship was used to detect Arabic fonts. In [9], the third and fourth-order moments were used as global texture features to recognize eight types of Spanish fonts. In [13], the authors proposed Sobel-Roberts gradient in sixteen dimensions for feature extraction to detect Farsi fonts. To classify fifteen Arabic fonts, the authors of [8] used scale-invariant detectors such as SIFT and DOG to extract keypoints and used the SIFT descriptor to describe the features. In [22], the authors used sixteen channels of Gabor filter in four directions and four sizes for feature extraction to detect eight types of English fonts and six types of Chinese fonts. In [23], Gaussian mixture model was used to extract features for detecting ten types of Arabic fonts. In [24], correlation coefficients were used to extract the features to detect the Farsi fonts. In [25], wavelet transform and neural network were used for feature extraction and classification respectively, to detect Arabic fonts. In [26], stack and points were used to extract features for detecting seven fonts. In [27], the holes in the characters and horizontal projection profile of text lines were used to extract features in detecting Farsi font. In [28], the SIFT algorithm was used to identify and describe the features and the matches based on the nearest neighbor technique to detect Farsi and Arabic fonts. In [29], redundant oriented LBP features were used for features

recognition and the nearest neighbor for the classification in the process of detecting ten types of Arabic fonts.

2-2-RKEM-SIFT Algorithm and Its Problems in Font Detection

In this section, the RKEM-SIFT algorithm is described briefly, and then the disadvantages of this algorithm in the font detection application are reported.

2-2-1-RKEM-SIFT Algorithm

The RKEM-SIFT is an improved form of the SIFT algorithm; which is used to remove redundant features generated by the SIFT algorithm. The feature extraction step in this algorithm consists of four phases, respectively including: extracting scale-space extrema, improving accuracy of localization and eliminating unstable extrema, allocating orientation to each generated feature, and removing unnecessary keypoints. In the step of removing redundant keypoints, it computes the distances between the keypoints in each image. Afterwards, for any pair of keypoints with a distance less than a pre-determined threshold value, one keypoint is deleted and the other one is kept for the matching process, according to a redundancy index. For more details, we refer the reader to [18].

2-2-2-RKEM-SIFT Algorithm Problems in Font Detection

Despite the high performance of the RKEM-SIFT algorithm, experiments of the present study showed that this method has some problems in the font detection task. The major shortcoming is that the mentioned threshold value for the keypoints' distances should be determined experimentally. In choosing the threshold value in the RKEM-SIFT, the image type (e.g., natural images, texts image, etc.) is not considered as an operational factor. Accordingly, some redundant keypoints may not be eliminated or some useful ones be removed unwantedly. Furthermore, this threshold value is considered the same for both the query and training images and the distortion between images is not considered. In addition, the RKEM-SIFT is not suitable for real-time applications. As one of the improved versions of the SIFT, the SURF algorithm was proposed by Bay [21] in 2006 for the feature matching in images. This algorithm has advantages including time efficiency, robustness against scale and rotation changes and also intensity variations; but it detects several redundant keypoints.

3- Proposed Method

The proposed font detection process consists of three phases, as Fig. 1 shows. At first, the initial features of each image (input images, pattern image) are detected using the proposed A.RKEM-SURF method and then the descriptors are extracted using the SURF algorithm. Finally, the matching process is done by the nearest neighbor distance ratio criteria.

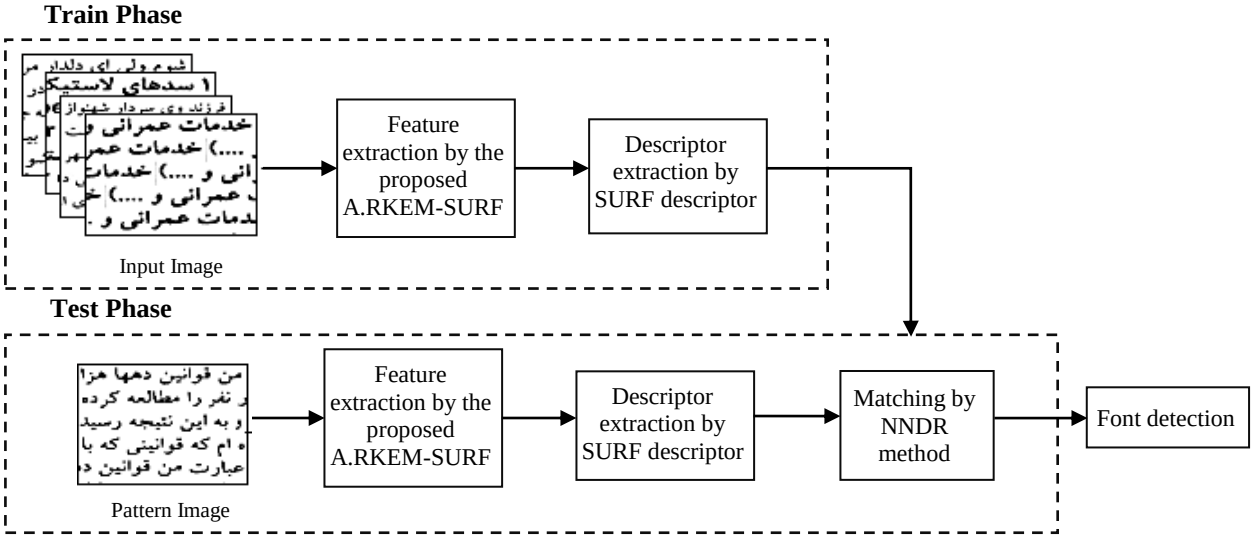

Fig.1 Block diagram of proposed method for Farsi font detection

3-1-Feature Extraction

In this subsection, the A.RKEM method is proposed and then used for the feature extraction. The details are described as follows.

3-1-1-Initial Futures Detection

At the first step, the scale-space extrema are detected, the keypoints are accurately localized and the orientation for each keypoint is assigned based on the classical SURF algorithm [17].

3-1-2-Final Futures Detection using the A.RKEM Method

In this step, the A.RKEM method is proposed and used for the identification of the final features. The aim is to find feature vectors which are too close to each other; then remove unnecessary ones and keep the rest. Notice that the following stages are performed for each image individually. The Manhattan distance between any two keypoints (e.g., p_m and p_j) is calculated (i.e., $d(p_m, p_j)$) for all the keypoints according to (1) [18].

$$d(p_m, p_j) = \sum_{i=1}^{l} \left| p_m(i) - p_j(i) \right| \quad (1)$$

In which, $p_m(i)$ and $p_j(i)$ are the i^{th} coordinate of the keypoints p_m and p_j, respectively and l is the length of any keypoint vector in the image.

An integer value $n_{\max}$ is determined to represent the maximum number of threshold integer values (i.e., $1, 2, \cdots, n_{\max}$). Now, the following two stages are performed for all the $n_{\max}$ number of threshold values:

- 1st stage: If the distance of p_m to any other keypoint is greater than the threshold value n, then p_m is kept in R_n. The set R_n collects those keypoints whose distances to all others are greater than n.

$$R_n = \left\{ p_m \,|\, d(p_m, p_j) > n \;;\; m, j = 1, 2, \cdots, M \right\} \quad n = 1, 2, \cdots, n_{\max} \quad (2)$$

In (2), M is the total number of keypoints.

- 2nd stage: The variance of the set R_n is calculated according to (3).

$$\sigma_n^2 = \mathrm{var}(R_n) \qquad n = 1, 2, \cdots, n_{\max} \quad (3)$$

The purpose of this algorithm is selecting the optimal threshold value for removing redundant keypoints. It deserves to be noticed that the original RKEM sets this value experimentally at 3 [18], without considering the type or other specifications of the images. To the optimal selection aim, the threshold value with minimum variance of the keypoints' distances is selected according to (4). The reason is that smaller dispersion of keypoints is due to existence of less redundant points.

$$\text{Optimal Thershold} = \arg\min(\sigma_n^2) \quad (4)$$

If the distance between each two distinct keypoints in the image is less than the optimal threshold, the unnecessary keypoint should be removed. In this condition, the keypoint with higher Redundancy Index (RI), defined in (5), is considered redundant and thus removed [18].

$$RI(p_m) = 1/SD(p_m) \quad (5)$$

In (5), $SD(p_m)$ is the summation of the distance values between the keypoint p_m and all other ones.

The presented A.RKEM method automatically finds the threshold value for each image, independent of the others. Accordingly, the image type and distortions are considered when adjusting the threshold value. This method leads to accurate removal of redundant keypoints and ultimately increases the matching accuracy. The A.RKEM is not limited to the font detection application, as it can be used in any task that SIFT and its variants are applied.

3-2-Descriptor Extraction

To carry out the image matching, different descriptors could be applied. These descriptors are generally categorized into three groups: distribution-based descriptors, special frequency techniques-based descriptors, and differential descriptors [30]. The distribution-based descriptors use histograms to represent different appearance characteristics. They are robust against geometric aberrations. One main disadvantage of these descriptors is that their dimensions are large. Shape context, SIFT and its improved versions (e.g., SURF and GLOH) are some examples of these descriptors. The special frequency techniques-based methods describe the frequency content of an image. Fourier transform is one of the basic techniques of this group of descriptors that breaks an image content down into basic functions. However, the spatial relationships between points are not clear and the basic functions are unlimited; thus, it is not suitable for adapting local approaches. Other examples of these descriptors are Gabor and Wavelet filters; which overcome the mentioned problems in the Fourier transform. But a large number of these filters are needed to describe small changes in frequency. Differential descriptors use image derivatives for description. Steerable and complex filters are two examples of these descriptors. Among the above-mentioned methods, the distribution-based descriptors such as the SIFT, SURF and the GLOH have higher matching accuracies than others; while the differential descriptors perform the least [31].

SURF is an example of the distribution-based descriptors that was proposed by Herbert Bay in 2006 [21]. As an extended speed-up version of the SIFT, the SURF is both a detector and a descriptor. The SURF algorithm consists of four stages including (1) keypoints detection, (2) keypoints positioning, (3) direction assignment, and (4) descriptors

creation for keypoints. SURF descriptor uses integral images in conjunction with Haar wavelet filters in order to increase the robustness and decrease computation time [21]. Haar wavelets are simple filters which can be used to find gradients in the x and y directions. Extracting the descriptor can be divided into two distinct steps. The first step is to construct a square window around the required point. This square window contains the pixels which form entries in the descriptor vector and its size is 20σ; where σ refers to the scale at which the point was detected. Furthermore, the window is oriented along a computed direction. Since all subsequent calculations are relative to this direction, this direction is important to be found to be repeatable under varying conditions. To determine the orientation, Haar wavelet responses of size 4σ are calculated for a set of pixels within a radius of 6σ of the detected point. The specific set of pixels is determined by sampling those inside the circle using a step size of σ. The responses are weighted with a Gaussian function, centered at the required point. In keeping with the rest the Gaussian is dependent on the scale of the point and chosen to have standard deviation equal to 2.5σ. Once weighted the responses are represented as points in vector space, with the x- responses along the abscissa and the y-responses along the ordinate. The dominant orientation is selected by rotating a circle segment covering an angle of $\pi/3$ around the origin. At each position, the x and y-responses within the segment are summed and used to form a new vector. The longest vector lends its orientation the interest point. The descriptor window is divided into 4×4 regular sub regions. Within each of these sub regions Haar wavelets of size 2σ are calculated for 25 regularly distributed sample points. If we refer to the x and y wavelet responses by dx and dy respectively, then for these 25 sample points, we collect the vector $\left[\sum dx, \sum dy, \sum |dx|, \sum |dy|\right]$ for each sub-region to create the 64-D descriptor vector. The resulting SURF descriptor is invariant to rotation, scale, brightness. In this paper, the SURF descriptor is used. After creating one descriptor for each feature, matching between the target page image descriptor and the training site pages images.

3-3-Matching

In this paper, the matching operation is performed based on the descriptors of each feature. By calculating the Euclidean distance between descriptors in both images and using an appropriate criterion, matching is done. In general, there are three criteria for correct matching between descriptors in two images: threshold-based matching, nearest-neighbors-based matching, and the nearest neighbor distance ratio (NNDR), each of which is described in the following [30].

• Threshold-based matching: if the distance between the descriptors of two keypoints in two images is less than a threshold, the two keypoints are matched. This method, however, has disadvantages; e.g., a descriptor can have several matches.
• Nearest-neighbor-based matching: two regions *A* and *B* are matched if the D_B descriptor is the closest neighbor to D_A, and the distance between the two descriptors is less than the threshold. Through this method, a descriptor has only one match.
• Nearest-neighbor distance ratio (NNDR): this method is similar to the nearest-neighbors-based matching. In this method, *A* and *B* keypoints are matched if (6) is satisfied [31].

$$\frac{\|D_A - D_B\|}{\|D_A - D_C\|} < T_{ED} \tag{6}$$

In which, D_B is the descriptor of the first nearest neighbor to the descriptor D_A, and D_C is that of the second nearest neighbor to D_A. If the ratio of 'the distance between the first nearest neighbor to the descriptor' to 'the distance of the second nearest neighbor to a given one' is smaller than a threshold value T_{ED}, the matching is done. The value of T_{ED} is considered equal to 0.8. Since the matching based on the ratio of the first and second nearest neighbor is more accurate than other methods, this criterion is used in this paper for matching [30].
Each pattern page is compared with all the pages in the database. The font of the training page with the maximum number of matches is assigned to the pattern page. If this number for a pattern page is less than a pre-determined threshold, the font of that page is not included in the font bag of the training database.

4- Experimental Results

In this section, we evaluate the performance of the proposed A.RKEM-SURF algorithm and compare it with the RKEM-SIFT[18] , also the method of method [28], the Sobel–Roberts features in [13] and the SIFT [8]. All the experiments are performed on a personal computer with a 2.28 GHz Intel Core i7, 16G RAM using the MATLAB® 2015A software. The database, evaluation criteria, and experimental results are presented in the next subsections.

4-1-Databases

We used four datasets to evaluate the proposed *Adaptive* RKEM-SURF method. The first dataset is provided by the authors of this paper via printing and scanning the Farsi translation of 'Le Petit Prince' (The Little Prince) book, written by Antoine de Saint-Exupéry originally in French. It contains 46 pages with 425×550 pixels printed in 20 different Farsi fonts. Each font is written in four

sizes: 6, 10, 14, 18 with four different styles: normal, **bold**, *italic* and ***bold-italic***. The second dataset includes 1400 text images. It contains 500 pages printed in 10 different Farsi fonts; each of which is written in sizes 11-16 [13]. The third and the fourth databases are the printed/scanned versions of the Arabic and English translations of 'The Little Prince' book, produced by this paper authors.

4-2-Evaluation Criteria

Classical evaluation criteria including the recognition rate (matching accuracy) and recall according to (7-8) are used to evaluate the effectiveness of the font detection methods [32].

$$Accuracy = TP/m \quad (7)$$

$$Recall = TP/P \quad (8)$$

In (7-8), TP is the number of correct matches, P is the number of correspondences and m is the total number of matches. If the accuracy and recall are high, the performance of the system is acceptable.

4-3-Setup of Experiments

Six sets of experiments were performed to evaluate the performance of the proposed *Adaptive* RKEM-SURF method. In the first and second sets, the performance on different sizes and different styles scenarios were evaluated, respectively. In the third set, the performance was investigated in both different sizes and styles. In the fourth set, comparison with other classical methods such as RKEM-SIFT [18], methods of [28], the Sobel–Roberts features in [13] and the SIFT [8] were presented.. In the fifth set, the performance in multi-language texts was evaluated. Finally, to evaluate the performance of the proposed A.RKEM-SURF method on images with simulated noise was evaluated.

4-3-1-Experiments on Different Sizes

In this test, text images with different sizes are used, and the performance of the proposed A.RKEM-SURF method is assessed. Fig. 2 and Table 1 validated that the effect of applying the proposed A.RKEM-SURF method is appropriate in the font detection application, according to the high rates of the recognition (accuracy) and the recall criteria.

4-3-2-Experiments on Different Styles

In this experiment, text images with different styles are used, and the performance of the A.RKEM-SURF is compared with the RKEM-SIFT. The results shown in Table 2 confirm than the performance of the proposed A.RKEM-SURF method is high in detecting the fonts for texts with different styles.

4-3-3-Experiments on Different Sizes and Styles

In this test, we used images with different sizes and styles to evaluate the performance of the proposed font detection method. The results of this test are shown in Fig. 3; from which, it is easy to conclude that the proposed A.RKEM SURF works well on images with different sizes and styles.

4-3-4-Comparison to other Methods

An experiment was conducted to compare the performance of the proposed font-detection method with other classical methods, such as [8], [13], and [28]. The results are reported in Table 3, which show that the proposed A.RKEM-SURF method outperformed the methods of [8] and [13], in term of the recognition rate. Although the proposed method achieved the accuracy value same as that of [28]; it was faster as the last column demonstrates.

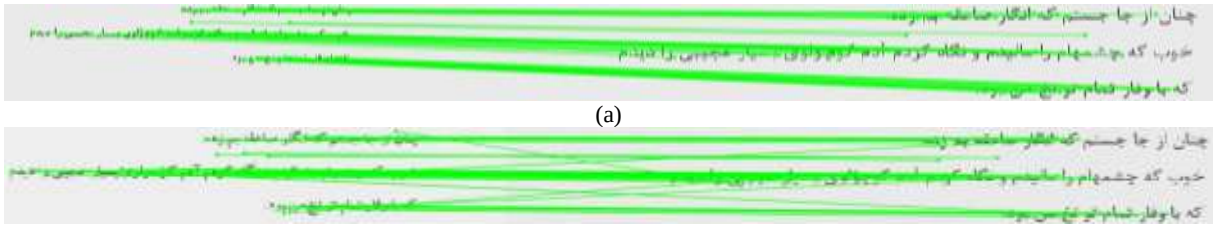

(a)

(b)

Fig. 2 Font detection using the proposed method for texts with different sizes. (a) texts with sizes (10,18), (b) texts with sizes (14,18). The first/second number in the parenthesis represents the size of the text characters in the pattern/database image.

Table 1: Font detection results on text images with different sizes.

Sizes	*Method*	*Recall (%)*	*Accuracy (%)*
(6,10)	RKEM-SIFT	94.6	98.2
	A.RKEM-SURF	97	99.5
(6,18)	RKEM-SIFT	83.15	89.3
	A.RKEM-SURF	92.7	97.7
(10,14)	RKEM-SIFT	78	87.7
	A.RKEM-SURF	88.1	95.8
(10,18)	RKEM-SIFT	72.65	85.1
	A.RKEM-SURF	85.42	94.6
(14,18)	RKEM-SIFT	68.09	84.2
	A.RKEM-SURF	80.6	93.2

Table 2: performance comparison in different styles scenario.

Sizes	***Method***	***Recall (%)***	***Accuracy (%)***	***Run time (s)***
Normal	RKEM-SIFT	91.03	100	14.62
	A.RKEM-SURF	98.78	100	10.45
Italic	RKEM-SIFT	90	99.9	13.81
	A.RKEM-SURF	95.43	100	11.94
Bold	RKEM-SIFT	86.52	100	16.43
	A.RKEM-SURF	92	100	13.07
Bold-Italic	RKEM-SIFT	75.18	97.6	18.72
	A.RKEM-SURF	89.32	99.2	15.61

Table 3: Comparison of the proposed method with some others

Method	*Number of fonts*	*Recognition rate*	*Required time per sample (ms)*
[8]	15	99.5	4.02
[13]	10	94	3.78
[28]	20	100	3.25
A.RKEM-SURF	**20**	**100**	**2.14**

Table 4: Recognition rates for texts written in English and Arabic

Language	*Method*	*Accuracy* (%)
English	*A*.RKEM-SURF	100
Arabic	Method of [8]	98.1
	A.RKEM-SURF	100

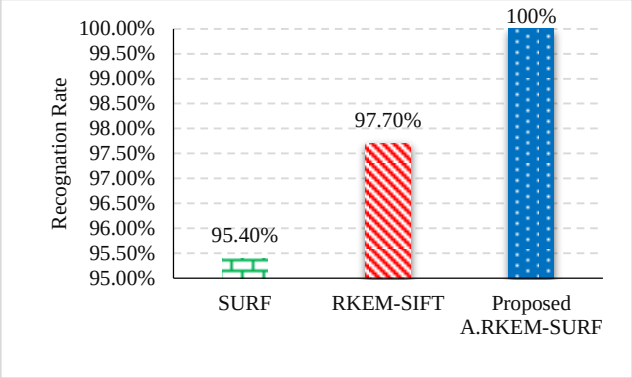

Fig. 3 Overall recognition rate in images with different sizes and styles

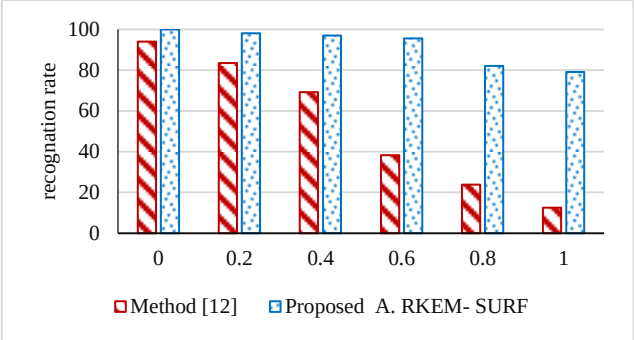

Fig. 4 Comparison of font detection rate on images contaminated by additive Gaussian noise with one mean and different variances.

4-3-5-Experiments on other Languages

In this test, the performance of the proposed method in detecting fonts of texts written in English and Arabic is assessed. The results are shown in Table 4, which show that the proposed A.RKEM-SURF method works well in the font detection task for English and Arabic texts. Also, this method performs better than the method [8].

4-3-6-Experiments on Images with Simulated Noise

In this test, to evaluate the performance of the A.RKEM-SURF method on noisy images, Gaussian noise with a mean of one and a variance between zero to one is added to the text images with ten types of fonts. This test is important since images are usually taken using low quality scanners. The results are shown in Fig. 4. It is easy to infer that the font detection rate in both compared methods decreases with the increase of the noise variance. Yet, the accuracy of the A.RKEM-SURF method is higher than that of the method of [13]. This indicates the appropriate functioning of the proposed A.RKEM-SURF method against noise.

5- Conclusion

Farsi language has challenging characteristics for OCR that elevates the need for the FOFR. Font detection is an essential step in the OCR systems. Thus, one main phase of recognizing Farsi characters is to detect the Farsi font of the written text. In this paper, a new three-step algorithm is presented for the purpose. The A.RKEM-SURF is introduced and used for the feature extraction step. Then SURF is used as the descriptor and NNDR is utilized for the matching step. The simulation results of the proposed method show a promising performance in the font detection task. Not only very good recognition rates are obtained in general, but also particular fonts (e.g. Tabassom) which are known to be weak points for other FOFR methods, are successfully identified. Additionally,

the proposed method was shown to work well in recognizing fonts in texts written in English and Arabic.

Acknowledgments

The authors would like to thank the Journal of Information Systems and Telecommunication (JIST) and Applications Associate Editor and the anonymous reviewers for their valuable comments.

References

[1] Mostafa Rahmandoust, "The Death of Pitcher: Persian Parables and its Stories," Tehran: School Publications, 1387.
[2] University of Texas: New Persian Language.
https://w3techs.com/technologies/overview/content_language/all/
[4] A. Zramdini and R. Ingold, "Optical font recognition using typographical features," IEEE Transactions on pattern analysis and machine intelligence, Vol. 20, pp. 877-882, 1998.
[5] M. Rajdev, D. Sahay, S. Khare, and S. Nainan, "Optical Character and Font Recognizer," in International Conference on Advances in Computing and Data Sciences, 2019, pp. 477-486.
[6] B. Bataineh, S. N. H. S. Abdullah, and K. Omar, "A statistical global feature extraction method for optical font recognition," in Asian Conference on Intelligent Information and Database Systems, 2011, pp. 257-267.
[7] S. Ghosh, P. Roy, S. Bhattacharya, and U. Pal, "Large-Scale Font Identification from Document Images," in Asian Conference on Pattern Recognition, 2019, pp. 594-600.
[8] M. A. Mousa, M. S. Sayed, and M. I. Abdalla, "An efficient algorithm for Arabic optical font recognition using scale-invariant detector," International Journal on Document Analysis and Recognition (IJDAR), Vol. 18, pp. 263-270, 2015.
[9] C. Avilés-Cruz, R. Rangel-Kuoppa, M. Reyes-Ayala, A. Andrade-Gonzalez, and R. Escarela-Perez, "High-order statistical texture analysis—font recognition applied," Pattern Recognition Letters, Vol. 26, pp. 135-145, 2005.
[10] V.-C. Juan and A.-C. Carlos, "Font recognition by invariant moments of global textures," in Proceedings of international workshop VLBV05 (very low bit-rate video-coding 2005), 2005, pp. 15-16.
[11] M. Lutf, X. You, Y.-m. Cheung, and C. P. Chen, "Arabic font recognition based on diacritics features," Pattern Recognition, Vol. 47, pp. 672-684, 2014.
[12] G. D. Joshi, S. Garg, and J. Sivaswamy, "A generalised framework for script identification," International Journal of Document Analysis and Recognition (IJDAR), Vol. 10, pp. 55-68, 2007.
[13] H. Khosravi and E. Kabir, "Farsi font recognition based on Sobel–Roberts features," Pattern Recognition Letters, Vol. 31, pp. 75-82, 2010.
[14] J. H. AlKhateeb, J. Ren, S. S. Ipson, and J. Jiang, "Knowledge-based baseline detection and optimal thresholding for words segmentation in efficient pre-processing of handwritten Arabic text," in Fifth International Conference on Information Technology: New Generations (itng 2008), 2008, pp. 1158-1159.
[15] C. ERGÜN and S. Norozpour, "Farsi document image recognition system using word layout signature," Turkish Journal of Electrical Engineering & Computer Sciences, Vol. 27, pp. 1477-1488, 2019.
[16] A.Mohammadkhani, F.Marvari, and M. Moshki, "Font Recognition of Persian Letters and Printed Words," 16th Iranian Electrical Engineering Student Conference, Kashan, Electrical Engineering Student Scientific Organization, 2013.
[17] D. G. Lowe, "Distinctive image features from scale-invariant keypoints," International journal of computer vision, Vol. 60, pp. 91-110, 2004.
[18] Z. Hossein-Nejad and M. Nasri, "RKEM: Redundant Keypoint Elimination Method in Image Registration," IET Image Processing, Vol. 11, pp. 273-284, 2017.
[19] Z. Hossein-Nejad and M. Nasri, "Copy-Move Image Forgery Detection Using Redundant Keypoint Elimination Method," in Cryptographic and Information Security Approaches for Images and Videos, S. Ramakrishnan, Ed. Boca Raton: CRC Press, pp. 773-797, 2019.
[20] Z. Hossein-Nejad and M. Nasri, "Natural Image Mosaicing based on Redundant Keypoint Elimination Method in SIFT algorithm and Adaptive RANSAC method," Signal and Data Processing, 2020.
[21] H. Bay, A. Ess, T. Tuytelaars, and L. Van Gool, "Speeded-up robust features (SURF)," Computer vision and image understanding, Vol. 110, pp. 346-359, 2008.
[22] Y. Zhu, T. Tan, and Y. Wang, "Font recognition based on global texture analysis," IEEE Transactions on pattern analysis and machine intelligence, Vol. 23, pp. 1192-1200, 2001.
[23] F. Slimane, S. Kanoun, A. M. Alimi, R. Ingold, and J. Hennebert, "Gaussian mixture models for arabic font recognition," in 2010 20th International Conference on Pattern Recognition, 2010, pp. 2174-2177.
[24] E. Rashedi, E. Nezam abadipour, and a. S. Saryazdi, "Farsi font recognition using correlation coefficients (in Farsi)," 4th Conf. on Machine Vision and Image Processing, Ferdosi Mashhad, 2007.
[25] N. E. B. Amara and S. Gazzah, "Une approche d'identification des fontes arabes," in Conférence Internationale Francophone sur l'Ecrit et le Document (CIFED 04), 2004.
[26] Y. Pourasad, H. Hassibi, and A. Ghorbani, "Farsi font recognition using holes of letters and horizontal projection profile," in International Conference on Innovative Computing Technology, 2011, pp. 235-243.
[27] Y. Pourasad, H. Hassibi, and A. Ghorbani, "Farsi font recognition in document images using PPH features," International Journal of Natural and Engineering Sciences (IJNES) E-ISSN: 2146-0086, Vol. 2, pp. 17-20, 2011.
[28] M. Zahedi and S. Eslami, "Farsi/Arabic optical font recognition using SIFT features," Procedia Computer Science, Vol. 3, pp. 1055-1059, 2011.
[29] A. Nicolaou, F. Slimane, V. Maergner, and M. Liwicki, "Local binary patterns for arabic optical font recognition," in 2014 11th IAPR International Workshop on Document Analysis Systems, 2014, pp. 76-80.
[30] K. Mikolajczyk and C. Schmid, "A performance evaluation of local descriptors," Pattern Analysis and Machine

Intelligence, IEEE Transactions on, Vol. 27, pp. 1615-1630, 2005.
[31] K. Mikolajczyk and C. Schmid, "A performance evaluation of local descriptors," IEEE transactions on pattern analysis and machine intelligence, Vol. 27, pp. 1615-1630, 2005.
[32] H. Agahi, A. Mahmoodzadeh, and M. Salehi, "Handwritten Digits Recognition Using an Ensemble Technique Based on the Firefly Algorithm," Information Systems & Telecommunication, pp. 136, 2018.

Zahra Hossein-Nejad received the B.Sc. and M.Sc. degrees in Electrical Engineering from the Islamic Azad University, Jahrom, and Sirjan branches, Iran, in 2013 and 2016, respectively. She is a Ph.D. student in Electrical Engineering at Shiraz University, Shiraz, Iran. Her research interests include image processing and computer vision.

Hamed Agahi received B.Sc. M.Sc. and Ph.D. degrees in Electrical Engineering from University of Shiraz, Amirkabir University of Technology and University of Tehran, Iran, in 2005, 2008 and 2013, respectively. From 2009, he was with the Islamic Azad University, Shiraz Branch, Shiraz, Iran. His research interests include pattern recognition, image and signal processing, and fault detection and diagnosis applications.

Azar Mahmoodzadeh received B.Sc., M.Sc. and Ph.D. degrees in Electrical Engineering from University of Shiraz, University of Shahed and University of Yazd, Iran, in 2005, 2008 and 2013, respectively. From 2009, she was with the Islamic Azad University, Shiraz Branch, Shiraz, Iran. Her research interests include pattern recognition and image and signal processing.

Evaluation of Pattern Recognition Techniques in Response to Cardiac Resynchronization Therapy (CRT)

Mohammad Nejadeh
Department of Computer Engineering, Islamic Azad University, Rasht Branch, Rasht, Iran
m.nejadeh@fshiau.ac.ir
Peyman Bayat*
Department of Computer Engineering, Islamic Azad University, Rasht Branch, Rasht, Iran
bayat@iaurasht.ac.ir
Jalal Kheirkhah
Department of Cardiology, Healthy Heart Research Center, School of Medicine, Guilan university of Medical Sciences, Rasht, Iran
kheirkhah@gums.ac.ir
Hassan Moladoust
Healthy Heart Research Center, School of Medicine, Guilan university of Medical Sciences, Rasht, Iran.
hmoladoust@gums.ac.ir

Received: 30/Aug/2020 Revised: 05/Oct/2020 Accepted: 08/Nov/2020

Abstract

Cardiac resynchronization therapy (CRT) improves cardiac function in patients with heart failure (HF), and the result of this treatment is decrease in death rate and improving quality of life for patients. This research is aimed at predicting CRT response for the prognosis of patients with heart failure under CRT. According to international instructions, in the case of approval of QRS prolongation and decrease in ejection fraction (EF), the patient is recognized as a candidate of implanting recognition device. However, regarding many intervening and effective factors, decision making can be done based on more variables. Computer-based decision-making systems especially machine learning (ML) are considered as a promising method regarding their significant background in medical prediction. Collective intelligence approaches such as particles swarm optimization (PSO) algorithm are used for determining the priorities of medical decision-making variables. This investigation was done on 209 patients and the data was collected over 12 months. In HESHMAT CRT center, 17.7% of patients did not respond to treatment. Recognizing the dominant parameters through combining machine recognition and physician's viewpoint, and introducing back-propagation of error neural network algorithm in order to decrease classification error are the most important achievements of this research. In this research, an analytical set of individual, clinical, and laboratory variables, echocardiography, and electrocardiography (ECG) are proposed with patients' response to CRT. Prediction of the response after CRT becomes possible by the support of a set of tools, algorithms, and variables.

Keywords: Cardiac resynchronization therapy; Neural Networks; Particle swarm optimization; HESHMAT_CRT dataset; Machine Learning.

1- Introduction

The unsuccessful function of the heart can result from different causes such as vascular occlusion and high blood pressure, and this problem is referred to as heart failure (HF). In this condition, cardiac muscle is not able to pump enough blood in the body [1]. Arrhythmia is a disorder of heartbeat rhythm. This disorder makes the heart unable to effectively pump blood all over the body and patients with arrhythmia usually experience the symptoms of rapid and slow heartbeat [2]. Patients with HF and arrhythmia may be appropriate candidates for CRT [3]. In addition to improvement of cardiac output in a short time, it helps to increase patients' lifetime and decrease of HF hospitalization cases [4]. Doctors' suggestions may be different depending on their observation of the patient's condition, and the results of selecting candidate patients in the past do not seem to be good.

Many risks can occur during the CRT process and there might be various side effects [5]. The majority of patients (35-40%) do not respond to CRT due to unknown causes [6], and it has a negative effect on function and efficiency of this treatment for HF patients [7]. The research idea is about proposing a new feature vector and creating a pattern detection solution for identifying appropriate candidates for CRT with high accuracy. It can increase the rate of response to CRT and practically decrease the rate

* Corresponding Author

of no response. Machine learning is a powerful computation method that can provide the possibility of a better description of effective parameters. Decision support tools are developed for the prediction of clinical results and create better decisions for similar cases of patients [8]. The possibility of prediction based on intelligent algorithms is a step forward to identifying candidates for CRT. These operations are non-invasive and used for optimizing the treatment process, and they can significantly help doctors provided that they are properly operated [9]. After the implant, there are very few and sometimes impossible ways to overcome the cases of no response [10]. The process of machine learning-based prediction requires using the collected medical data [11]. In order to create analysis features in most of the datasets relevant to the research topic, three methods are used including (1) extracting feature from cardiac imaging [12], (2) a combination of the features extracted from ECG and the patient's laboratory data [13, 8], and (3) combining an important parameter such as (NYHA) classification function and analysis of medical examinations with other techniques such as natural language processing (NLP) [14], or using QRS variable international suggestions [15]. The research data set consists of 67 independent attributes and 1 dependent attribute. Independent characteristics were obtained according to the patient's medical record, laboratory results, imaging, and independent characteristics were obtained according to postoperative results.

The main purpose of this study is to introduce a set of cardiac synchronization therapy data, identify patients suitable for treatment with machine learning algorithms, determine the role of important features and their priorities. The determination of effective features by the medical doctor is collected from the feature vector, the prioritization of features by intelligent algorithms, and their effective role in obtaining a better classification answer are discussed.

In the following, related works on the analysis of CRT patients are reviewed. All the researches have been performed aimed at proposing a method for making HF treatment efficient. Various researches have addressed the results by predictors [16, 8, 10, 17]. The research [18] investigated the relationship between the variables aimed at improving prediction of CRT response, and the research [19] investigated the analysis of data after optimizing the device and setting the device in different locations. In the researches [20, 9, 21, 22], the effect of other cardiac factors in patients under CRT was investigated. Some studies such as [23] provided statistical reports of the related works and so, helped to prepare a new dataset. In spite of the same instructions, [24] indicates that CRT is not still fully used everywhere. Regarding the datasets of previous works, we can mention [21] with 25 features and 54 samples, [25] with 18 features and 428 samples, [26] with 25 features and 679 samples, [27] with 32 features and 23 samples, and [8] with 45 features and 595 samples for predicting CRT condition. The three studies of [8, 10, 27] used machine learning for selecting CRT candidate patients. In the research [8], the effective variables were analyzed based on four quartiles. These charts were composed of two variables of LBBB and QRS. The variable QRS was defined at two states of QRS $\geq$ 150 ms and QRS $<$ 150 ms, and LBBB was defined in a binary manner. Efficiency of the random forest (RF) algorithm was evaluated by reviewing the classifiers. Since the collected data including class variables have different levels, and determination of importance and priority of features by RF algorithm is not reliable, increasing and decreasing the samples in [8] resulted in many changes in classification error. On the other hand, with the existence of unknown parameters in the provided dataset that can play the role of noise, using the RF algorithm will cause over-fitting (OF). However, the research method classifies QRS variable in three levels of short, medium, and long. Back-propagation of error neural network model is prioritized is used for decreasing implementation classification error and the variables selected by the doctor are prioritized by PSO algorithm. The results will show that neural models such as backpropagation of error neural network and Learning Vector Quantization compared to other machine learning algorithms such as Naive Bayes (NB), support vector machine (SVM), random forest (RF), k-Nearest Neighbors has higher efficiency on research data sets. Also, 7 out of 9 features by the medical doctor were prioritized.

The following sections of the paper are organized as the following. First, the general properties of the research dataset, features, and primary pre-processing are described by transformation and discretization, and the research method is explained for the implementation of the dataset. The results are discussed by evaluating the algorithms and conclusion of the research is presented. Also, some suggestions are proposed for developing decision making systems for working on the present dataset.

2- Medical dataset

The data was collected by individual, laboratory, clinical, electrocardiogram, and echocardiography. The limited number of surgeries in treatment centers (Heshmat Hospital of Rasht), no access to the patients after the surgery, the need to a specialist for reviewing the medical files, and incompleteness of the files are some of the data collection constraints. Feature extraction was done by using a questionnaire before and after implanting CRT device, medical examinations, blood sampling, ECG observations, and echocardiography. Table (1) presents a full description of the extracted features. The research dataset includes 209 cardiac patients gotten CRT-D implant. 38 people did not respond to the treatment and 171 people indicated a positive response. Some of the personal information of patients was excluded for security considerations and also, some of the deficient and calculable were removed. The main features and their range are specified in Table (1).

Table 1: The features extracted for prediction of CRT response

Type	*Feature Name*	*Range*
Register	File Number	-
	Patient Name	-
	Patient contact number	-
	Companion patient ‘s contact number	-
	Surgical Date	-
	Doctor's name	-
Demographic	Age	25-86
	Sex	1=Male, 2=Female
	DM (Diabetes Mellitus)	Yes, No
	HTN (Hyper Tension)	Yes, No
	Current Smoker	Yes, No
	Ex-Smoker	Yes, No
	FH (Family History)	Yes, No
	CRF (Chronic Renal Failure)	Yes, No
	CVA (Cerebrovascular Accident)	Yes, No
	CABG(Coronary artery bypass surgery)	Yes, No
	Airway Disease	Yes, No
	Thyroid Disease	Yes, No
	CHF (Congestive Heart Failure)	Yes, No
	DLP (Dyslipidemia)	Yes, No
Symptom and Examination	BP (Blood Pressure: mmHg)	90-190
	Edema	Yes, No
	Weak peripheral pulse	Yes, No
	Lung Rales	Yes, No
	Systolic murmur	Yes, No
	Diastolic murmur	Yes, No
	Typical Chest Pain	Yes, No
	Dyspnea	Yes, No
	NYHA (New York Heart Association Function Class)	1, 2, 3, 4
	Atypical	Yes, No
	Nonanginal CP	Yes, No
	Exertional CP (Exertional Chest Pain)	Yes, No
	Low Th Ang (low Threshold angina)	Yes, No
Laboratory	FBS (Fasting Blood Sugar) (mg/dl)	62- 400
	Cr (creatine) (mg/dl)	0.5- 2.2
	TG (Triglyceride) (mg/dl)	37- 1050
	Total chol	-
	LDL (Low density lipoprotein) (mg/dl)	18- 232
	HDL (High density lipoprotein) (mg/dl)	15- 111
	BUN (Blood Urea Nitrogen) (mg/dl)	6- 52
	ESR (Erythrocyte Sedimentation rate) (mm/h)	1- 90
	HB (Hemoglobin) (g/dl)	8.9- 17.6
	K (Potassium) (mEq/lit)	3.0- 6.6
	Na (Sodium) (mEq/lit)	128- 156
	WBC (White Blood Cell) (cells/ml)	3700- 18000
	CKMB	-
	Troponin	-
	Lymph (Lymphocyte) (%)	7- 60

Type	***Feature Name***	***Range***
	Neut (Neutrophil) (%)	32- 89
	PLT (Platelet) (1000/ml)	25- 742
ECG & Echo	Rhythm	Sin, AF
	Q Wave	Yes, No
	HR	50-110
	PR Interval	-
	QT Interval	-
	QRS Duration	-
	Fragment	Yes, No
	Number of fragment	0-8
	ST Elevation	Yes, No
	ST Depression	Yes, No
	T inversion	Yes, No
	LVH (Left Ventricular Hypertrophy)	Yes, No
	Poor R Progression(Poor R Wave Progression)	Yes, No
	LV EF (left ventricular ejection fraction) (%)	Number
	AI (Normal,mild,moderate,severe)	1-4
	MR (Normal,mild,moderate,severe)	1-4
	Device Type	-
Result	CRT Response	Yes, No

In the present dataset, there are many features that provide useful information by discretization. Discretization is done based on standard medical ranges and other methods such as class entropy, bucketing, range frequency-varying domain, numbers distance determination, and clustering. Table (2) presents the method of discretization of general and laboratory features. General features refer to the features related to symptoms, examination, and demography. The most important variables of the final feature vector for prediction of CRT response are resulted from ECG and the patient's echocardiography.

Table 2: Discretization of general and laboratory features

Feature	***Low***	***Normal***	***High***
Cr2	$Cr < 0.7$	$0.7 \leq Cr \leq 1.5$	$Cr > 1.5$
FBS2	$FBS < 70$	$70 \leq FBS \leq 105$	$FBS > 105$
LDL2		$LDL \leq 130$	$LDL > 130$
HDL2	$HDL < 35$	$HDL \geq 35$	-
BUN2	$BUN < 7$	$7 \leq BUN \leq 20$	$BUN > 20$
ESR2	-	if male & $ESR \leq Age/2$ or if female & $ESR \leq Age/2+5$	if male & $ESR > Age/2$ or if female & $ESR > Age/2+5$
Hb2	if male & $Hb < 14$ Or If female & $Hb < 12.5$	if male & $14 \leq Hb \leq 17$ Or if female & $12.5 \leq Hb \leq 15$	if male & $Hb > 17$ Or if female & $Hb > 15$
K2	$K < 3.8$	$3.8 \leq K \leq 5.6$	$K > 5.6$
Na2	$Na < 136$	$136 \leq Na \leq 146$	$Na > 146$
WBC2	$WBC < 4000$	$4000 \leq WBC \leq 11000$	$WBC > 11000$
PLT2	$PLT < 150$	$150 \leq PLT \leq 450$	$PLT > 450$
EF2	$EF \leq 50$	$EF > 50$	-
Age2	-	if male & $Age \leq 45$ or if female & $Age \leq 55$	if male & $Age > 45$ Or if female & $Age > 55$
BP2	$BP < 90$	$90 \leq BP \leq 120$	$BP > 120$
PR2	$PR < 60$	$60 \leq PR \leq 100$	$PR > 100$
Neut 2	-	$Neut \leq 65$	$Neut > 65$
TG2	-	$TG \leq 200$	$TG > 200$
Function Class2	-	1	2,3,4
HR2	$HR < 60$	$60 \leq HR \leq 100$	$HR > 100$
Total chol2	$200 \leq$ Total chol ≤ 240 is desirable	Total chol<200	Total chol > 240
Lymph2	Lymph < 20	$20 \leq Lymph \leq 40$	$Lymph > 40$

Table (3) and Table (4) present the discretization of some of the most important features obtained from ECG that decrease the data.

Table 3: Discretization of ECG features

Feature	*Short*	*Normal*	*Long*
PR Interval 2	PR Interval <0.12	0.12 ≤ PR Interval≤ 0.20	PR Interval >0.20
QT Interval 2	QT Interval <0.35	0.35 ≤ QT Interval≤ 0.45	QT Interval >0.45

Table 4: Discretization of QRS feature

Feature	*Narrow*	*Normal*	*Wide*
QRS2	QRS <0.08	0.08 ≤ QRS ≤ 0.12	QRS >0.12

3- Method

Extraction of effective features for classifying the risk of patients under CRT is important for improving CRT response. This research is aimed at evaluating the prediction of CRT response by analysis of clinical, laboratory, and ECG data. The most important measures in this research are using the most well-known machine learning algorithms for creating a prediction model and proposing a comparative method for optimal classification on the proposed feature vector. Fig. (1) presents the overall phases of the research for prediction of CRT response in patients, prioritizing the variables from the experts' viewpoints, and their effectiveness in prediction.

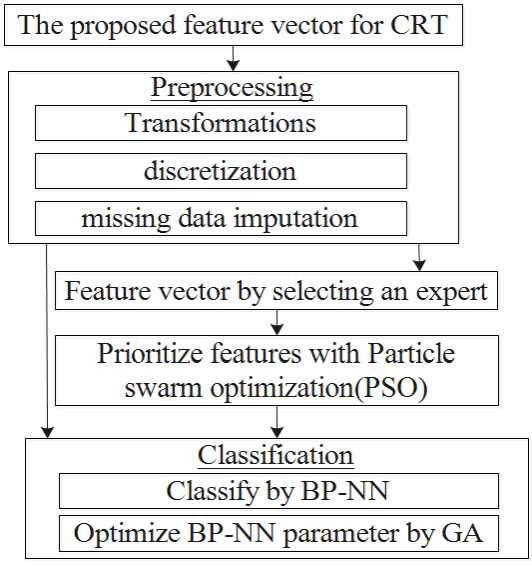

Fig. 1: Overall research method for recognizing the priorities of prediction variables

In the preprocessing section, three operations of transformation, discretization, and imputation are performed to improve the input data. The transformation operation transforms some qualitative attributes into quantitative ones. For example, the Device_Type attribute has two types of CRT-P and CRT-D, or the Rhythm attribute has two types of AF and Sin, which can take zero and one value, respectively. Quantification provides the conditions for the use of many machine learning algorithms. In discretization, the goal is to reduce data. Many variables have large numerical dispersions that reduce the efficiency of the classifier in detection. By discretizing the attributes based on the medical doctor's knowledge, more favorable conditions can be created based on clinical trial intervals in decision making for the classifier. The aim is to reduce the data and easier decision making for the algorithm. The predictive imputation process can prevent presenting sets with lost data. In this dataset, very little data is lost due to incomplete patient records. The results of the predicted imputation were evaluated based on the patient's other data with the supervision of a medical doctor. The imputation process was performed by prediction by the K-Nearest Neighbor (K-NN) algorithm with one neighborhood. The subject of the number of neighborhoods in producing a logical answer was examined from the perspective of a medical doctor. It revealed that the higher number of neighborhoods provide inappropriate answers for prediction due to the distance of neighbors from the studied samples.

3-1- Backpropagation of Error Neural Network

In the following sections, the most important used algorithms are briefly introduced and then, the method of calculating efficiency is described. The architecture of the back propagation neural networks (BP-NN) is the most popular model for complex and multilayer networks. The training process is usually done by delta rule that starts with the calculated difference between the real outputs and the desired outputs. The neural network determines the primary prediction by using Eq. (1), and in the case of $y \neq Target$, the weights become updated based on the error value [28].

$$y = f(b + \sum_{i=1}^{n} w_i x_i) \quad (1)$$

In this study, a multilayer perceptron back propagation neural network with a hidden layer was presented. Since

some features lacked information and some features were not computational, they were removed from the set for analysis. 61 features were given to the neural network input and 34 nodes were considered as hidden layer nodes for greater productivity. This number has been set based on the logic of adequate accuracy and fewer nodes in the hidden layer. At the beginning of the experiment, the hidden layer nodes were equal to 61 nodes and the number 34 was selected with different iterations, which the algorithm offers better speed without reducing the classification accuracy. At the network output, two nodes were placed to determine the status of cardiac synchronization treatment which the prediction results are determined based on the reliability of each output node.

3-2- Particle Swarm Optimization (PSO)

Particle swarm optimization begins with a random initialization to particles population. These particles show the dataset properties of the research. The value of each property is random to adjust the initial position of the particle while the initial particle velocity is set to zero. The particle density should not exceed the maximum value of each property of the sample dataset. After initialization, each particle is evaluated with an evaluator function to find the value of pbest. From the value of pbest obtained, a value is selected as the best value of gbest. Then, the velocity and position of each particle are updated using Equation 2 and Equation 3.

$$Vi(t) = Vi(t-1) + c1r1(xpi - xi) + x2r2(xg - xi) \quad (2)$$

$$xi(t) = xi(t-1) + vi(t) \quad (3)$$

Here v is the velocity, x is the particle position, c is the learning rate, and r is a random number between zero and one and vi (t -1) inertia, which forces the particle to move in the same direction as before. c$r2r2$ (xg - xi) is a social expression that forces particles to move to the best position of all particles. The evaluation process by proportional function, position, and density update is performed as an iterative operation until the expected termination conditions are met. If the evaluation performance tends to improve very slightly, convergence is obtained whose output is a weight value for each property. In fact, the higher weight indicates the effect of the property to achieve a better position of the particle [29]. In the research method, the obtained weights are used to prioritize the vector recommended by the medical doctor.

3-3- Measuring Efficiency

Accuracy of a classifier is the probability of accurate prediction of the class of samples without a label. The experimental samples for prediction of CRT response are classified in one of the four variables below; in other words, accuracy criteria for binary classification can be explained in four categories:

- **TP** or positive true is the number of patients who faced with no CRT response in a true class.
- **TN** or true negative is the number of patients who responded to CRT in true class.
- **FP** or false positive is the number of patients who faced with no CRT response in a false class.
- **FN** or false negative is the number of patients who responded to CRT in a false class.

Classifier sensitivity or inclusiveness is determined by true positive division into the total positive true and false negative samples. Eq. (4) presents the percentage of reliability of no CRT response.

$$Sensitivity = \frac{TP}{TP + FN} \quad (4)$$

However, a specificity that is a kind of accuracy is determined by dividing true negatives by the total true negative and false positive samples. Actually, Eq. (5) indicates the way of determining the appropriate cases of CRT response.

$$Specificity = \frac{TN}{TN + FP} \quad (5)$$

The ability of accurate detection of patients needing and not needing CRT to become possible by accuracy metric. In order to evaluate the accuracy, the ratio of all the true predictions of response and no response to the total prediction is considered. Eq. (6) indicates this ratio.

$$Accuracy = \frac{TP + TN}{TP + FP + TN + FN} \quad (6)$$

For measuring F-measure, F score, or F1 score, a harmonic average of two scores multiplied with two is defined that is proposed for the balance of sensitivity and specificity. Eq. (7) indicates the calculation of the F score.

$$F = 2 \times \frac{Sensitivity \times Specificity}{Sensitivity + Specificity} \quad (7)$$

K-fold cross-validation (KCV) is a technique for precise evaluation in which, the created model is applied on rotated test sets for k times. In the proposed method, the k value is considered equal to 10. Measuring precision affects model selection.

4- Experimental Results

In this section, five machine learning algorithms are applied for prediction of the condition after implanting the device. Each of these algorithms will have different performance in pattern recognition and they will provide different predictions of CRT response or no response.

4-1- The Results of The Primary Classification

The tested algorithms include NB classifier, SVM, random forest, K-NN, and neural network algorithm. Since no CRT response is determined as the positive class, improvement of the total accuracy of classification mainly depends on the accuracy of the negative class. In order to get the highest classification accuracy, algorithms try to maximize the accuracy of this class and it will lead to a decrease in the accuracy of the positive class. Random Forest has the highest sensitivity rate, but it cannot have a high rate of accuracy due to low specificity. Three algorithms of neural network, support vector machine, and k-nearest neighbors have respectively the highest specificity. These three algorithms present the specificity criteria in a close range. So, they play a determinative role in selecting a better algorithm. Neural network provides a more optimal condition due to having the highest specificity compared with the other two algorithms. The low F-measure indicates the low sensitivity of the algorithms and it suggests that prediction of no CRT response has a low rate in the research dataset. Although high specificity indicates the quality of prediction in recognition of positive CRT response after total accuracy F-measure should be carefully investigated for comparing efficiency rates. In the primary test, a decision tree was selected, but a classifier similar to the random forest was replaced for that due to lack of sensitivity. In the primary evaluation, Table (5) presents the efficiency of error back propagation neural networks (BP-NN).

Table 5: The results of classifying the five algorithms in terms of CRT response

Performance	***NB***	***K-NN***	***BP-NN***	***SVM***	***RF***
Accuracy	69.36	71.73	**73.24**	66.54	68.9
F-Measure	17.95	19.22	9.68	12.5	**19.75**
Sensitivity	18.93	18.93	8.21	13.93	**21.79**
Specificity	80.32	83.13	**87.24**	78.05	79.14

4-2- Achieving a Higher Performance

With regard to the results of comparing the algorithms, it can be expected that parameter optimization of neural network models causes higher efficiency in the classification process. In the following of the test, two further neural networks including single layer perceptron and learning vector quantization neural network (NN-LVQ) were compared. Fig. (2) indicates that BP-NN parametric optimization significantly improves the total accuracy of detection. However, consequences of this optimization lead to a decrease in sensitivity. The genetic algorithm produces the initial population by producing different chromosomes from different parameters of the neural network algorithm. The proportional function evaluates the dataset based on the parameters of each chromosome. Selected chromosomes are passed on to the next generation and in the next generation, new compounds are made using crossovers. In this study, the mutation is not used to produce compounds. Ten percent of each generation's choices have been passed on to the next generation, and in 90 percent the intersections have been used. Finally, if there is no improvement in 3 generations or continuity for up to 50 generations, the exit from the algorithm will be done and the chromosome will show the optimal parameters of the algorithm with the highest accuracy of classification. Ultimately, if there is no improvement in 3 generations or continuity for up to 50 generations, the exit from the algorithm will be done and the chromosome with the highest accuracy of classification will show the optimal parameters of the algorithm.

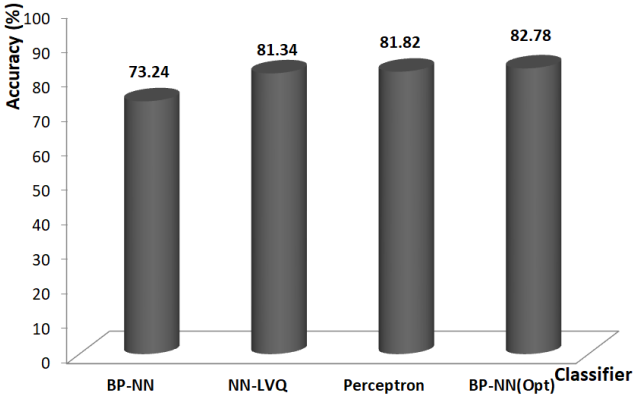

Fig. 2: The results of improvement of classification by neural network models

The two parameters of learning rate (0.561) and momentum (0.923) of the neural network were improved when being trained by genetic algorithm. Also, the other

two parameters of epoch number (1000) and error epsilon were set manually.

All the models of neural network indicated more optimal conditions than the studied machine learning algorithms. Therefore, more improvement in neural network models can be expected. Through separating a subset of the no response samples with the minimum number of samples from a different class, an appropriate model can be created for better recognition of this class by using BP-NN algorithm. Determining the effect of the variable in the prediction of CRT response on 9 important features from the doctor's viewpoint can indicate the priority of selecting the features as an optimization operation. Two features in the subset of the selected features do not have information gain (IG). So according to Table (6), the analysis continues without considering CHF.

Higher weights do not necessarily refer to the effect of a feature on prediction. However, zero weight refers to a lack of information variety for decision making. Creating various combinations of features by particle swarm optimization (PSO) algorithm and using 8 features can be an effective solution for recognizing the effect of variables. PSO algorithm was used for general minimization and weighting the features. First, the algorithm randomly created a group of particles. Then, it searched for the optimal solution by updating generations. Two possible local and global locations of the particle are effective in updating particles.

Table 6: Weighting the features with information gain (IG)

Attribute	***Weight***	***Select***
CHF	0	N
Lung_rales	7.80E-04	Y
QRS_Duration2	2.11E-03	Y
Dyspnea	5.44E-03	Y
Cr2	6.79E-03	Y
Function_Class	9.13E-03	Y
BUN2	1.01E-02	Y
LV_EF2	1.23E-02	Y
Number_of_fragment	1.24E-02	Y

BP-NN classifier was selected as the fitness function with optimal parameters, the population of 50, the generation number of 100, and the exclusion condition in the case of no improvement was considered equal to 2. Fig. (3), presents the results of weighting and the importance of each feature related to CRT response.

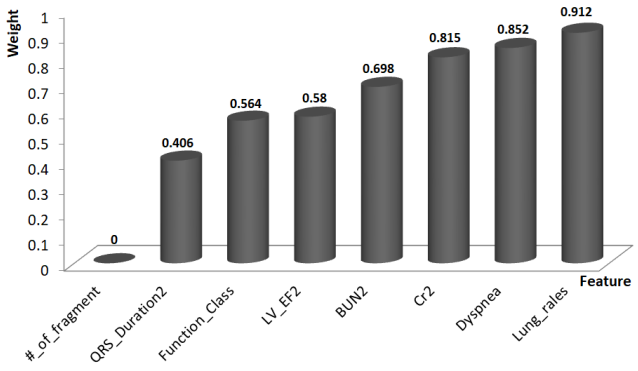

Fig. 3: Prioritization of variables based on the influence coefficient of the PSO algorithm

So, feature weighting method is about searching for the weight of a feature by PSO in order to specify its effect on output results.

4-3- Discussion

After selecting the CRT candidate patients, there are many challenges and problems before a successful treatment. In HF patients, CRT improves the quality of life and decreases the death rate. However, making a decision about different issues such as CRT heart pacemaker [30], and post-surgery suggestions [31] are effective in the improvement of treatment. Classification process provides the possibility of predicting CRT response before treatment of a patient in a probabilistic manner. Among the studied algorithms, neural network models indicated a higher efficiency. By setting the parameters for reaching a higher precision in NN training, it was found that the maximum increase in specificity leads to a maximum decrease in sensitivity and consequently, decreases of F-measure. So, the major technical challenge of this dataset is improving sensitivity without decrease of the total precision. In this paper, the PSO algorithm that is one of the collective intelligence algorithms was used for prioritizing the variables. Among the 8 important features selected by the doctor, Lung rales and Dyspnea were the most effective features. Since most of the patients faced with no response, they were considered as CHF=1; also since the number of fragments was predictable regarding the existence of other independent variables, they were less important than other features in decision making.

5- Conclusions

In this paper, we have presented two goals of a selection of appropriate candidates for CRT and machine prioritization of the feature vector limited by the doctor. In the evaluation of the 9 variables considered important by the doctor in making a decision about prediction, prioritizes of 8 features were determined by the PSO algorithm. The two variables of Lung rales and Dyspnea have the highest effectiveness in the prediction of no CRT response. The improvement in class separability resulted in a significant increase in individual class accuracy achieved by the ANN classifier, and an overall accuracy of 82.78% was reached. The future efforts will be aimed at evaluating the efficiency and the smaller feature vector and solving the problem of low sensitivity in the prediction of CRT response. According to the comparison of the proposed machine learning algorithms and advantages of neural network models in classifying the research dataset, and also regarding the possibility of extending neural network models and optimizing the various parameters of the neural network, it can be concluded that development of neural network models can be promising.

Compliance with ethical standards

Conflict of interest: The authors declare that they have no conflict of interest.

Ethical approval: Our research was approved by the Behavioral Research Ethics Board at the Islamic Azad University, Rasht Branch, Guilan, Iran.

References

[1] R. C. Deo, "Machine learning in medicine", Circulation, vol. 132, no. 20, 2015, pp. 1920-1930.

[2] H. Assodiky, I. Syarif, and T. Badriyah, "Deep Learning Algorithm for Arrhythmia Detection", International Electronics Symposium on Knowledge Creation and Intelligent Computing (IES-KCIC), 2017, pp. 26-32.

[3] A. K. Flügge, K. Wasmer, S. Orwat, H. Abdul-Khaliq, P. C. Helm, U. Bauer, H. Baumgartner, and G. P. Diller, "Cardiac resynchronization therapy in congenital heart disease: Results from the German National Register for Congenital Heart Defects," International Journal of Cardiology, vol. 273, 2018, pp. 108-111.

[4] J. Rickard, A. Cheng, D. Spragg, S. Bansal, M. Niebauer, B. Baranowski, D. J. Cantillon, P. J. Tchou, R. A. Grimm, W. H. W. Tang, B. L. Wilkoff, and N. Varma, "Durability of the survival effect of cardiac resynchronization therapy by level of left ventricular functional improvement: Fate of "nonresponders"," Heart Rhythm, vol. 11, no. 3, 2014, pp. 412-416.

[5] H. X. Niu, W. Hua , F. Z. Wang , S. Zhang , K. P. Chen, and X. Chen, "Complications of cardiac resynchronization therapy in patients with congestive heart failure," *Chinese Medical Journal*, vol. 119, no. 6, 2006, pp. 449-453.

[6] C. Leclercq, H. Burri, A. Curnis, P. P. Delnoy, C. A. Rinaldi, J. Sperzel, K. Lee, C. Cohorn, and B. Thibault, "Rationale and design of a randomized clinical trial to assess the safety and efficacy of multipoint pacing therapy: MOre REsponse on Cardiac Resynchronization Therapy with MultiPoint Pacing (MORE-CRT MPP–PHASE II)," *American Heart Journal*, vol. 209, 2019, pp. 1-8.

[7] H. Huang, L. Shen, R. Zhang, F. Makedon, B. Hettleman, and J. Pearlman, "Cardiac Motion Analysis to Improve Pacing Site Selection in CRT," *Academic Radiology*, vol. 13, no. 9, 2006, pp. 1124–1134.

[8] M. M. Kalscheur, R. T. Kipp, M. C. Tattersall, C. Mei, K. A. Buhr, D. L. DeMets, M. E. Field, L. L. Eckhardt, and C. D. Page, "Machine Learning Algorithm Predicts Cardiac Resynchronization Therapy Outcomes: Lessons From the COMPANION Trial," *Circ Arrhythm Electrophysiol*, vol. 11, no. 1, 2018, pp. 1-11.

[9] S. Giffard-Roisin, H. Delingette, T. Jackson, J. Webb, L. Fovargue, J. Lee, C. A. Rinaldi, R. Razavi, N. Ayache, and M. Sermesant, "Transfer Learning From Simulations on a Reference Anatomy for ECGI in Personalized Cardiac Resynchronization Therapy," *IEEE Transactions on Biomedical Engineering*, vol. 66, no. 2, 2019, pp. 343-353.

[10] K. Howe, P. Gladding, N. James, C. Prabhakar, L. Dawson, A. Gavin, and T. Schlegel, "Predicting CRT Response Using Machine Learning Analysis of Pre-Implant ECG Data," *Heart, Lung and Circulation*, vol. 26, no. 1, 2017, pp. S25-S26.

[11] I. Kononenko, "Machine learning for medical diagnosis: history, state of the art and perspective," *Artificial Intelligence in Medicine*, vol. 23, no. 1, 2001, pp. 89-109.

[12] P. K. Chao, C. L. Wang, and H. L. Chan, "An intelligent classifier for prognosis of cardiac resynchronization therapy based on speckle-tracking echocardiograms," *Artificial Intelligence in Medicine*, vol. 54, no. 3, 2012, pp. 181-188.

[13] M. Fedorco, A. Bulava, P. Šantavý, A. Mokráček, V. Lonský, L. Dušek, and M. Táborský, "Middle-term stability of epicardial left ventricular electrodes for cardiac resynchronization therapy," *Cor et Vasa*, vol. 59, no. 6, 2017, pp. e530-e539.

[14] R. Zhang, S. Ma, L. Shanahan, J. Munroe, S. Horn, and S. Speedie, "Discovering and identifying New York heart association classification from electronic health records," *BMC Medical Informatics and Decision Making*, vol. 18, no. 2, 2018, pp. 5-13.

[15] N. M. Hawkins, M. C. Petrie, M. I. Burgess, and J. J.V. McMurray, "Selecting Patients for Cardiac Resynchronization Therapy: The Fallacy of Echocardiographic Dyssynchrony," *Journal of the American College of Cardiology*, vol. 53, no. 21, 2009, pp. 1944-1959.

[16] J. Rickard, H. Michtalik, R. Sharma, Z. Berger, E. Iyoha, A. R. Green, N. Haq, and K. A. Robinson, "Predictors of response to cardiac resynchronization therapy: a systematic review," *International Journal of Cardiology*, vol. 225, 2016, pp. 345-352.

[17] M. Tokodi, W. Schwertner, P. Perge, A. Kosztin, B. Lakatos, S. Shrestha, A. Kovacs, and B. Merkely, "Unsupervised machine learning algorithm to identify high and low risk patients following crt implantation," *Journal of*

the American College of Cardiology, vol. 71, no. 11, 2018, pp. 947-948.

[18] M. Loutfi, M. Nawar, S. Eltahan, and A. A. Elhoda, "Predictors of response to cardiac resynchronization therapy in chronic heart failure patients," *The Egyptian Heart Journal*, vol. 68, no. 4, 2016, pp. 227-236.

[19] A. Grimaldi, E. Z. Gorodeski, and J. Rickard, "Optimizing Cardiac Resynchronization Therapy: an Update on New Insights and Advancements," Current Heart Failure Reports, vol. 15, no. 3, 2018, pp. 156-160.

[20] O. Adegbala, O. Olagoke, A. Adejumo, E. Akintoye, A. Oluwole, P. Alebna, K. Williams, R. Lieberman, and L. Afonso, "Incidence and outcomes of cardiac tamponade in patients undergoing cardiac resynchronization therapy," *International journal of cardiology*, vol. 272, 2018, pp. 137-141.

[21] C. J. Plummer, C. M. Frank, Z. Bári, Y. S. Al Hebaishi, R. N. Klepfer, R. W. Stadler, S. Ghosh, S. Liu, and S. Mittal, "A novel algorithm increases the delivery of effective cardiac resynchronization therapy during atrial fibrillation: The CRTee randomized crossover trial," *Heart Rhythm*, vol. 15, no. 3, 2018, pp. 369-375.

[22] E. Thomas, D. Toth, T. Kurzendorfer, K. Rhode, and P. Mountney, "Mechanical Activation Computation from Fluoroscopy for Guided Cardiac Resynchronization Therapy," in *2018 40th Annual International Conference of the IEEE Engineering in Medicine and Biology Society (EMBC)*, 2018, pp. 592-595.

[23] D. J. van Veldhuisen, A. H. Maass, S. G. Priori, P. Stolt, I. C. van Gelder, K. Dickstein, and K. Swedberg, "Implementation of device therapy (cardiac resynchronization therapy and implantable cardioverter defibrillator) for patients with heart failure in Europe: changes from 2004 to 2008," *European Journal of Heart Failure*, vol. 11, no. 12, 2009, pp. 1143-1151.

[24] G. Boriani, M. Ziacchi, M. Nesti, A. Battista, F. Placentino, V. L. Malavasi, I. Diemberger, and L. Padeletti, "Cardiac resynchronization therapy: How did consensus guidelines from Europe and the United States evolve in the last 15 years?," *International journal of cardiology*, vol. 261, 2018, pp. 119-129.

[25] J. Gorcsan, C. P. Anderson, B. Tayal, M. Sugahara, J. Walmsley, R. C. Starling, and J. Lumens, "Systolic Stretch Characterizes the Electromechanical Substrate Responsive to Cardiac Resynchronization Therapy," *JACC: Cardiovascular Imaging*, vol. 12, no. 9, 2018, pp. 1741-1752.

[26] M. A. Baturova, V. Kutyifa, S. McNitt, B. Polonsky, S. Solomon, J. Carlson, W. Zareba, and P. G. Platonov, "Usefulness of Electrocardiographic Left Atrial Abnormality to Predict Response to Cardiac Resynchronization Therapy in Patients With Mild Heart Failure and Left Bundle Branch Block," *The American Journal of Cardiology*, vol. 122, no. 2, 2018, pp. 268-274.

[27] D. Peressutti, W. Bai, T. Jackson, M. Sohal, A. Rinaldi, D. Rueckert, and A. King, "Prospective Identification of CRT Super Responders Using a Motion Atlas and Random Projection Ensemble Learning," in *International Conference on Medical Image Computing and Computer-Assisted Intervention*, 2015, vol. 9351, pp. 493-500.

[28] S. Shanmuganathan, "Artificial Neural Network Modelling: An Introduction," in *Studies in Computational Intelligence*, vol. 628, 2016, pp. 1-14.

[29] A. Dongoran, S. Rahmadani, M. Zarlis, and S. Zakarias, "Feature weighting using particle swarm optimization for learning vector quantization classifier," in *2nd International Conference on Computing and Applied Informatics*, 2017 vol.978, pp.1-6.

[30] D. Weber, M. Koller, D. Theuns, S. Yap, M. Kühne, C. Sticherling, T. Reichlin, T. Szili-Torok, S. Osswald, and B. Schaer, "Predicting defibrillator benefit in patients with cardiac resynchronization therapy: A competing risk study," *Heart Rhythm*, vol. 16, no. 7, 2019, pp. 1057-1064.

[31] F. Leyva, A. Zegard, O. N Okafor, J. de Bono, D. McNulty, A. Ahmed, H. J Marshall, D. Ray, and T. Qiu, "Survival after cardiac resynchronization therapy: results from 50 084 implantations," *EP Europace*, vol. 21, no. 5, 2019, pp. 754–762.

Mohammad Nejadeh received the B.S. degree in Computer Engineering from Islamic Azad University, Lahijan Branch, Iran, and M.S. degree in Information Technology from Guilan University , Iran. Currently He is Ph.D. Candidate in Islamic Azad University, Rasht Branch, Iran. His research interests include Information Technology, Network Security, Artificial Intelligence, Computer Engineering Sciences.

Peyman Bayat received the M.Sc. degree from Islamic Azad University, Arak Branch, Iran, and the Ph.D. degree in computer engineering from UPM University, Malaysia. He is currently an Assistant Professor with the Faculty of Computer Engineering, Islamic Azad University, Rasht Branch, Iran. His main research interests include distributed systems, Artificial Intelligence.

Jalal Kheirkhah received the Specialty Doctor in Cardiology in Shahid Beheshti University of Medical Sciences, Tehran, Iran, in 2004 and the Fellowship of Clinical Cardiac Electrophysiology in Tehran University of Medical Sciences, Tehran, Iran in 2011. His area research interests include Cardiac Electrophysiology and Cardiovascular Imaging.

Hassan Moladoust received the M.S. and Ph.D degrees in Medical Physics from Tarbiat Modares University, Tehran, Iran, in 2001 and 2008; respectively. His area research interests include Cardiovascular Imaging, Signal and Image analysis.